US008261602B2

(12) **United States Patent**
Degertekin

(10) **Patent No.: US 8,261,602 B2**
(45) **Date of Patent: Sep. 11, 2012**

(54) **THREE-DIMENSIONAL NANOSCALE METROLOGY USING FIRAT PROBE**

(75) Inventor: **Fahrettin L. Degertekin**, Decatur, GA (US)

(73) Assignee: **Georgia Tech Research Corporation**, Atlanta, GA (US)

(*) Notice: Subject to any disclaimer, the term of this patent is extended or adjusted under 35 U.S.C. 154(b) by 64 days.

(21) Appl. No.: **12/732,991**

(22) Filed: **Mar. 26, 2010**

(65) **Prior Publication Data**

US 2010/0180354 A1 Jul. 15, 2010

Related U.S. Application Data

(60) Division of application No. 12/136,399, filed on Jun. 10, 2008, now Pat. No. 7,707,873, which is a continuation of application No. 11/552,274, filed on Oct. 24, 2006, now Pat. No. 7,395,698.

(60) Provisional application No. 60/730,217, filed on Oct. 25, 2005.

(51) **Int. Cl.**
G01B 5/28 (2006.01)

(52) **U.S. Cl.** **73/105**

(58) **Field of Classification Search** ..... None
See application file for complete search history.

(56) **References Cited**

U.S. PATENT DOCUMENTS

5,276,672 A * 1/1994 Miyazaki et al. 369/126

* cited by examiner

Primary Examiner — Robert R Raevis

(74) *Attorney, Agent, or Firm* — Bryan W. Bockhop; Bockhop & Associates, LLC

(57) **ABSTRACT**

In accordance with an embodiment of the invention, there is a force sensor for a probe based instrument. The force sensor can comprise a detection surface and a flexible mechanical structure disposed a first distance above the detection surface so as to form a gap between the flexible mechanical structure and the detection surface, wherein the flexible mechanical structure is configured to deflect upon exposure to an external force, thereby changing the first distance over a selected portion of the gap, the change in distance at the selected portion orienting a probe tip of the force sensor for multi-directional measurement.

13 Claims, 43 Drawing Sheets

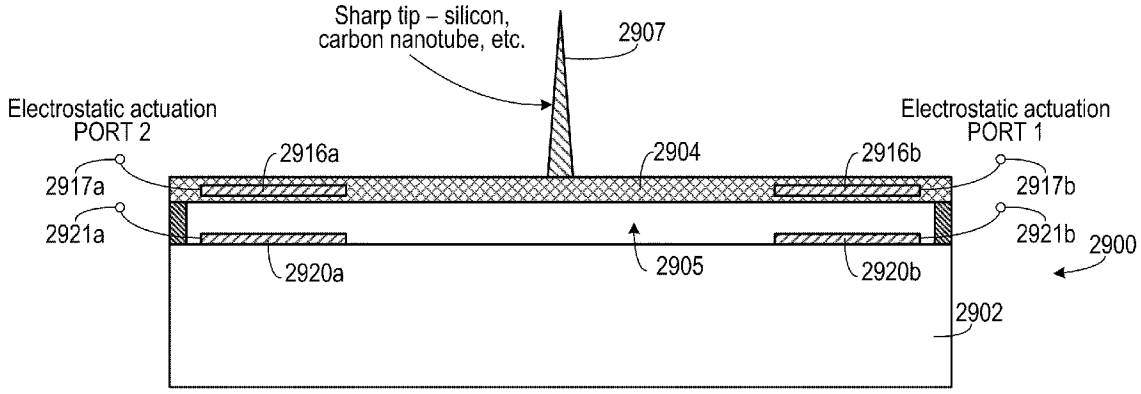

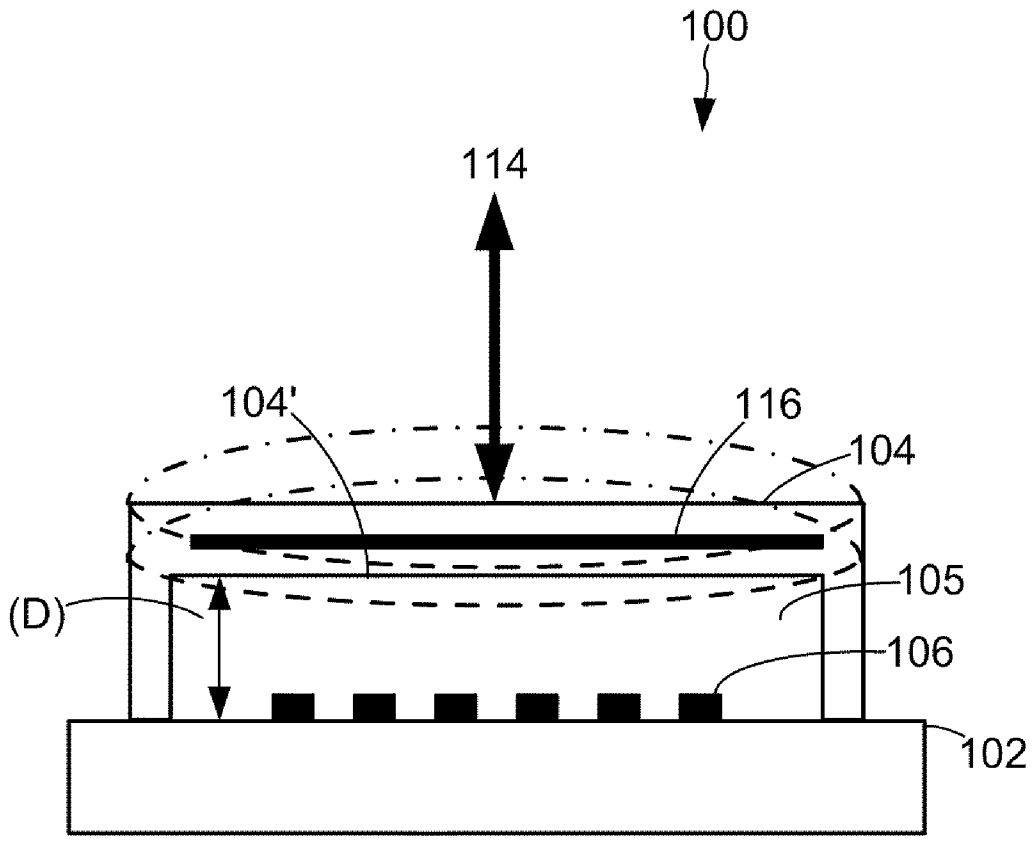

Fig. 1A

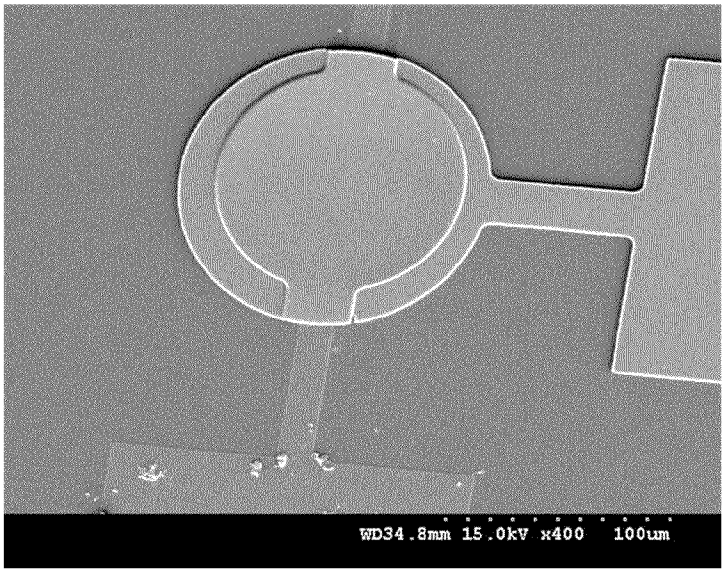

Fig. 1B

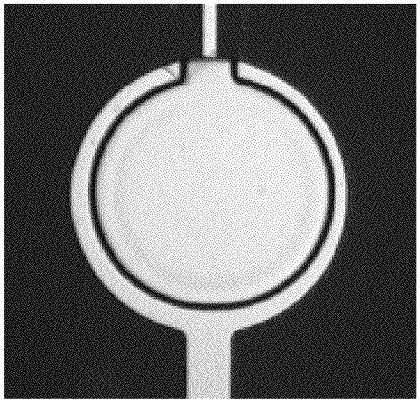

Fig. 1C

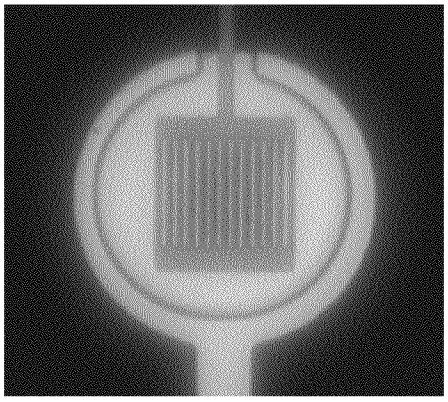

Fig. 1D

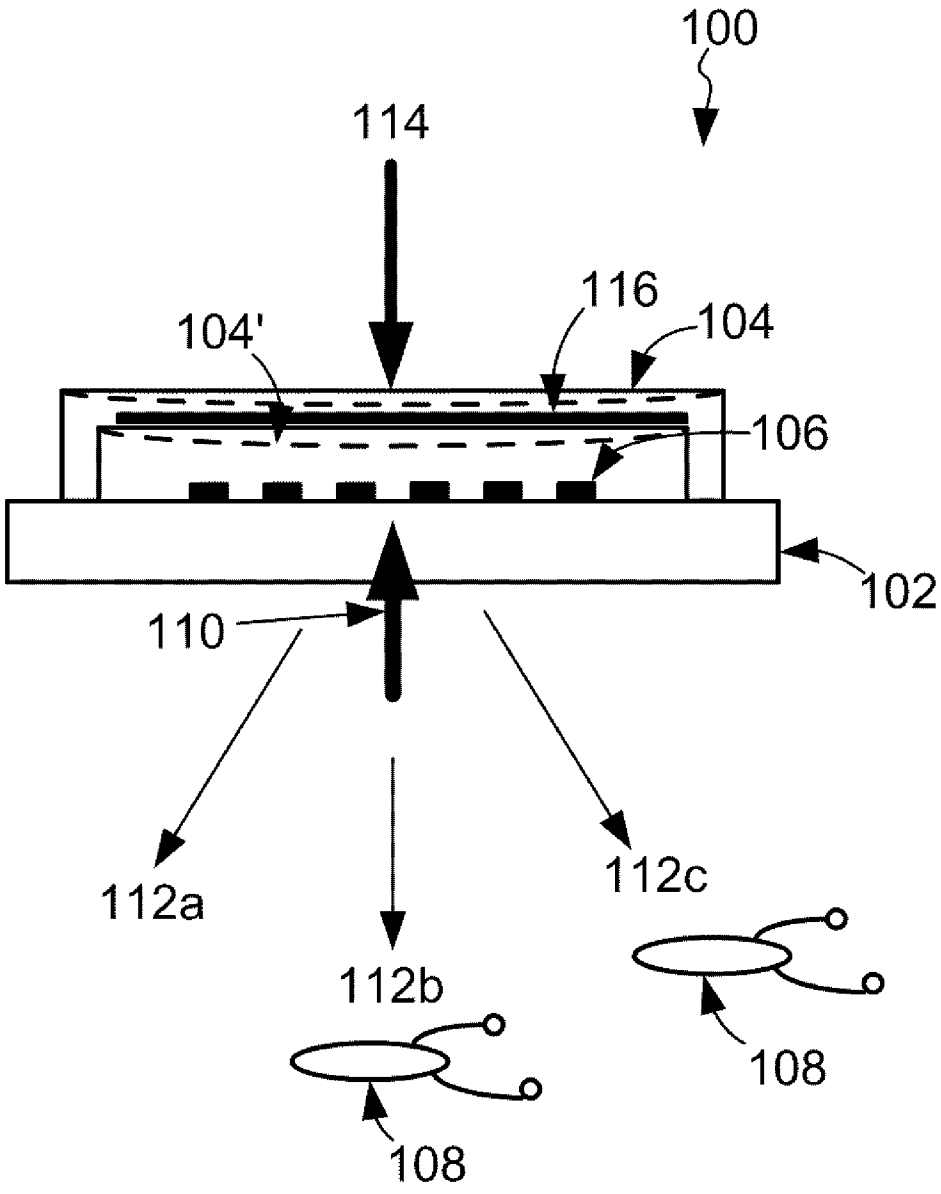

Fig. 1E

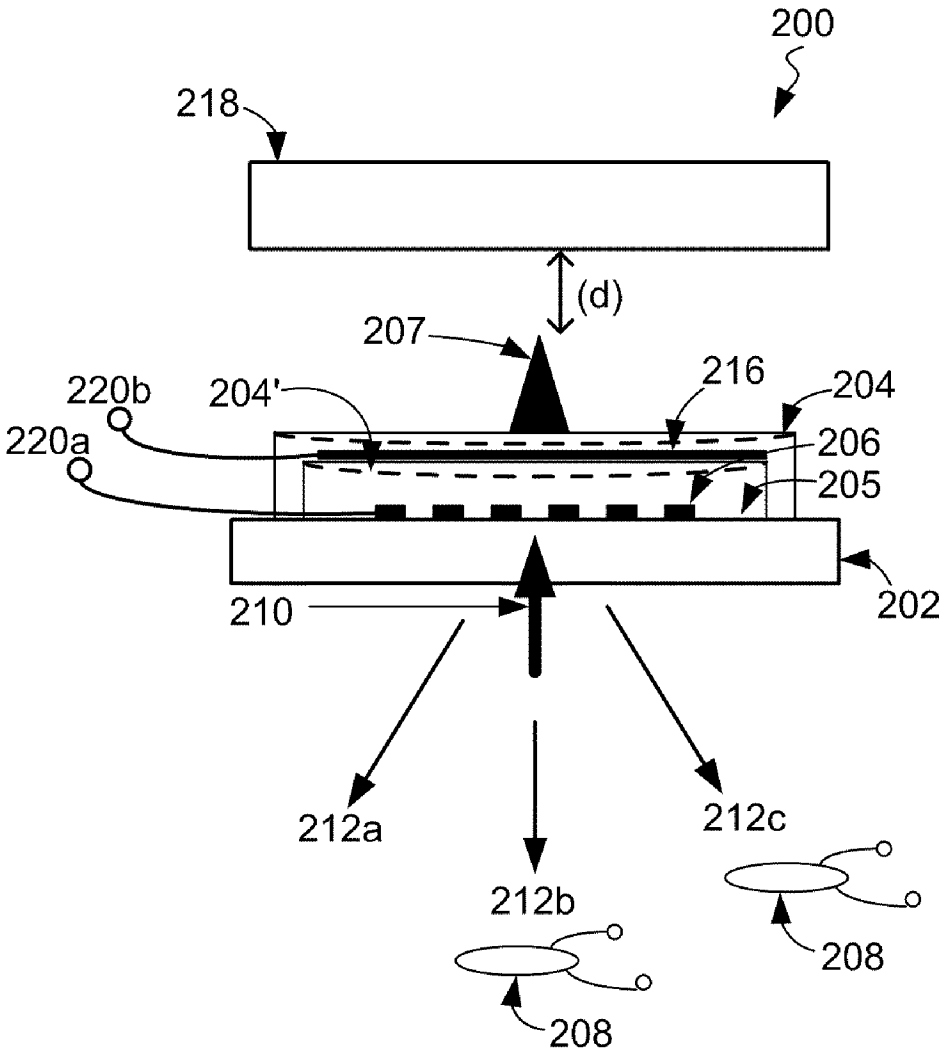
200
218
(d)
207
216
204
220b
204'
220a
206
205
210
202
212a
212c
212b
208
208

Fig. 2A

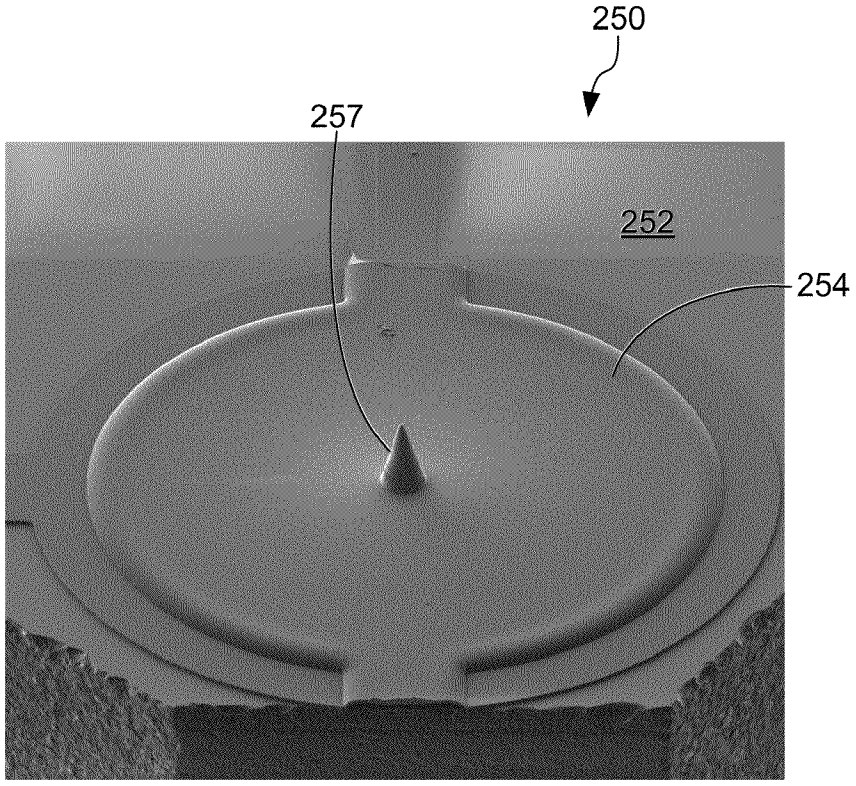

Fig. 2B

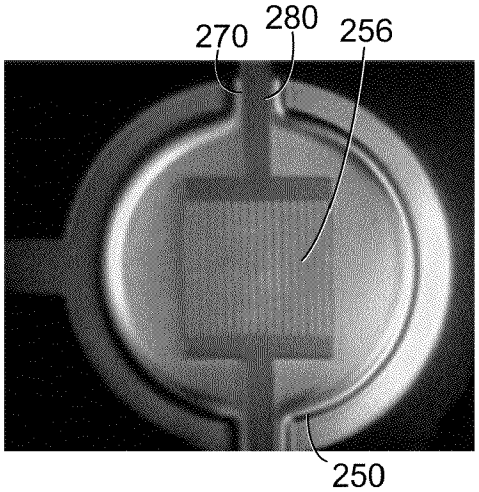

Fig. 2C

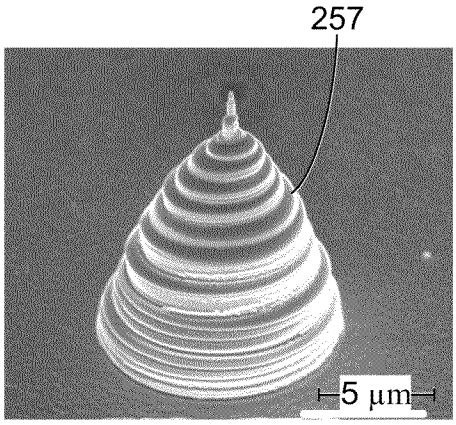

Fig. 2D

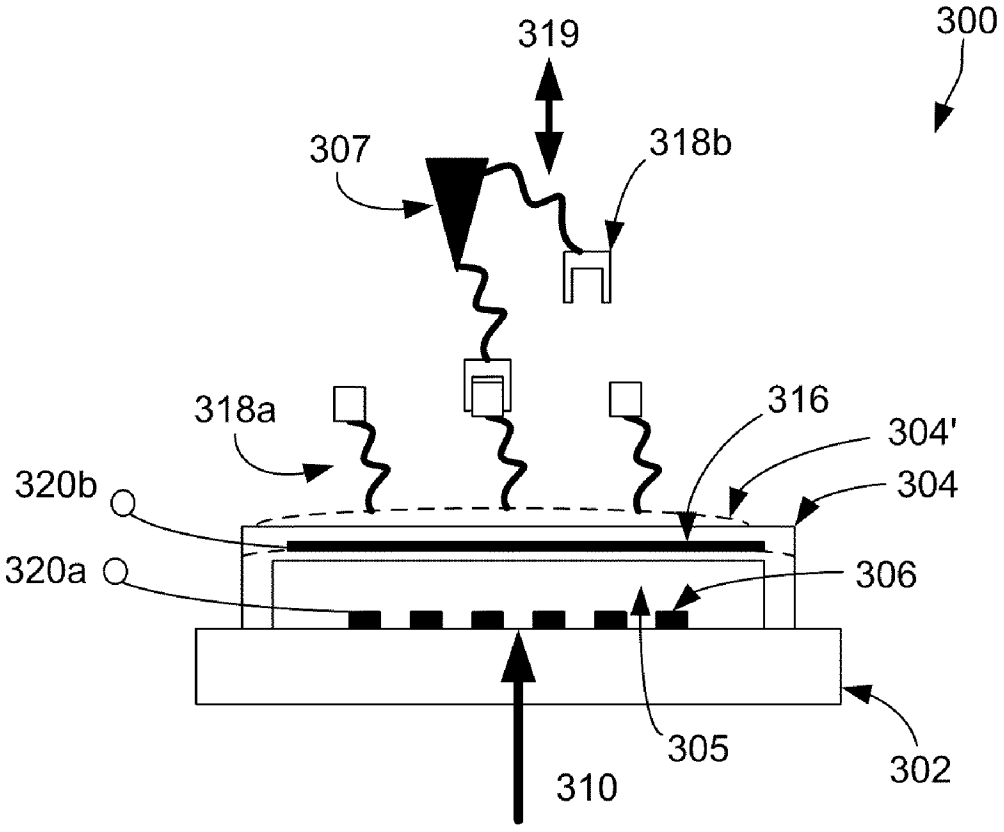

Fig. 3A

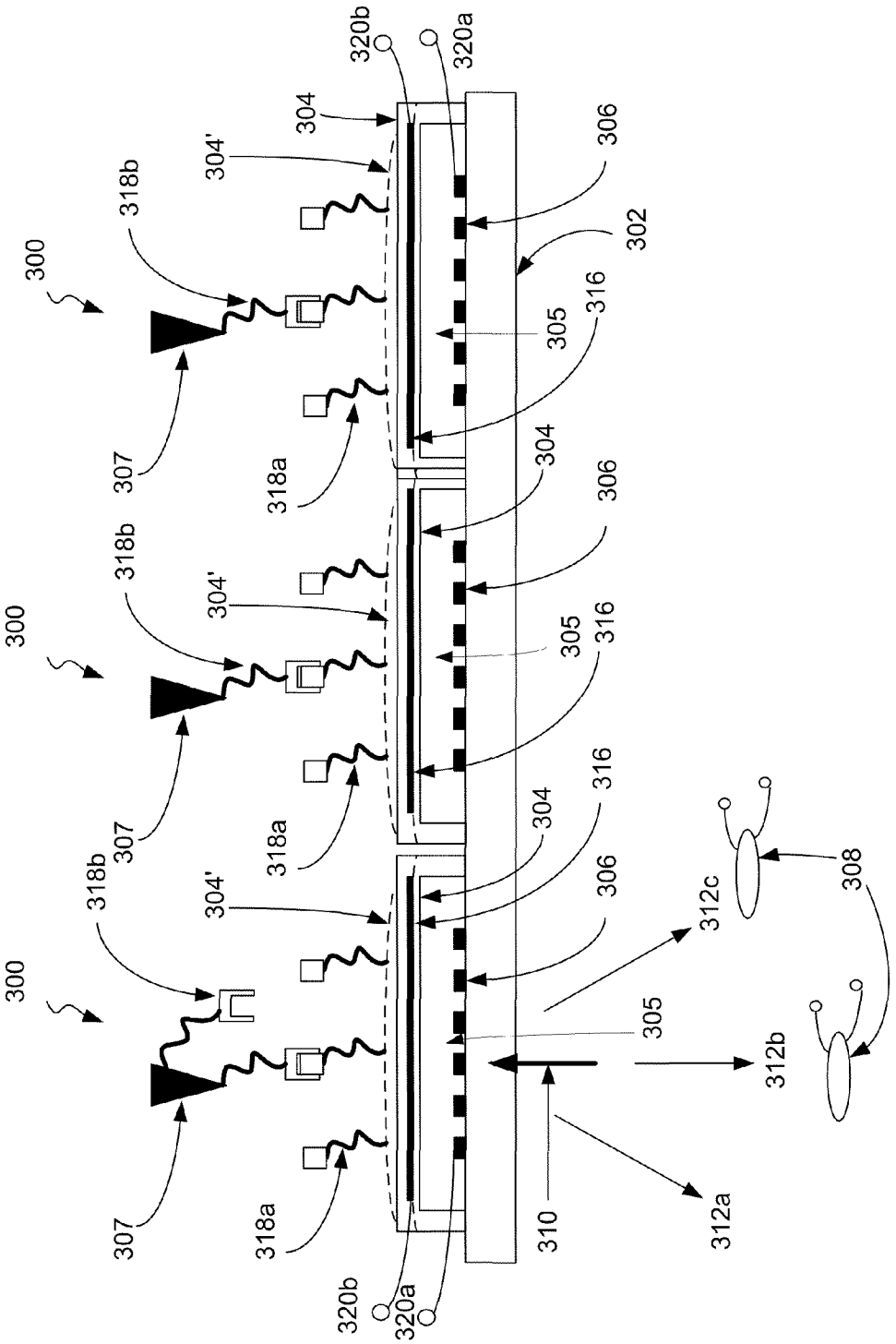
300
307
318b
318a
304
304'
306
302
305
316
320a
320b
310
312a
312b
312c
308

Fig. 3B

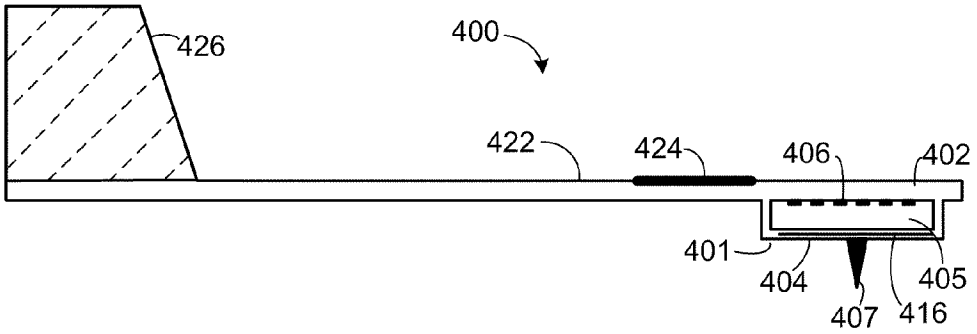

Fig. 4A

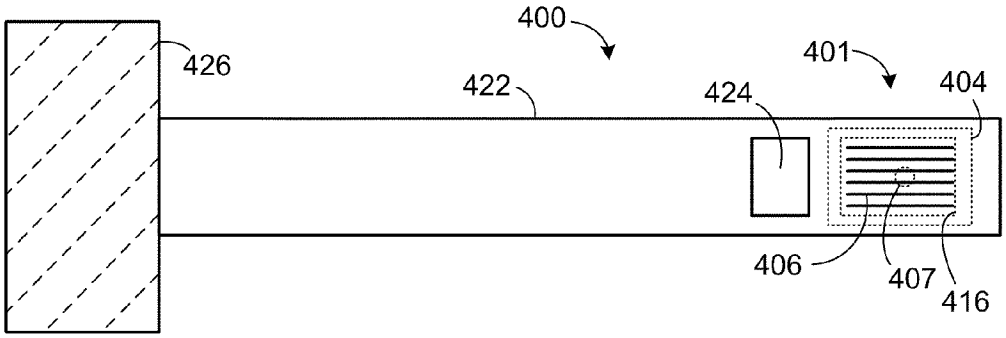

Fig. 4B

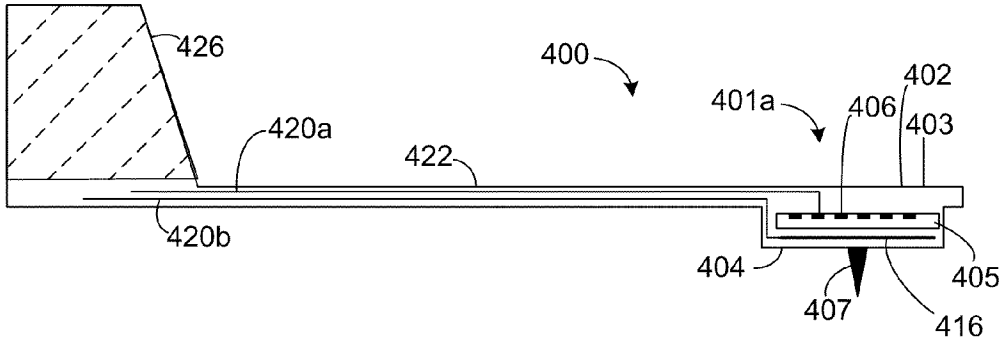

Fig. 4C

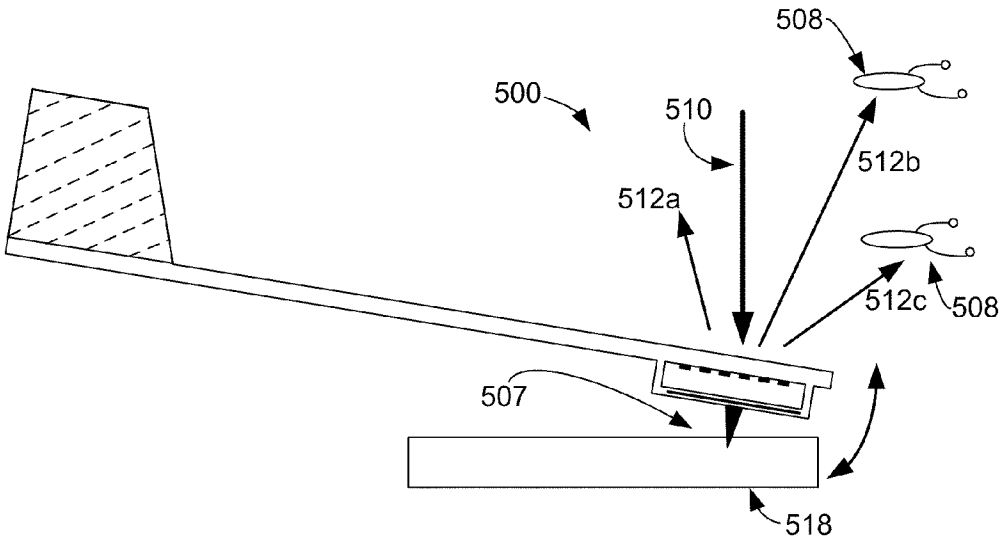

Fig. 5A

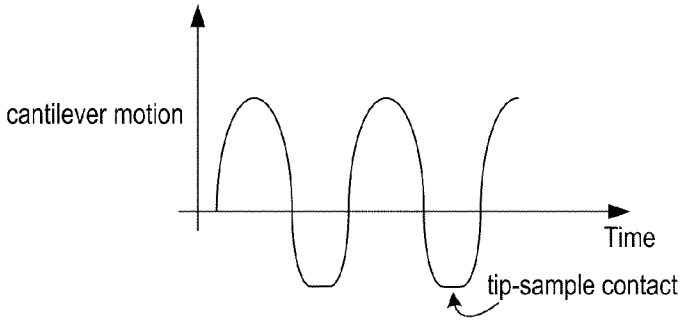

Fig. 5B

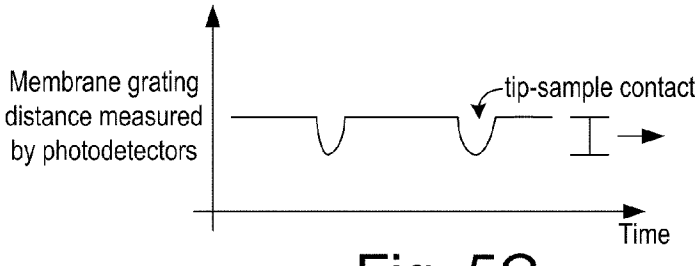

Fig. 5C

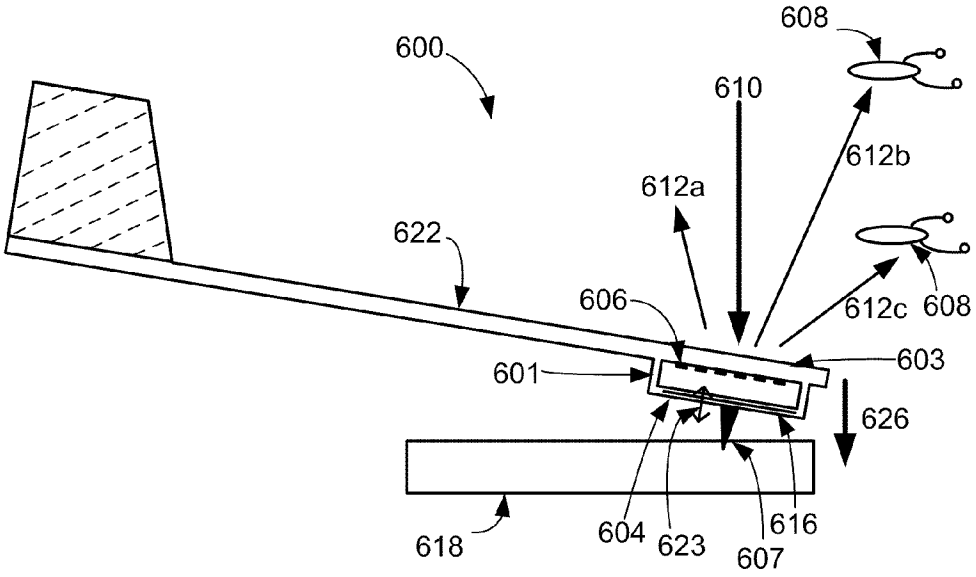
600
608
610
612b
612a
622
606
612c
608
603
601
626
618
604
623
616
607

Fig. 6

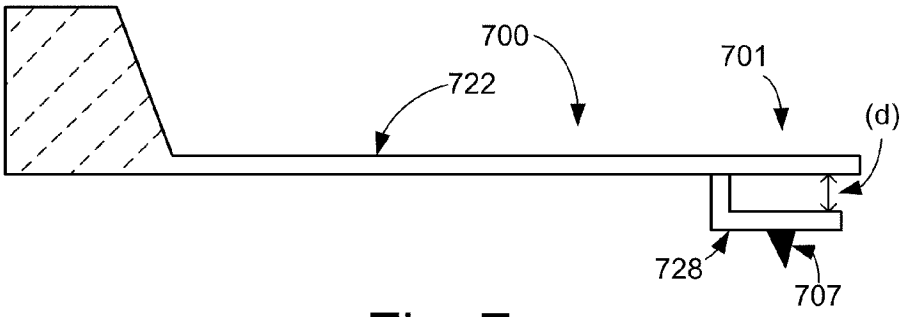
700
701
722
(d)
728
707

Fig. 7

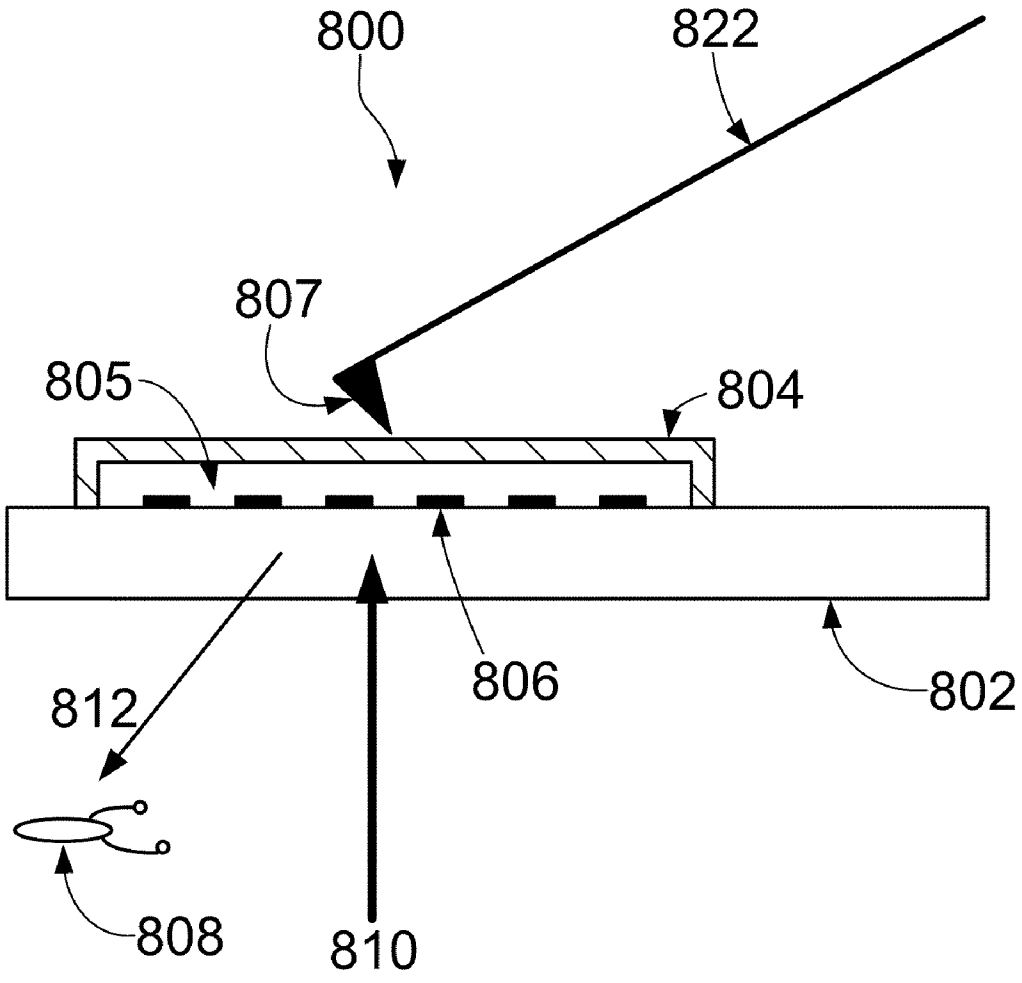

Fig. 8A

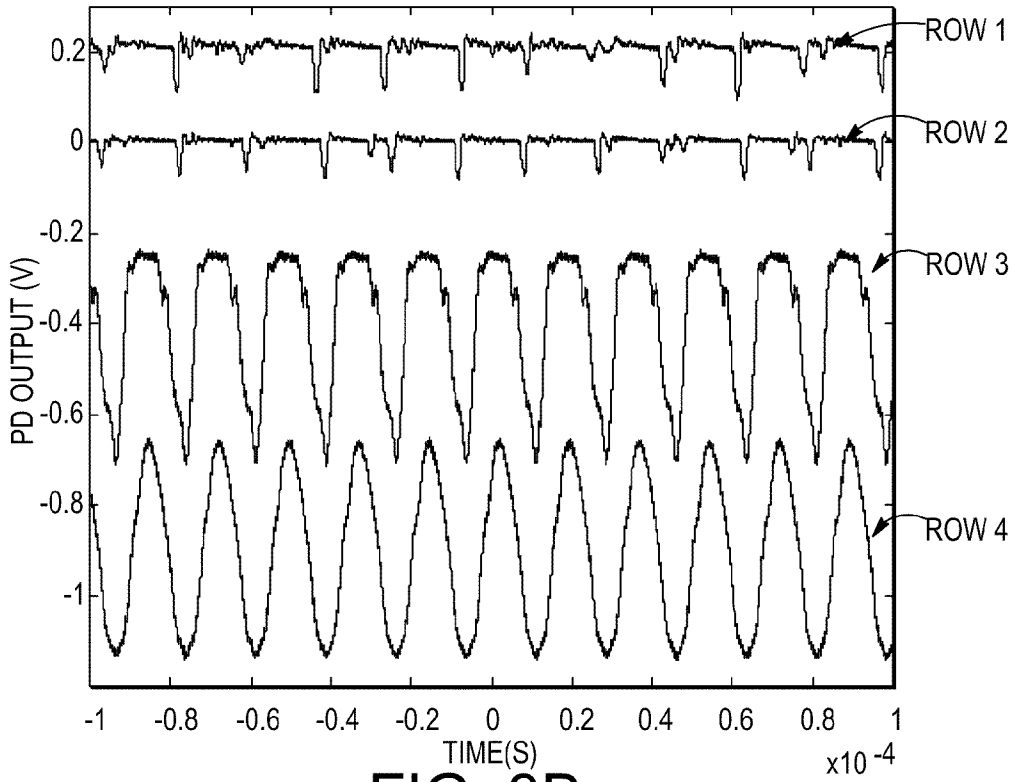
ROW 1
ROW 2
ROW 3
ROW 4
PD OUTPUT (V)
0.2
0
-0.2
-0.4
-0.6
-0.8
-1
-1 -0.8 -0.6 -0.4 -0.2 0 0.2 0.4 0.6 0.8 1
TIME(S)
x10 -4

FIG. 8B

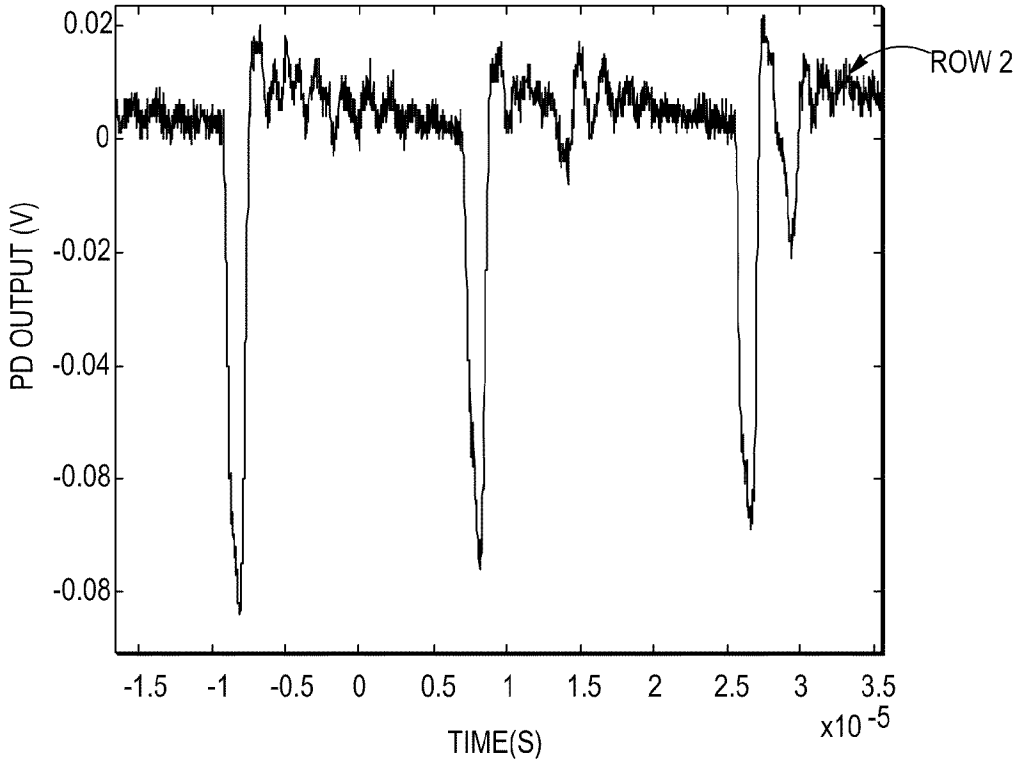
ROW 2
PD OUTPUT (V)
0.02
0
-0.02
-0.04
-0.08
-0.08
-1.5 -1 -0.5 0 0.5 1 1.5 2 2.5 3 3.5
TIME(S)
x10 -5

FIG. 8C

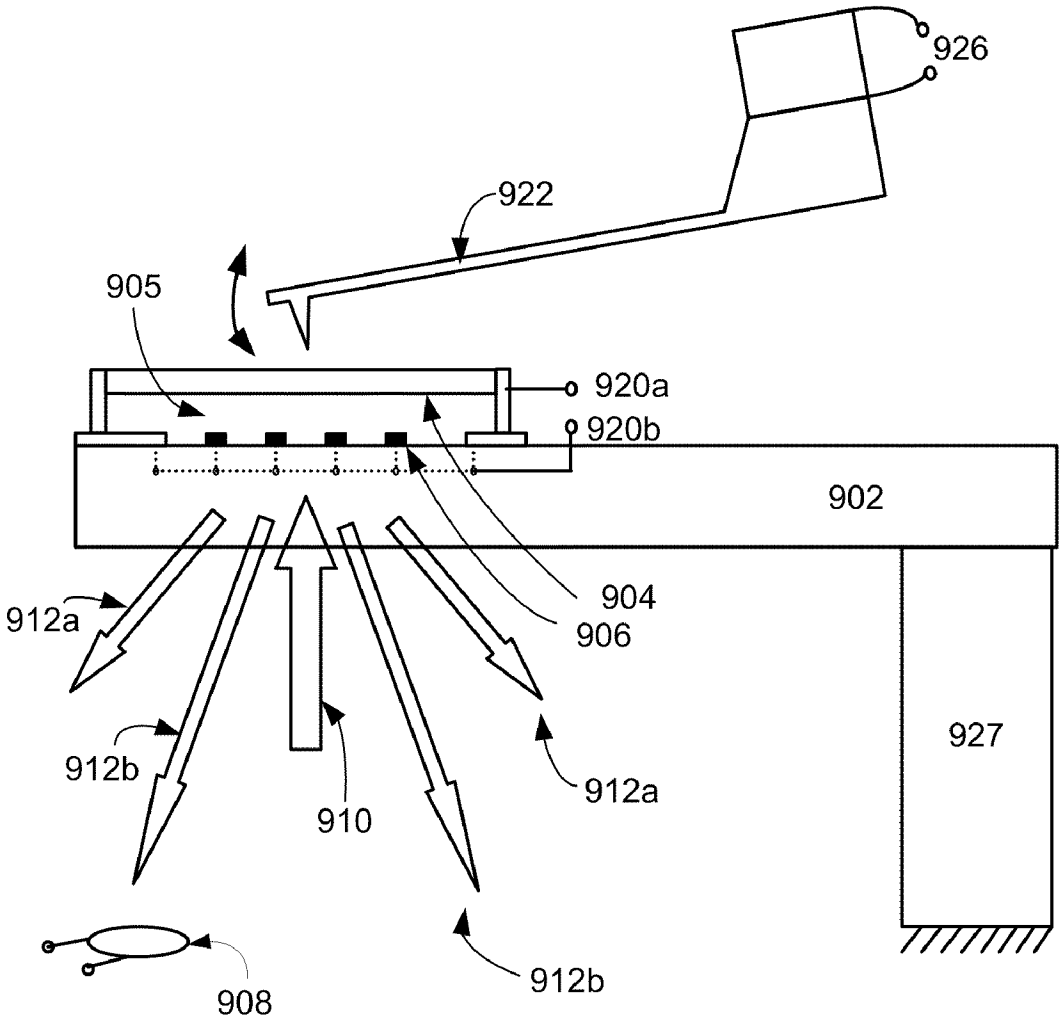
926
922
905
920a
920b
902
904
906
912a
912b
910
912a
927
912b
908

Fig. 9A

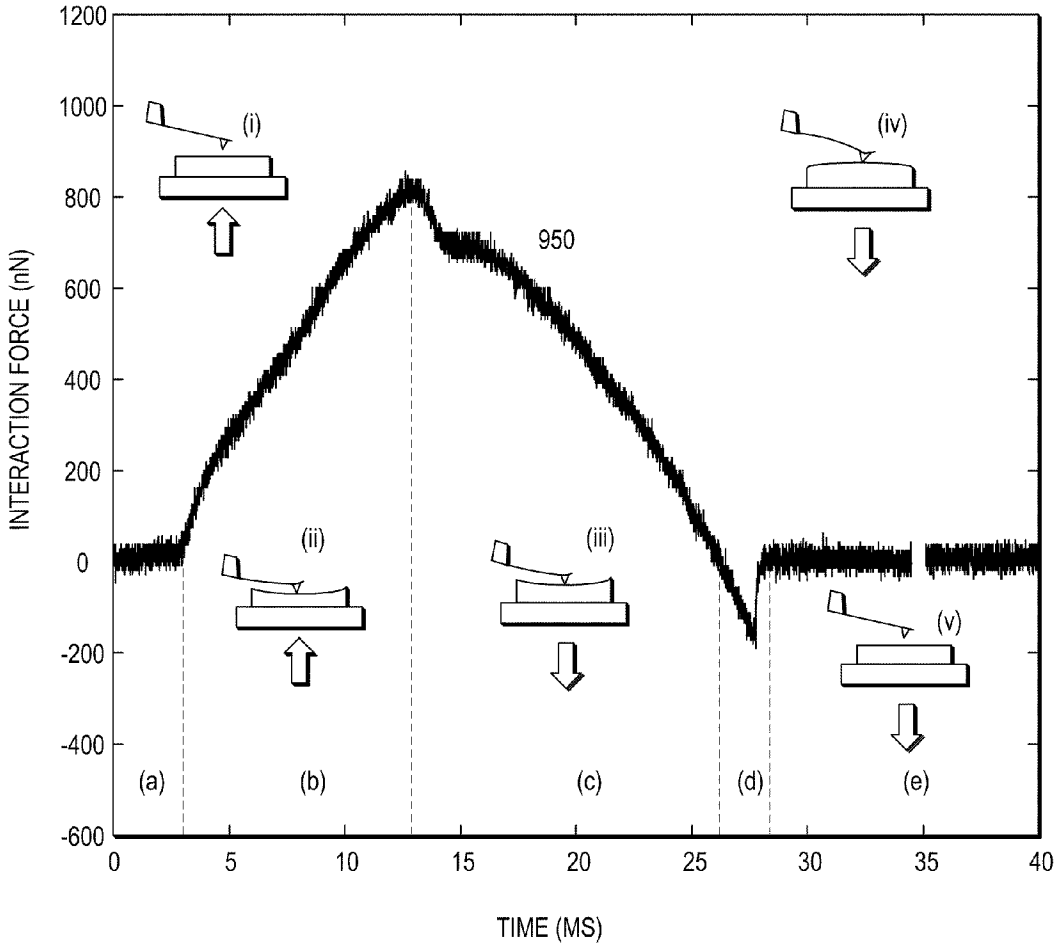
1200
1000
800
600
400
200
0
-200
-400
-600
INTERACTION FORCE (nN)
0
5
10
15
20
25
30
35
40
TIME (MS)
950
(i)
(ii)
(iii)
(iv)
(v)
(a)
(b)
(c)
(d)
(e)

FIG. 9B

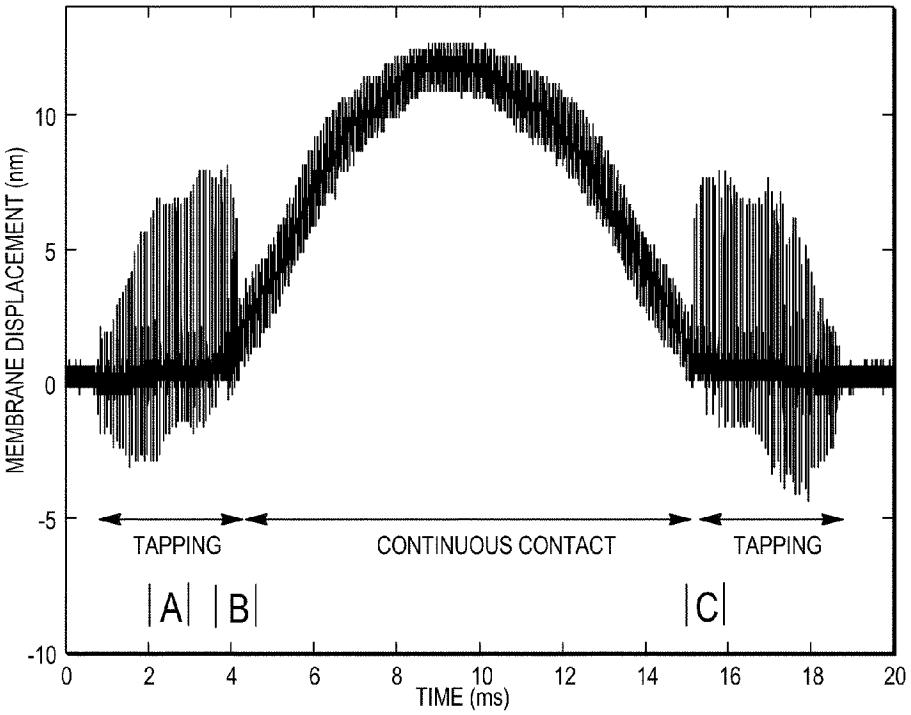

FIG. 9C

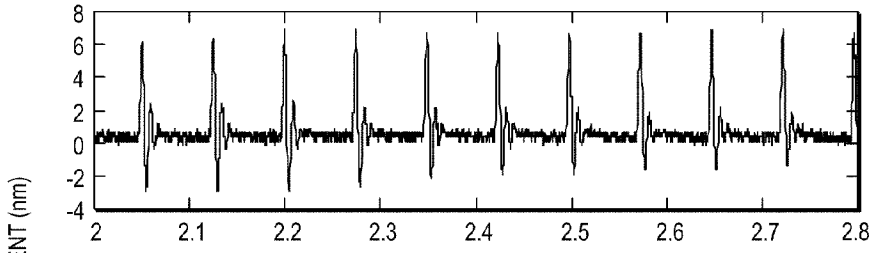

FIG. 9D

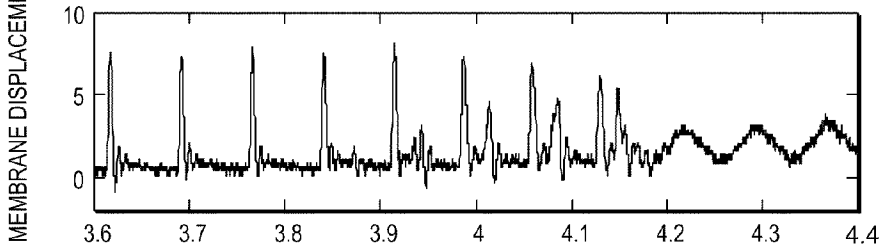

FIG. 9E

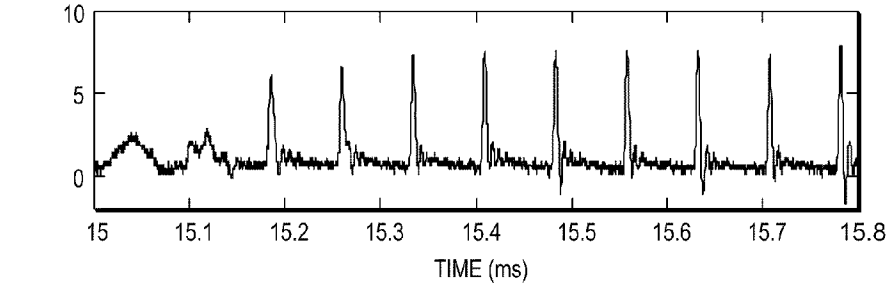

FIG. 9F

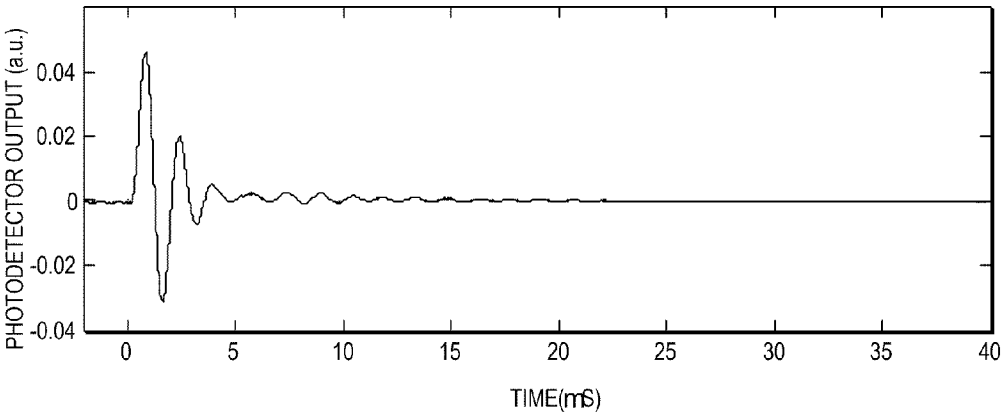
PHOTODETECTOR OUTPUT (a.u.)
0.04
0.02
0
-0.02
-0.04
0
5
10
15
20
25
30
35
40
TIME(mS)

FIG. 9G

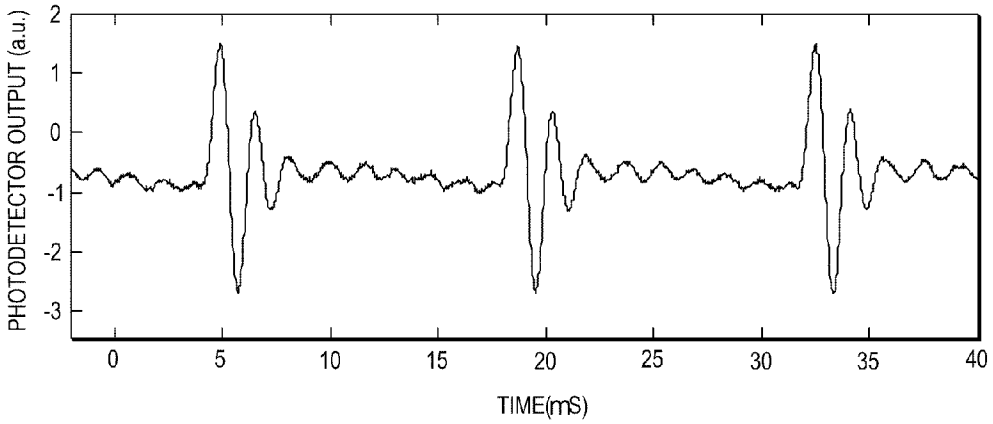
PHOTODETECTOR OUTPUT (a.u.)
2
1
0
-1
-2
-3
0
5
10
15
20
25
30
35
40
TIME(mS)

FIG. 9H

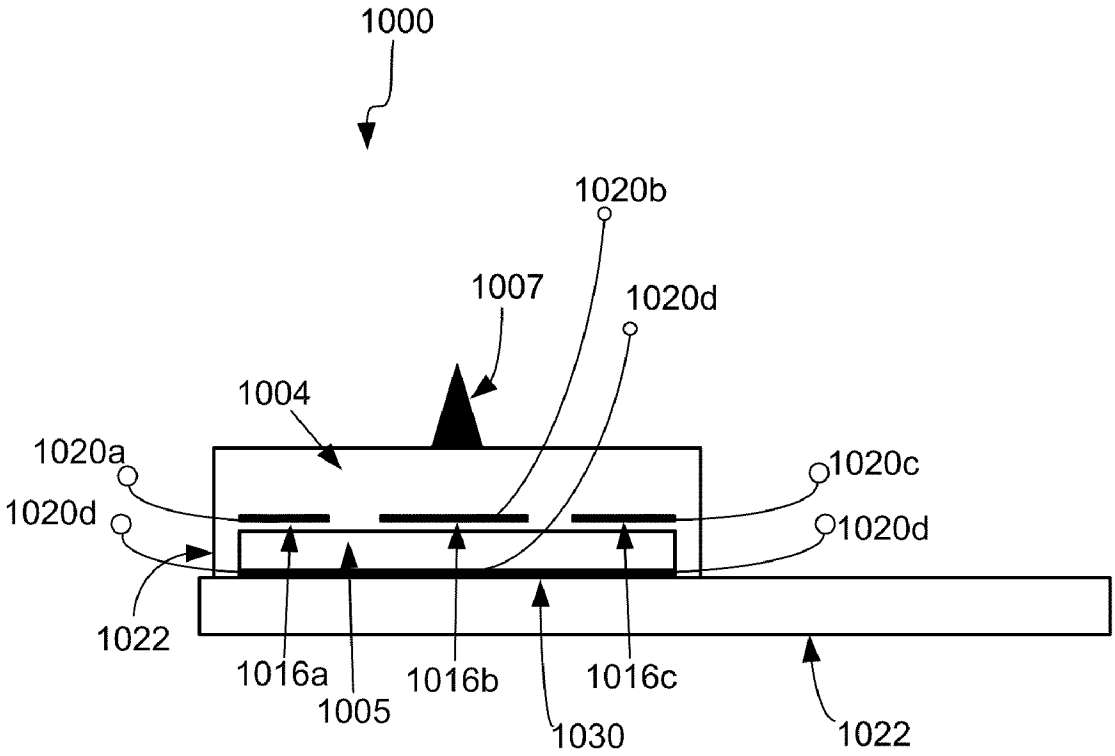
1000
1020b
1007
1020d
1004
1020a
1020c
1020d
1020d
1022
1016a
1005
1016b
1030
1016c
1022

Fig. 10A

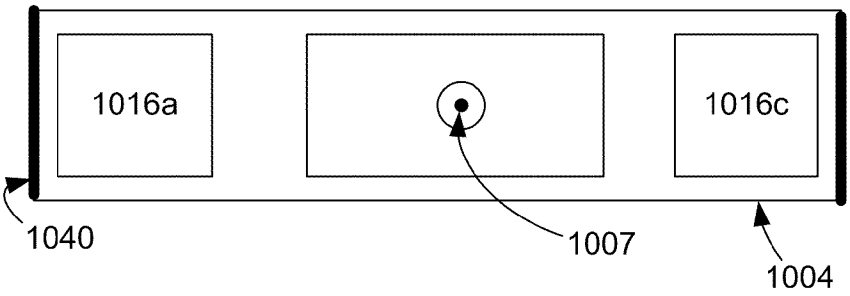

Fig. 10B

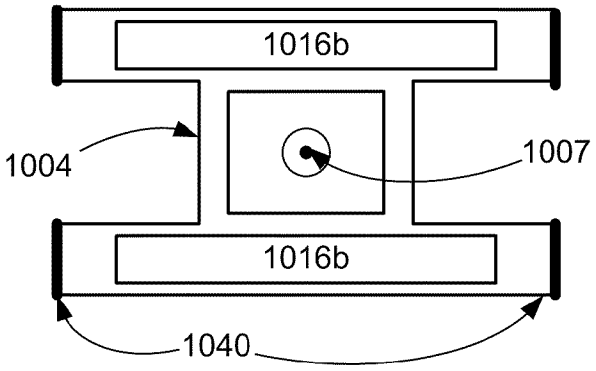

Fig. 10C

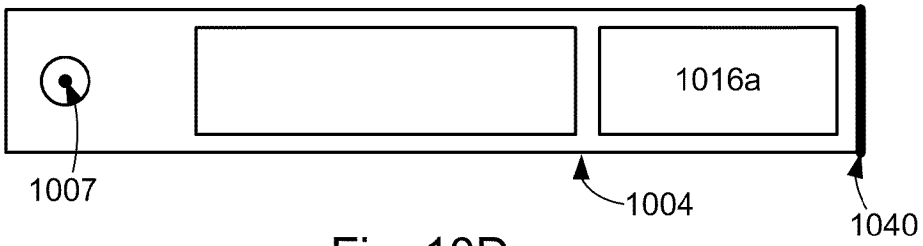

Fig. 10D

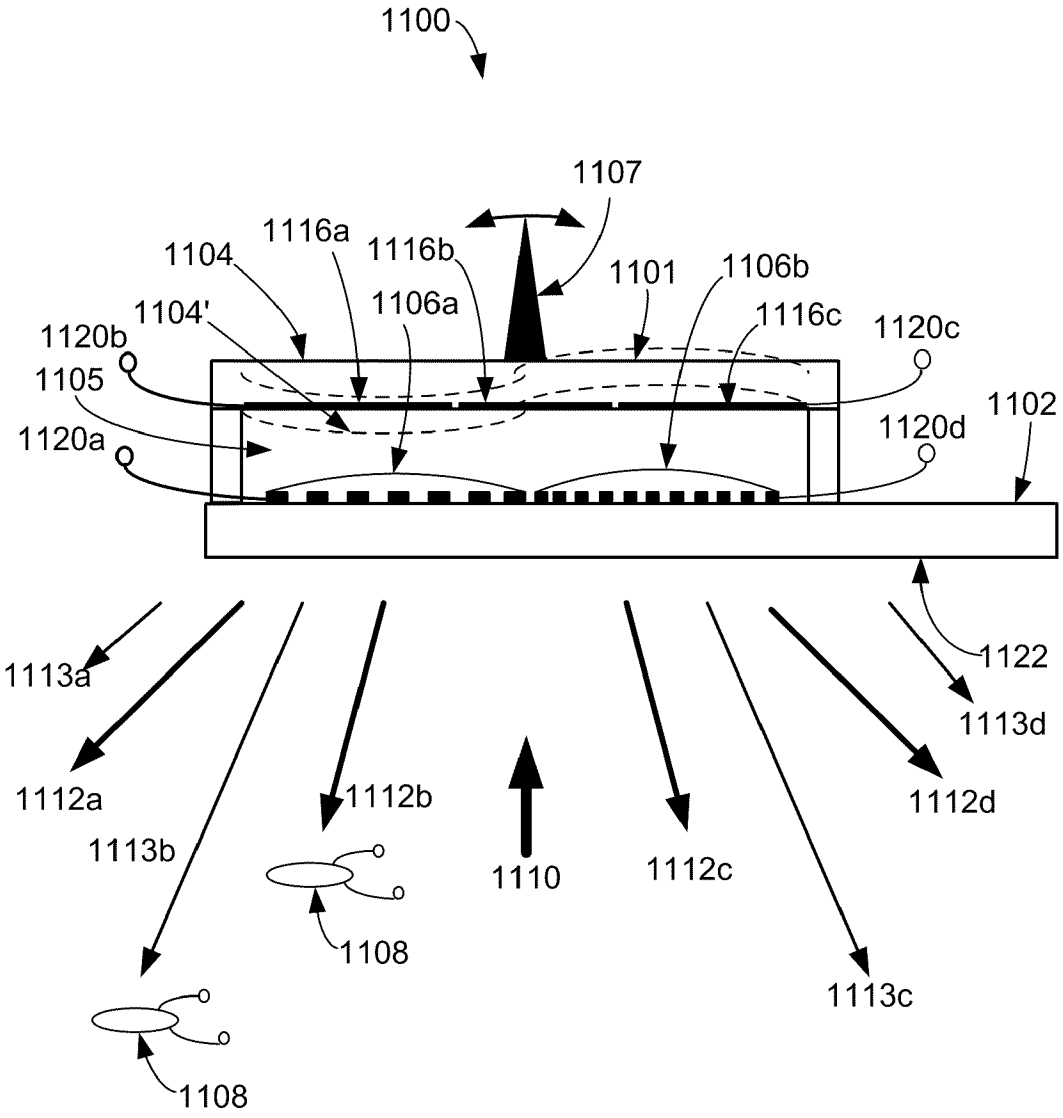
1100
1107
1116a
1104
1116b
1101
1106b
1104'
1106a
1116c
1120c
1120b
1105
1102
1120a
1120d
1122
1113a
1113d
1112a
1112b
1112d
1113b
1110
1112c
1108
1113c
1108

Fig. 11A

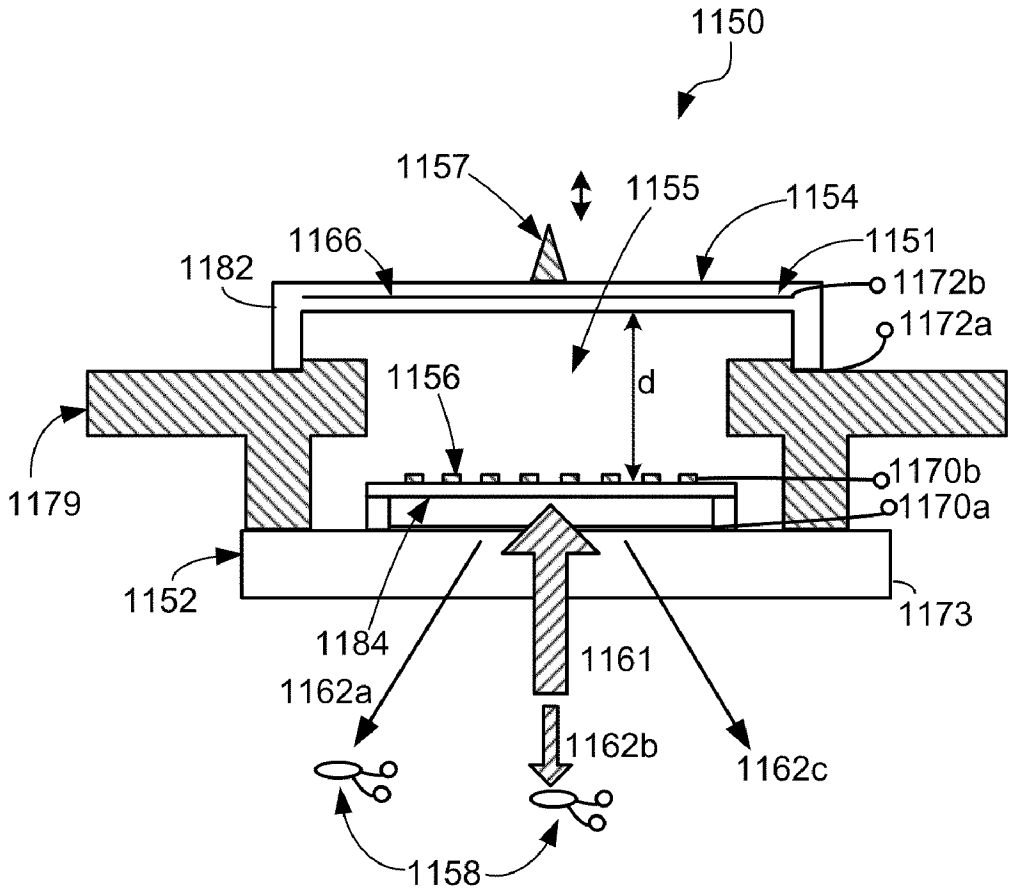

Fig. 11B

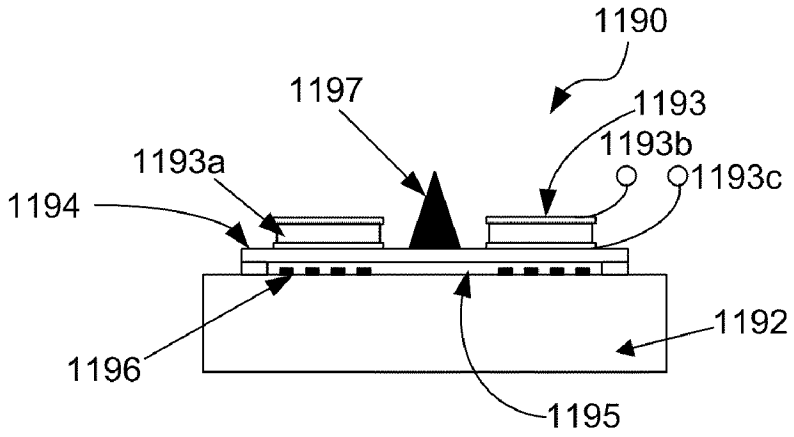

Fig. 11C

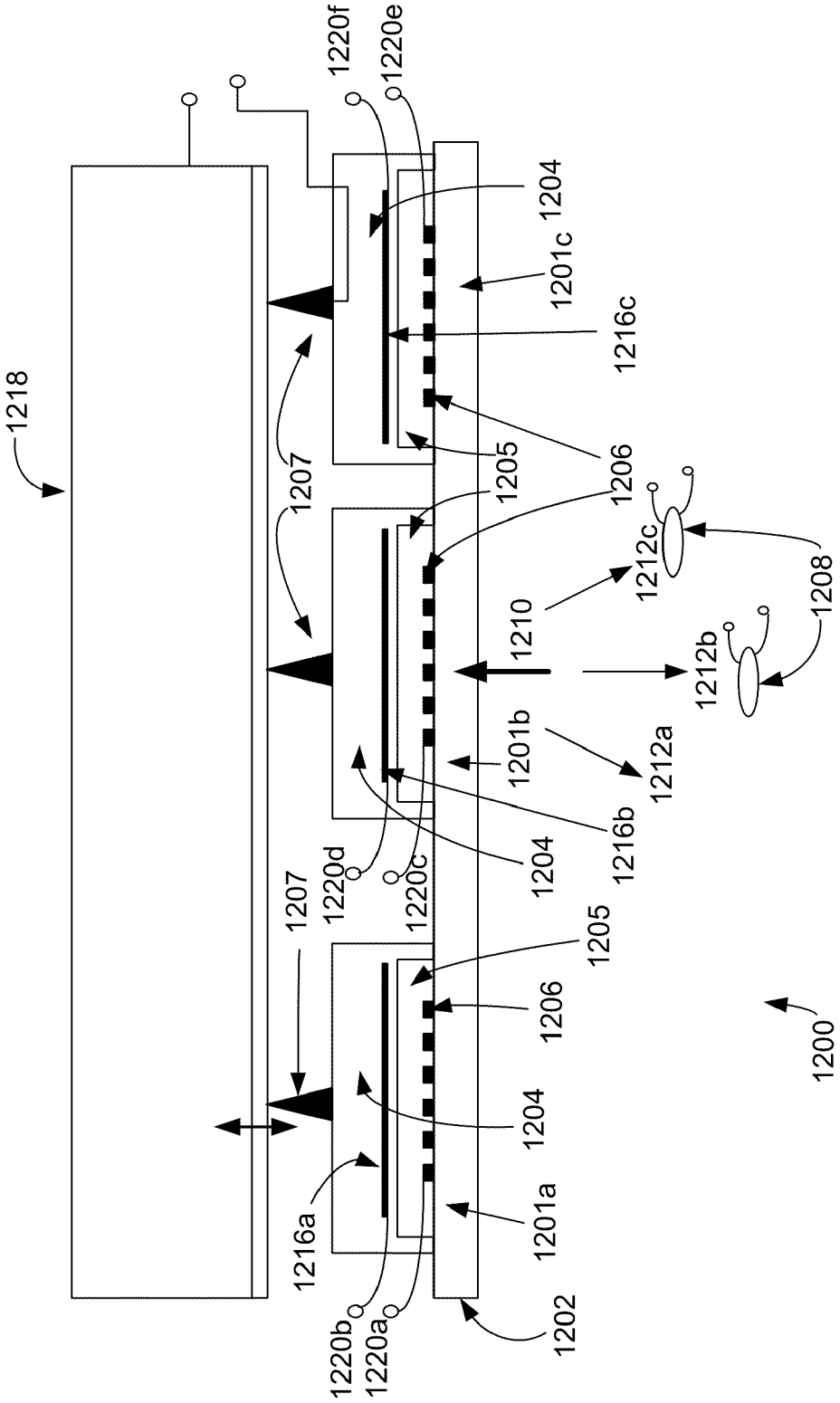
1218
1220f
1220e
1204
1201c
1216c
1207
1205
1206
1212c
1208
1210
1212b
1201b
1212a
1216b
1220d
1220c
1204
1207
1205
1206
1200
1204
1216a
1201a
1220b
1220a
1202

Fig. 12

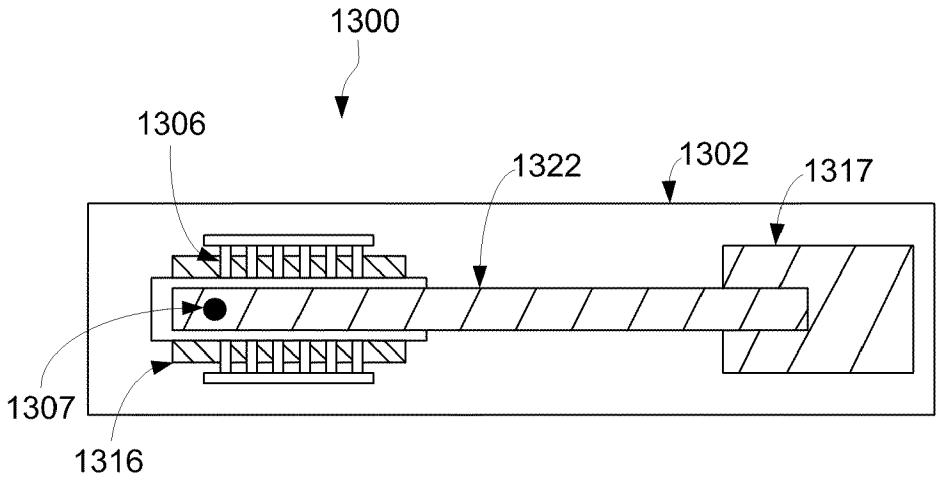

Fig. 13A

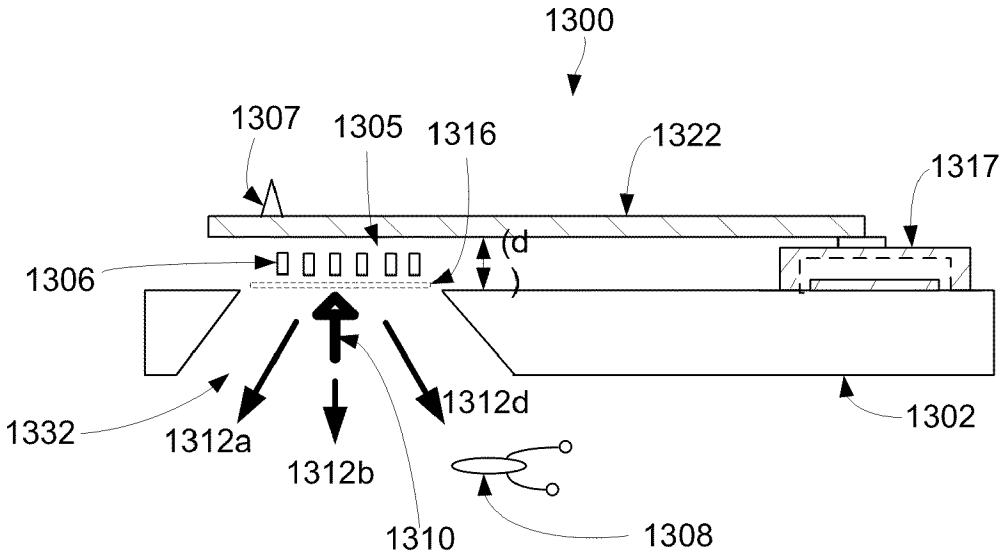

Fig. 13B

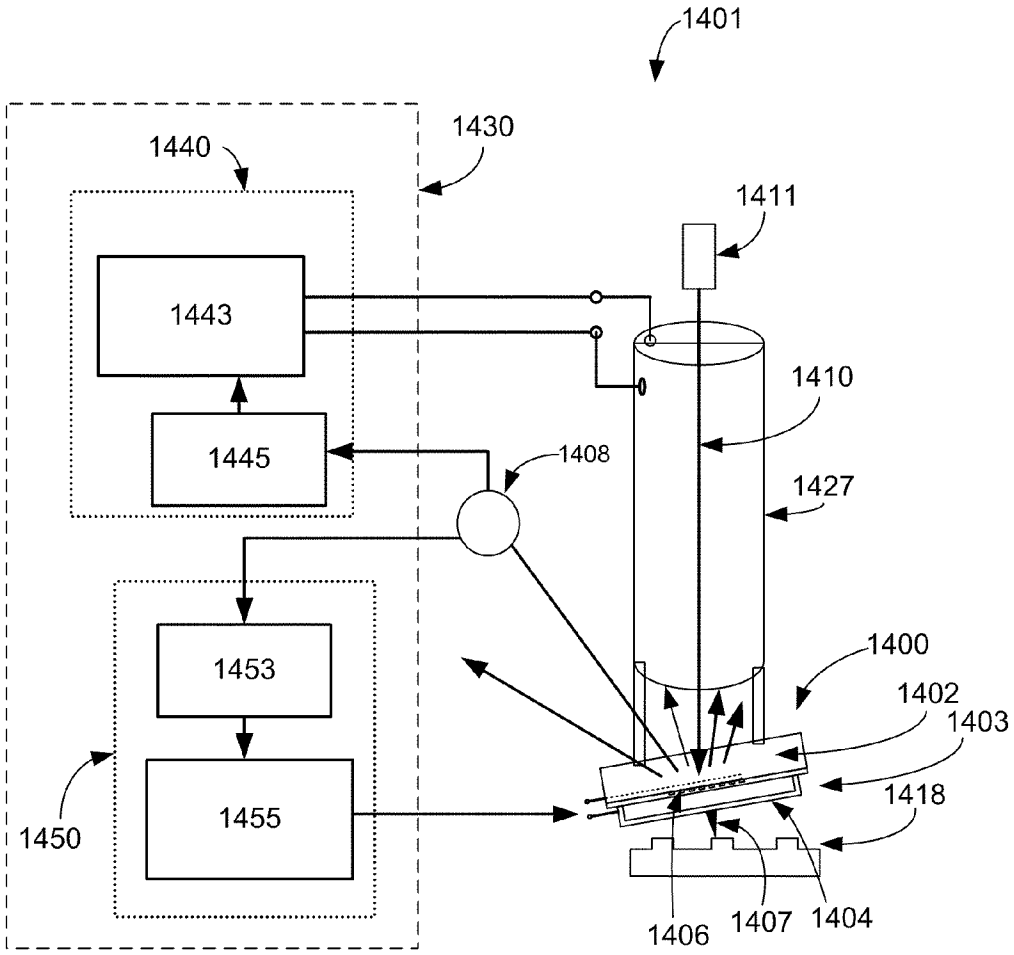
1401
1430
1440
1411
1443
1410
1445
1408
1427
1453
1400
1402
1403
1455
1418
1450
1406
1407
1404

Fig. 14

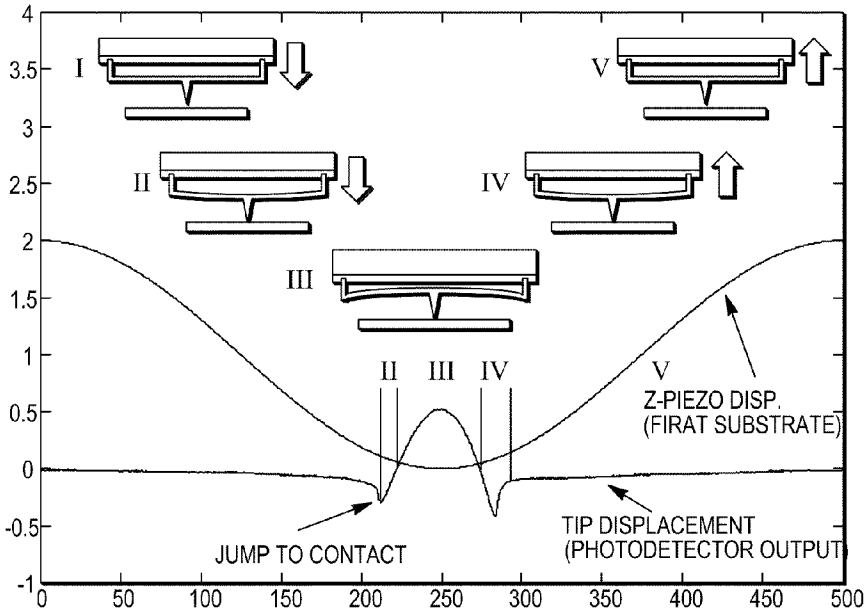

FIG. 15A

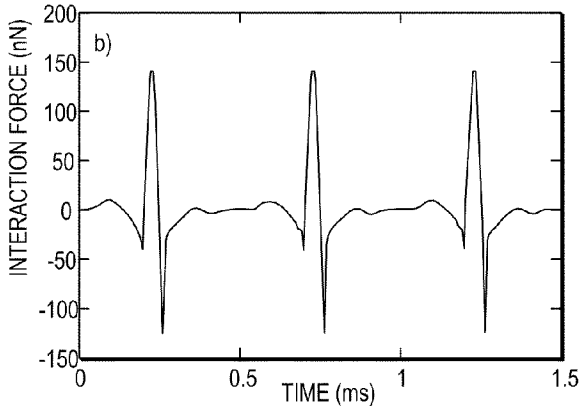

FIG. 15B

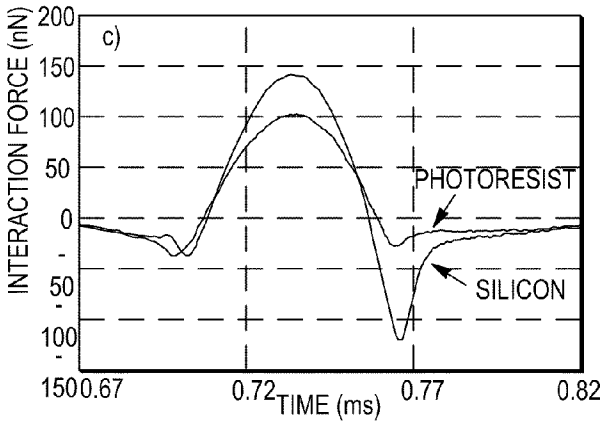

FIG. 15C

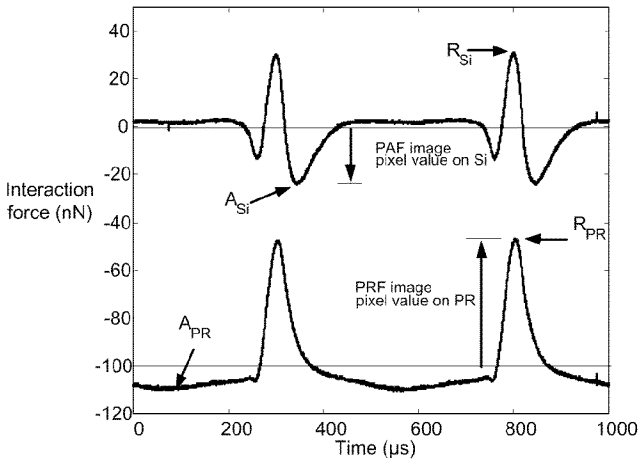

Fig. 16A

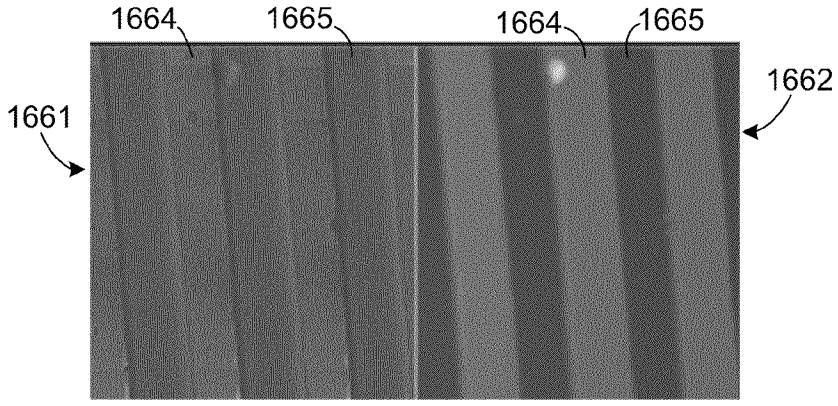

Fig. 16B

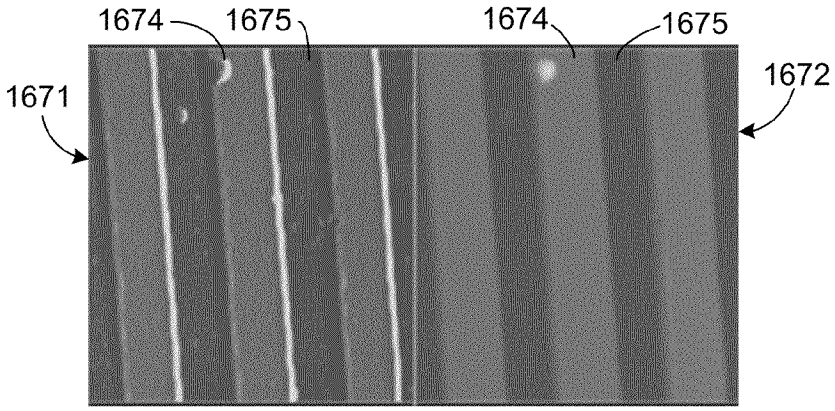

Fig. 16C

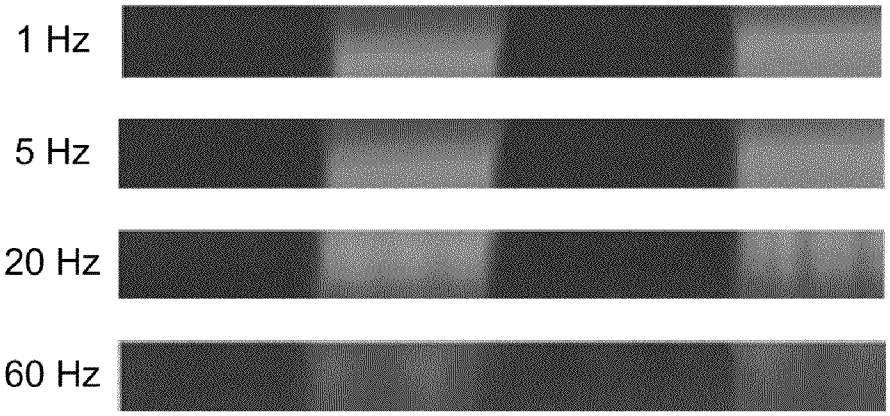

Fig. 17A

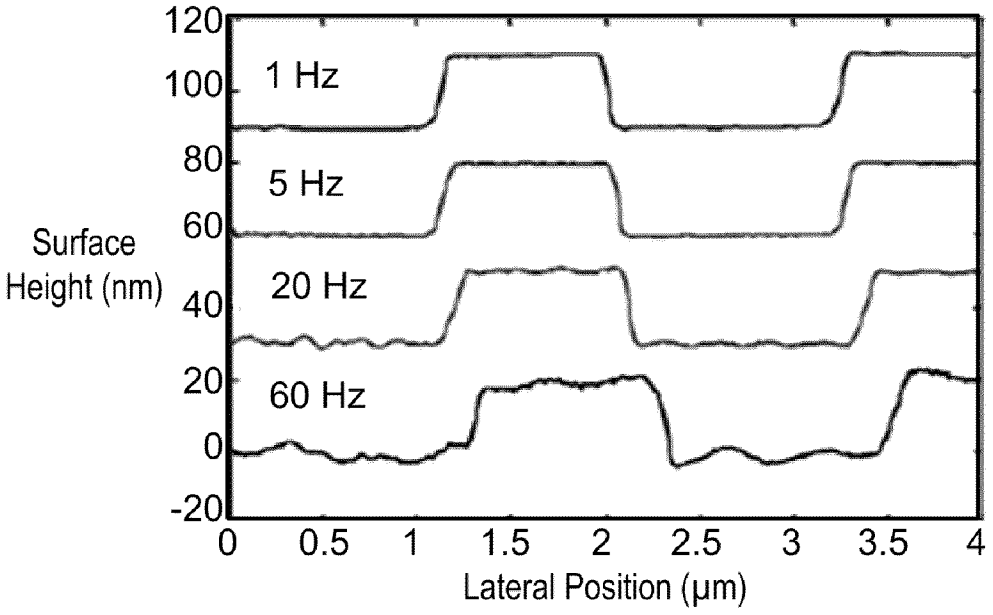

Fig. 17B

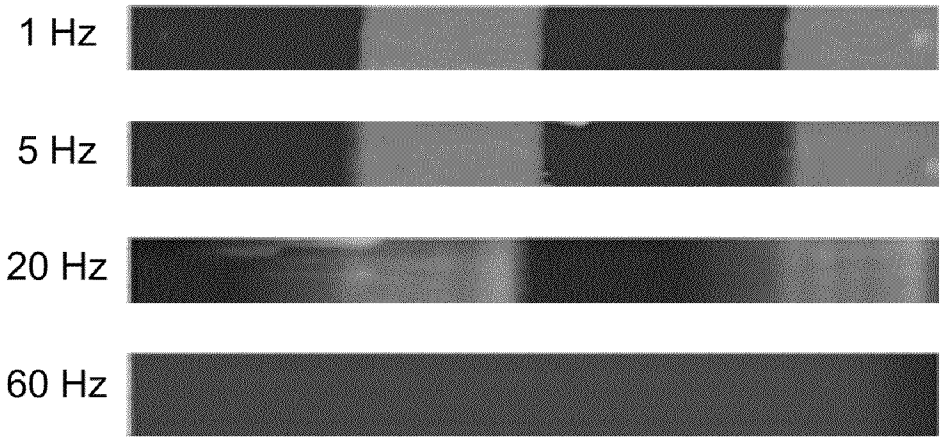

Fig. 17C

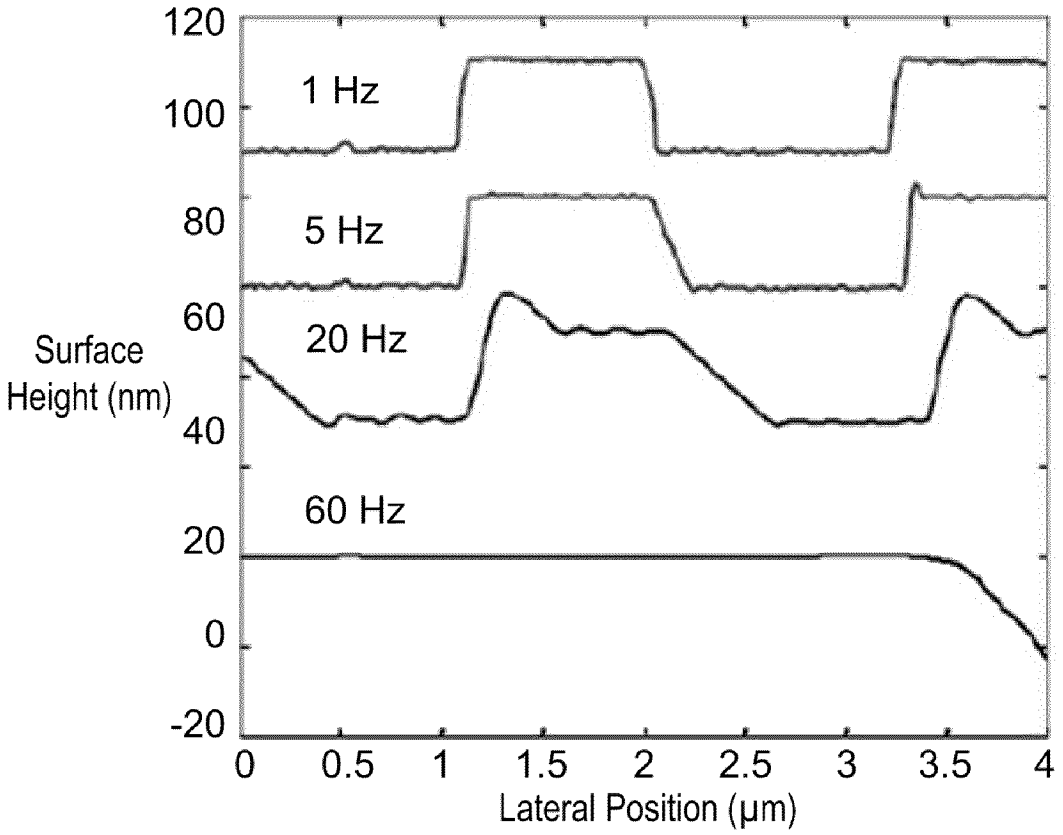

Fig. 17D

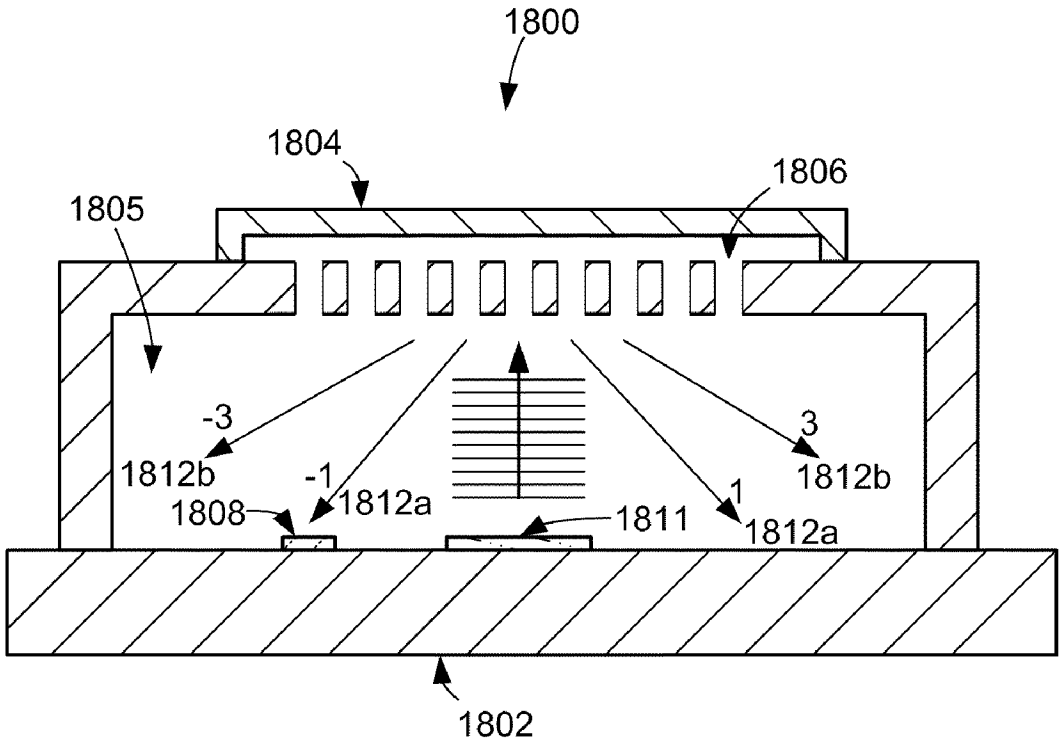
1800
1804
1806
1805
-3
1812b
-1
1812a
1808
1811
1
1812a
3
1812b
1802

Fig. 18

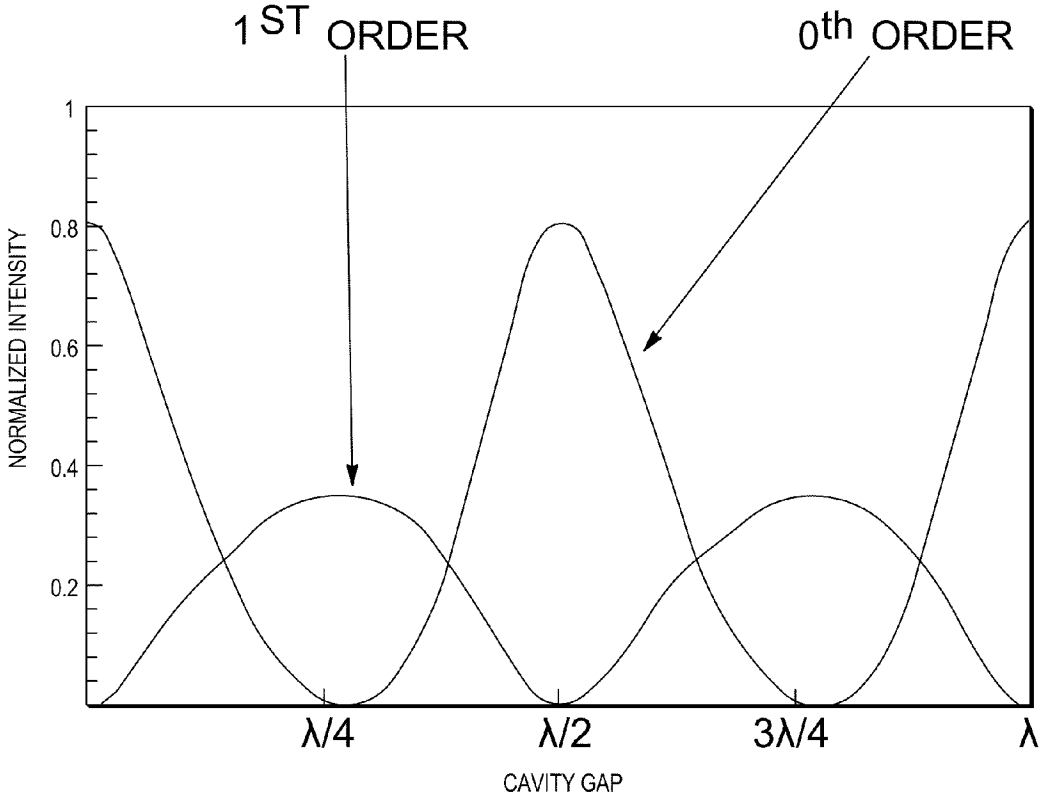
1 ST ORDER
0th ORDER
1
0.8
0.6
0.4
0.2
NORMALIZED INTENSITY
λ/4
λ/2
3λ/4
λ
CAVITY GAP

FIG. 19

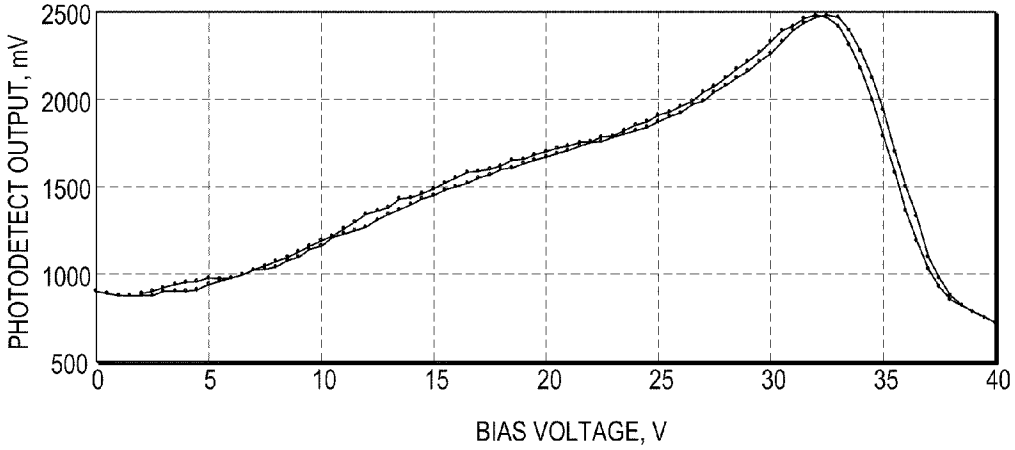

FIG. 20A

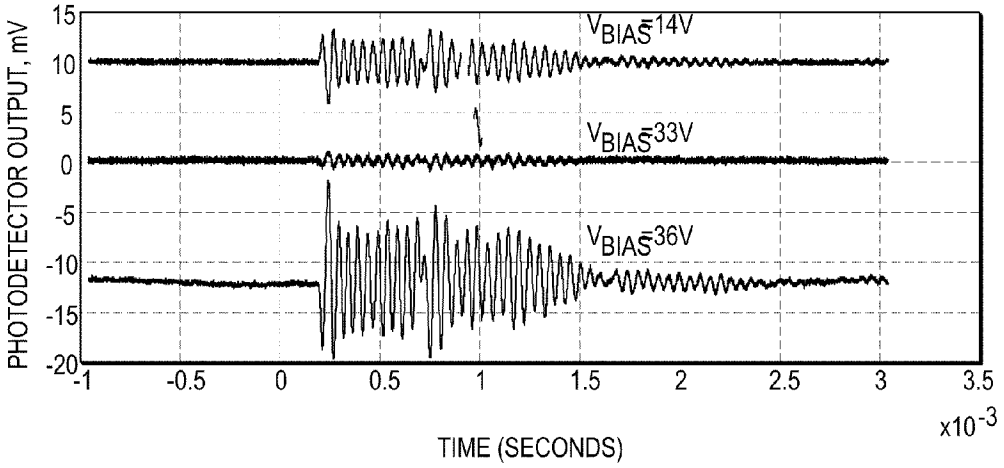

FIG. 20B

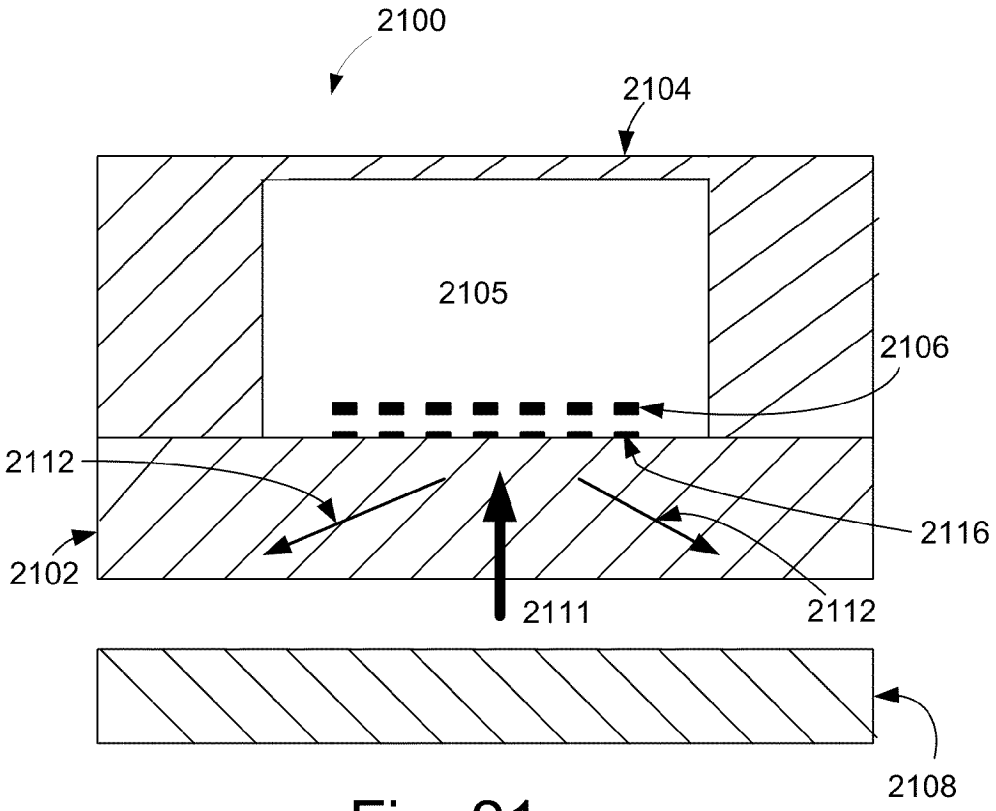
2100
2104
2105
2106
2112
2116
2102
2111
2112
2108

Fig. 21

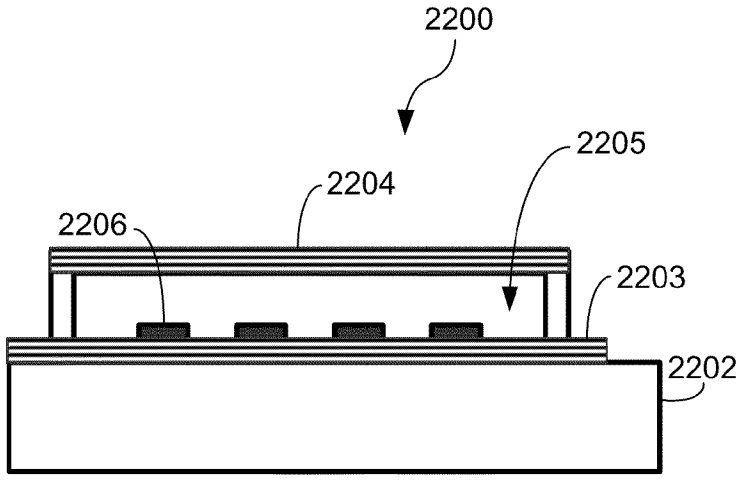
2200
2205
2204
2206
2203
2202

Fig. 22

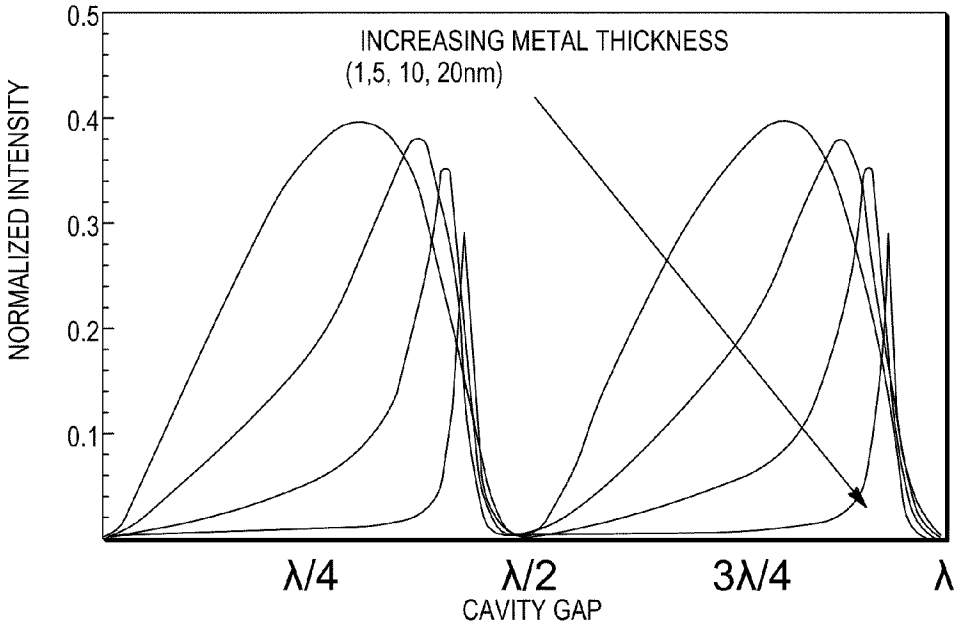

FIG. 23A

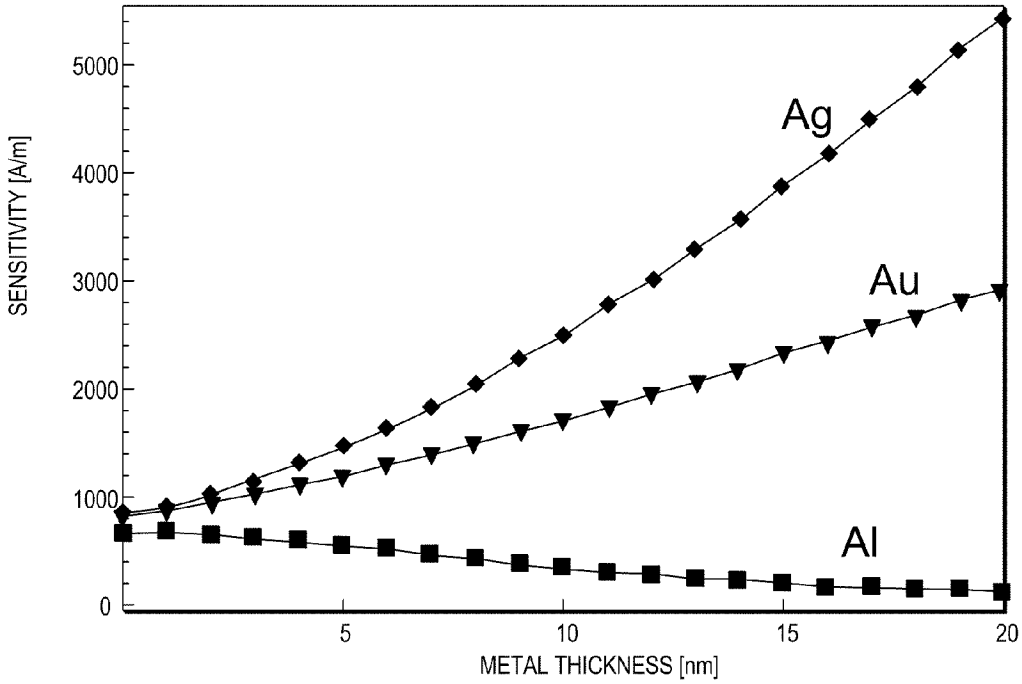

FIG. 23B

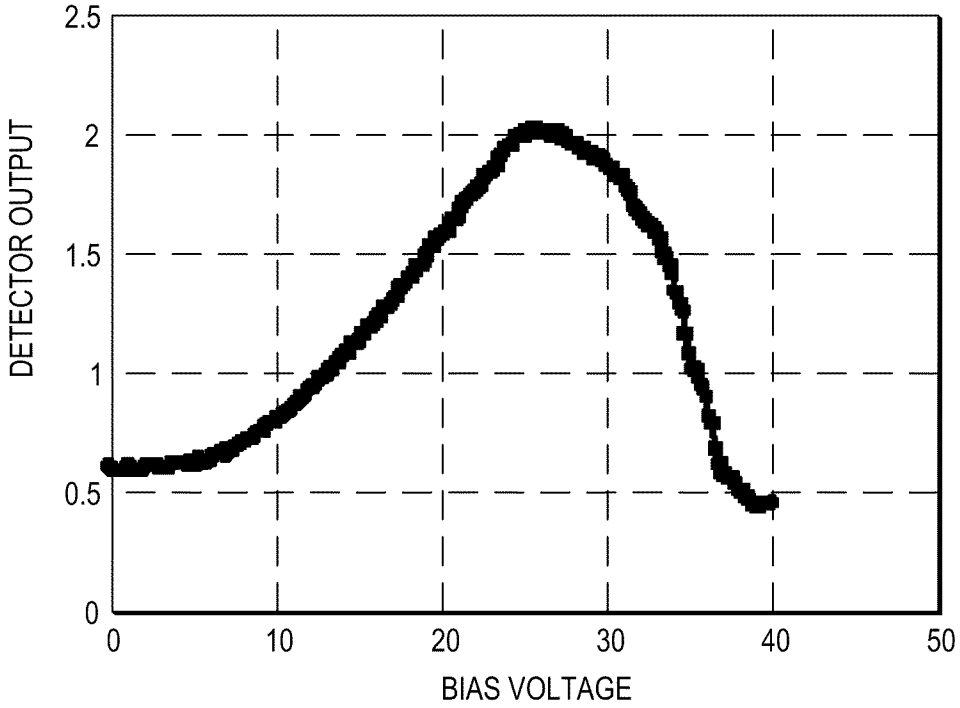

FIG. 24A

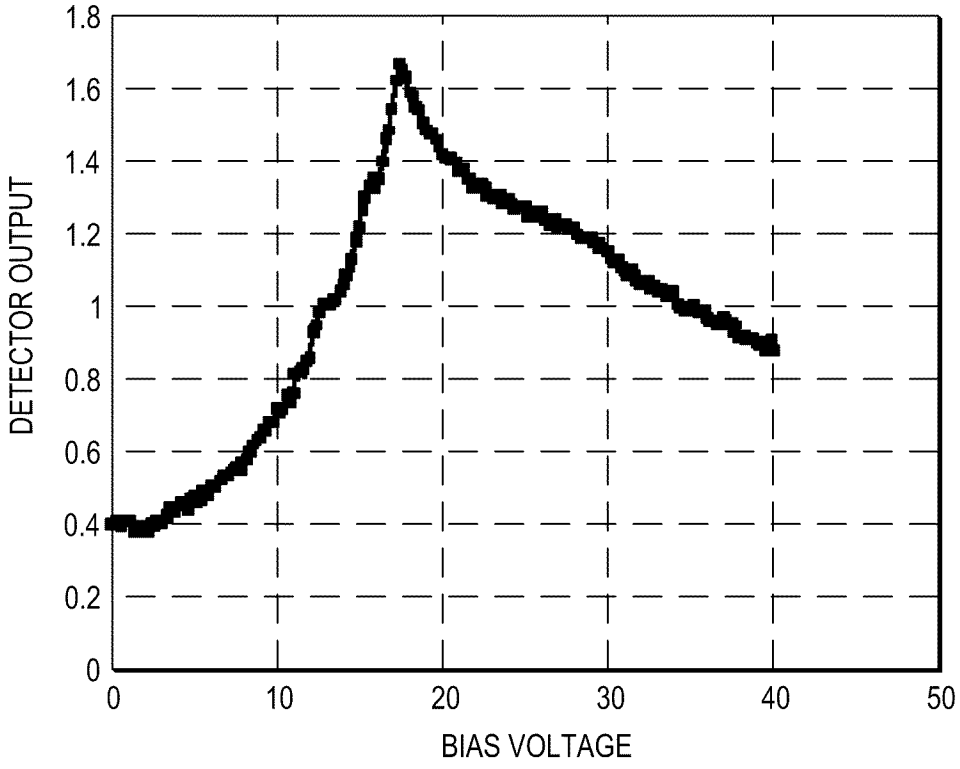

FIG. 24B

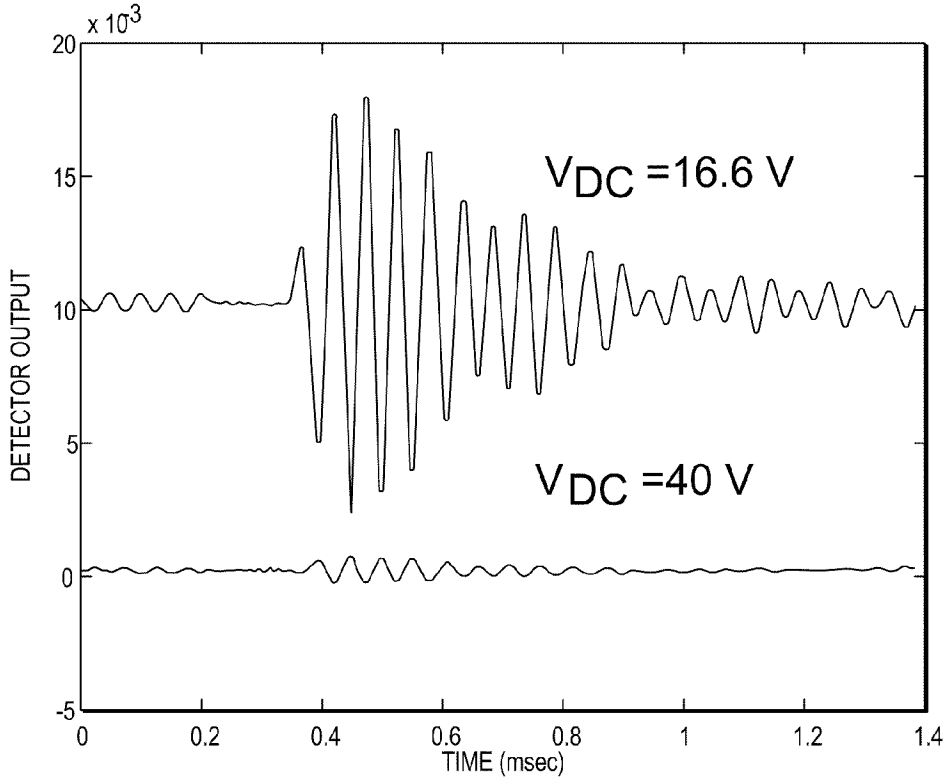

FIG. 24C

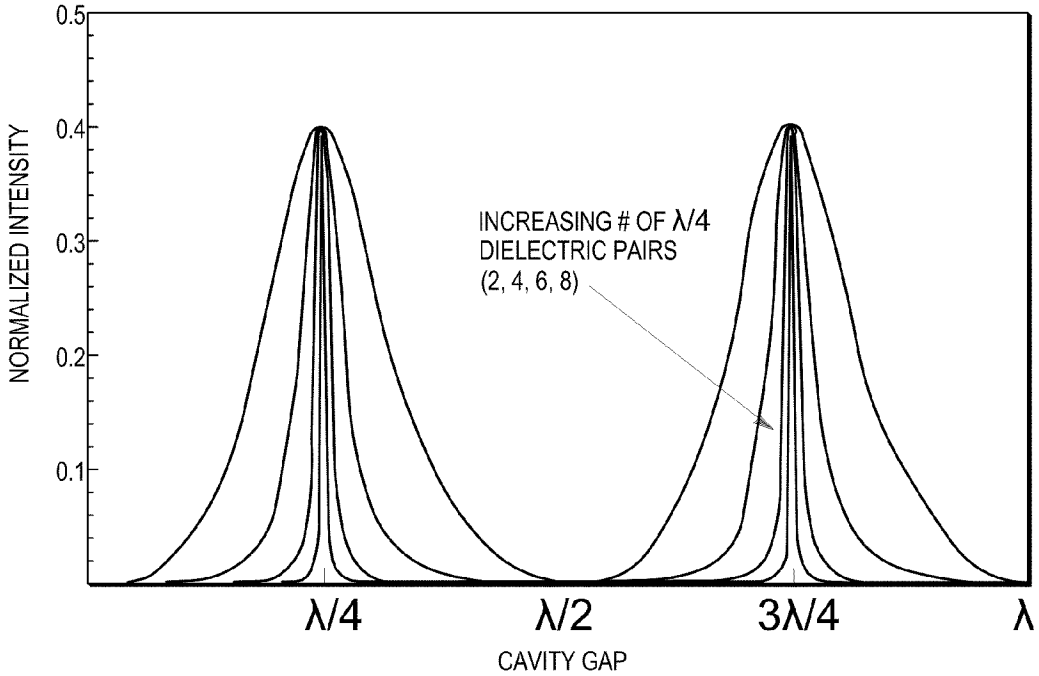

FIG. 25

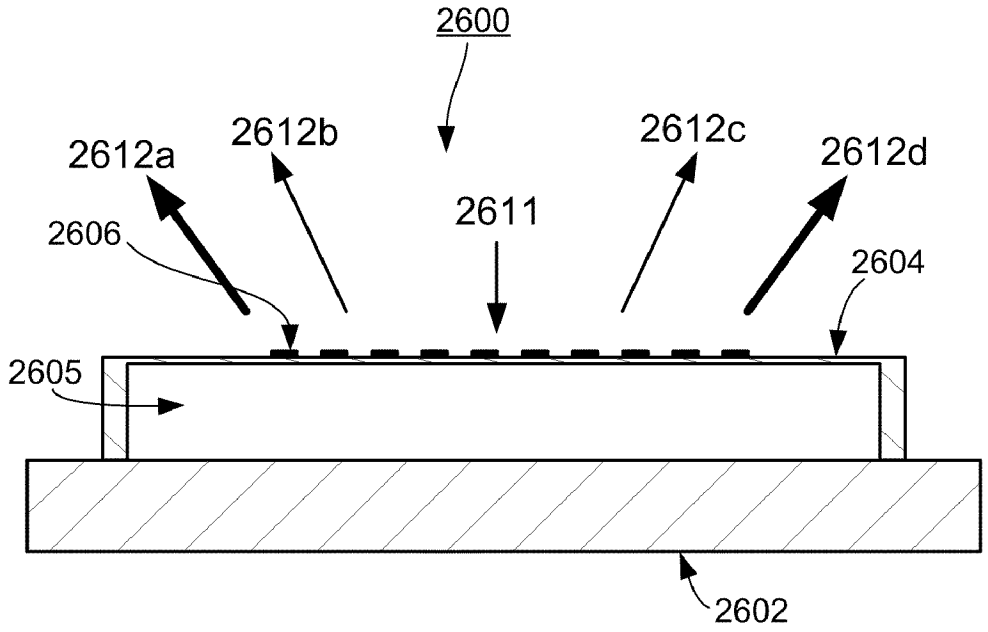
2600
2612a
2612b
2612c
2612d
2611
2606
2604
2605
2602

Fig. 26

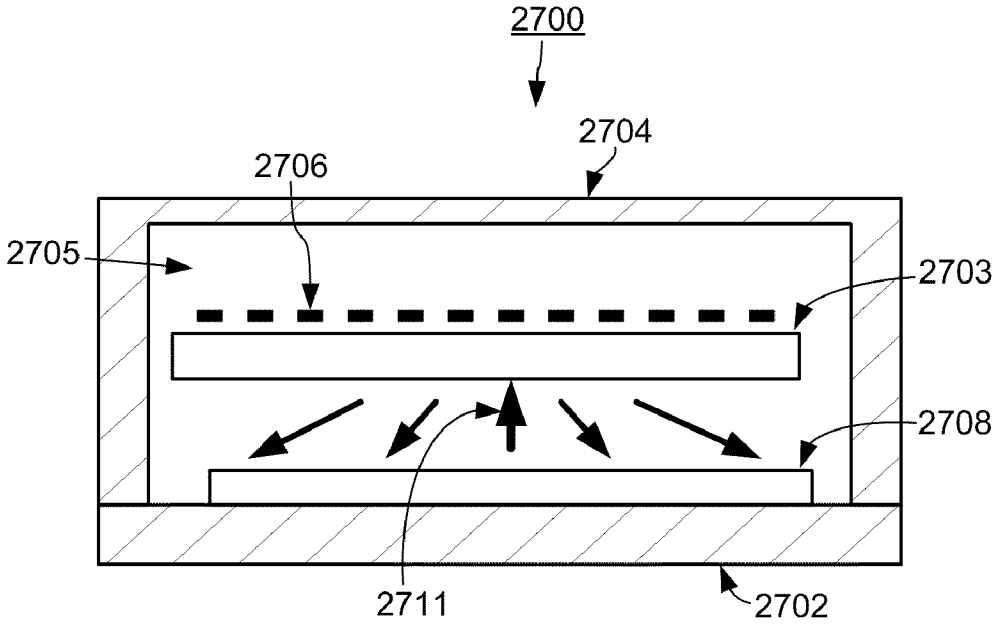
2700
2704
2706
2705
2703
2708
2711
2702

Fig. 27

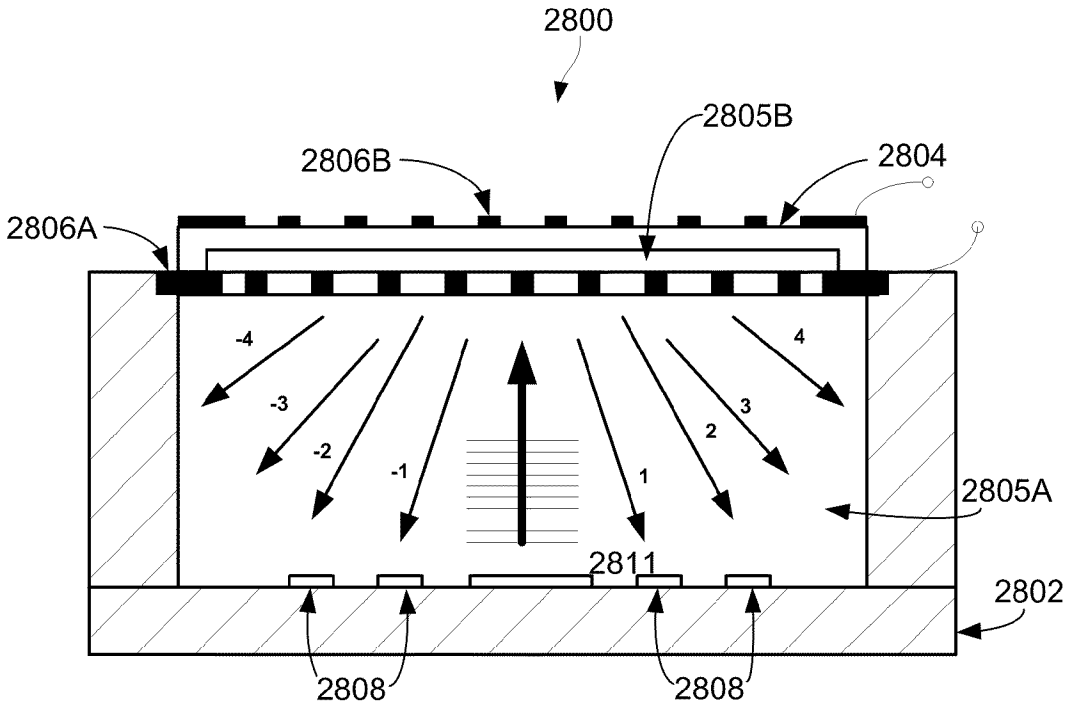

Fig. 28A

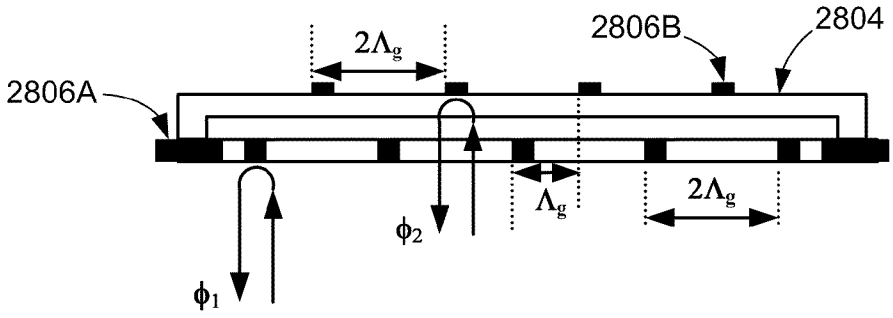

Fig. 28B

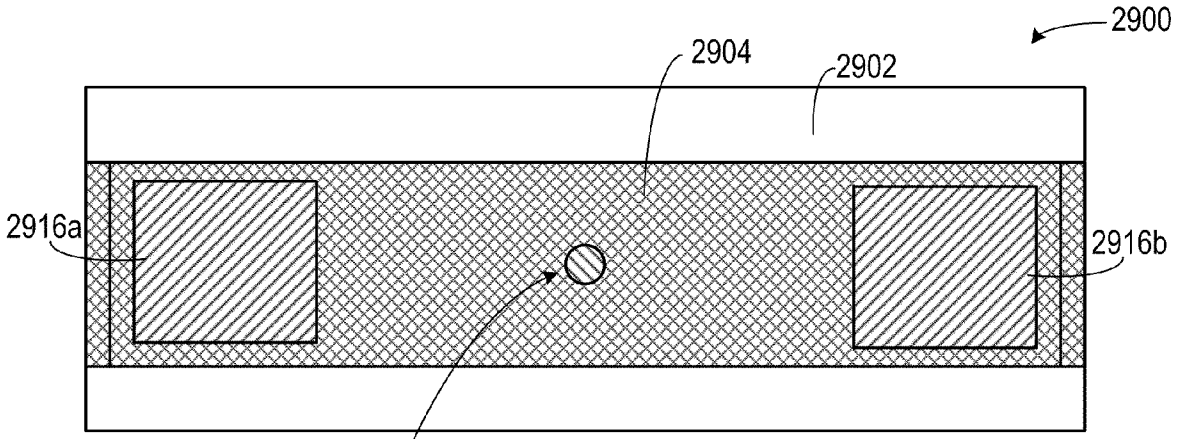

FIG. 29A

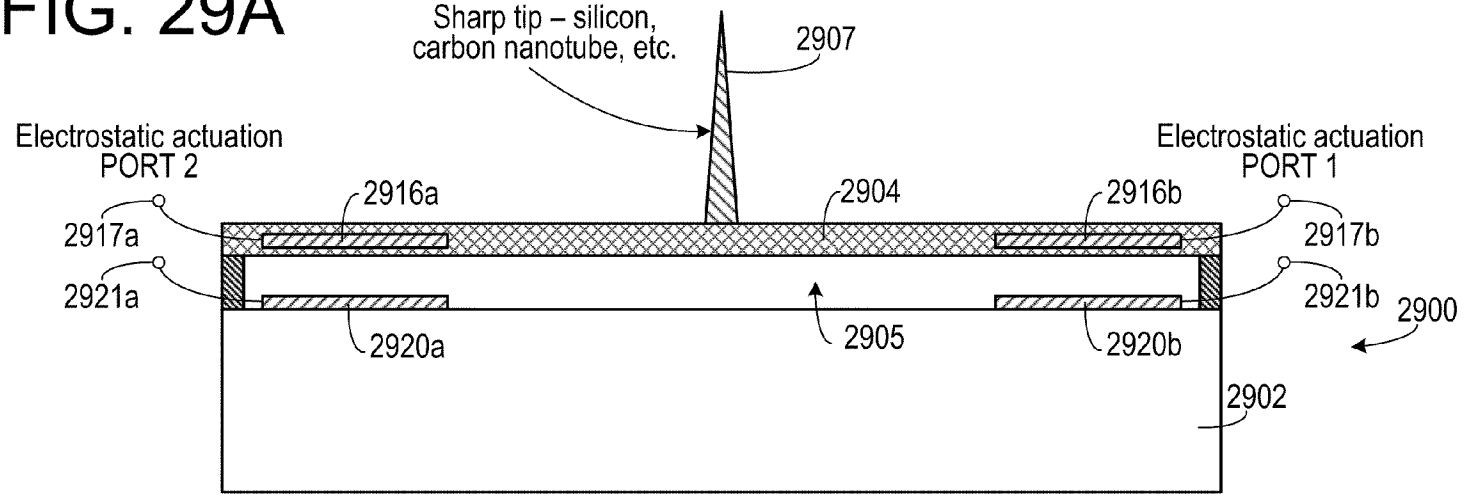

FIG. 29B

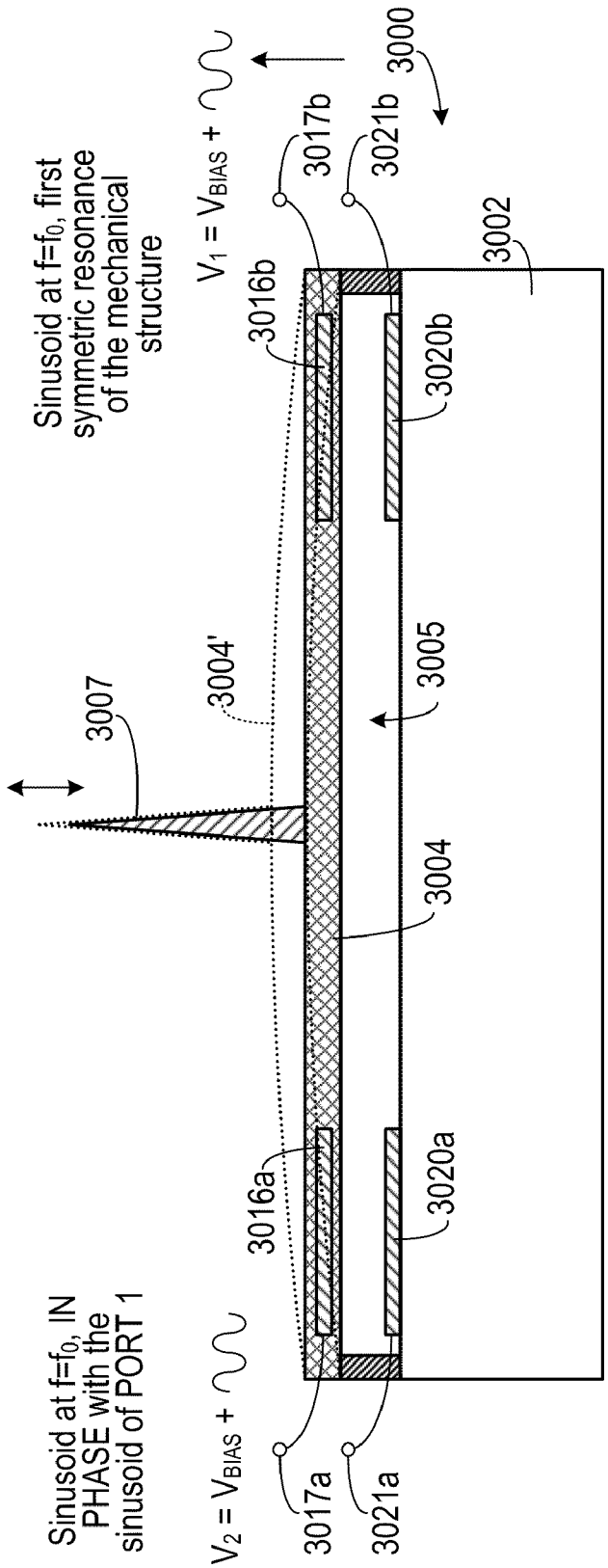
Sinusoid at f=f0, first symmetric resonance of the mechanical structure
V1 = VBIAS +
3000
3017b
3021b
3002
3016b
3020b
3007
3004'
3005
3004
3016a
3020a
Sinusoid at f=f0, IN PHASE with the sinusoid of PORT 1
V2 = VBIAS +
3017a
3021a

FIG. 30

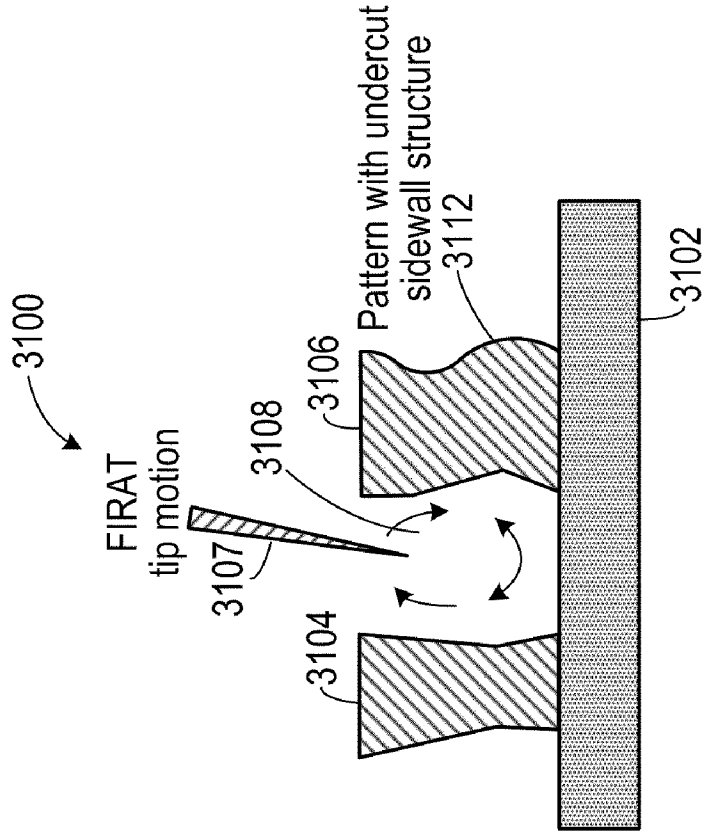

FIG. 31B

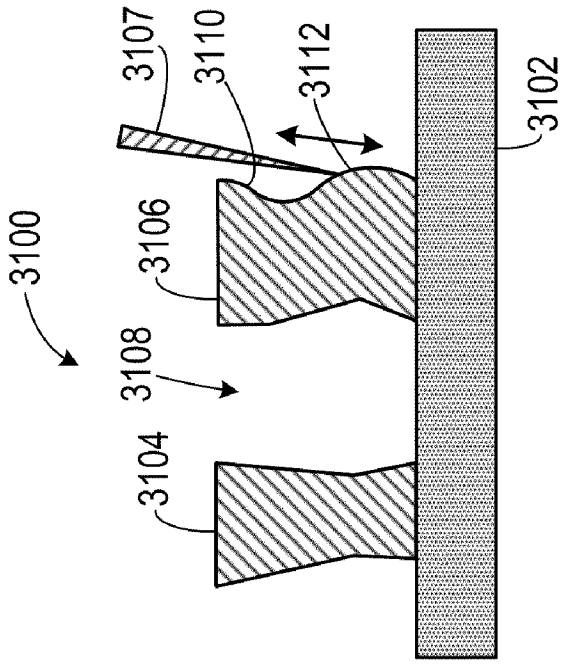

FIG. 31A

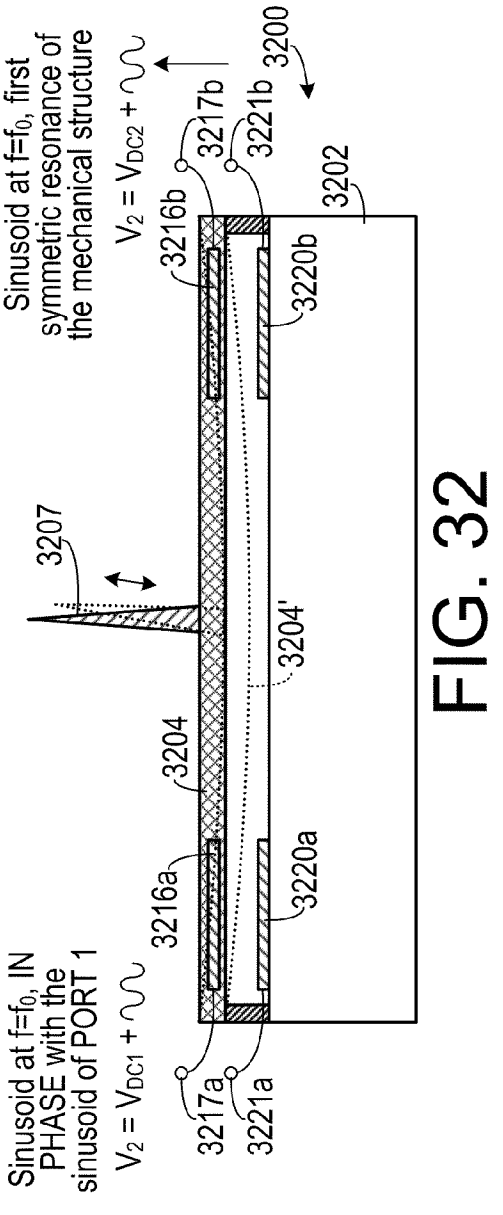
Sinusoid at f=f0, first symmetric resonance of the mechanical structure
V2 = VDC2 + ∿
3200
3217b
3221b
3216b
3202
3220b
3207
3204'
3204
3216a
3220a
Sinusoid at f=f0, IN PHASE with the sinusoid of PORT 1
V2 = VDC1 + ∿
3217a
3221a

FIG. 32

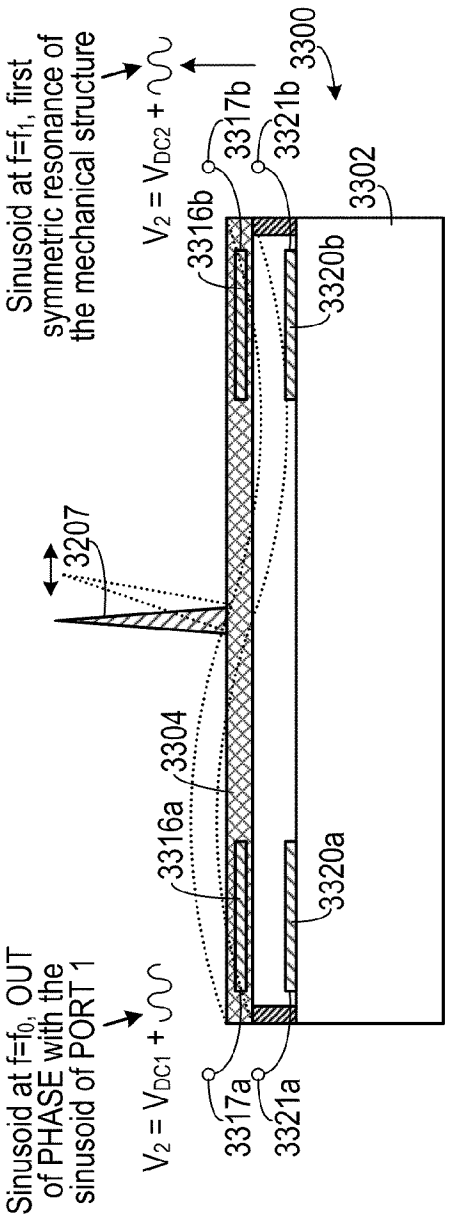
Sinusoid at f=f1, first symmetric resonance of the mechanical structure
V2 = VDC2 + ∿
3300
3317b
3321b
3316b
3302
3320b
3207
3304
3316a
3320a
Sinusoid at f=f0, OUT of PHASE with the sinusoid of PORT 1
V2 = VDC1 + ∿
3317a
3321a

FIG. 33

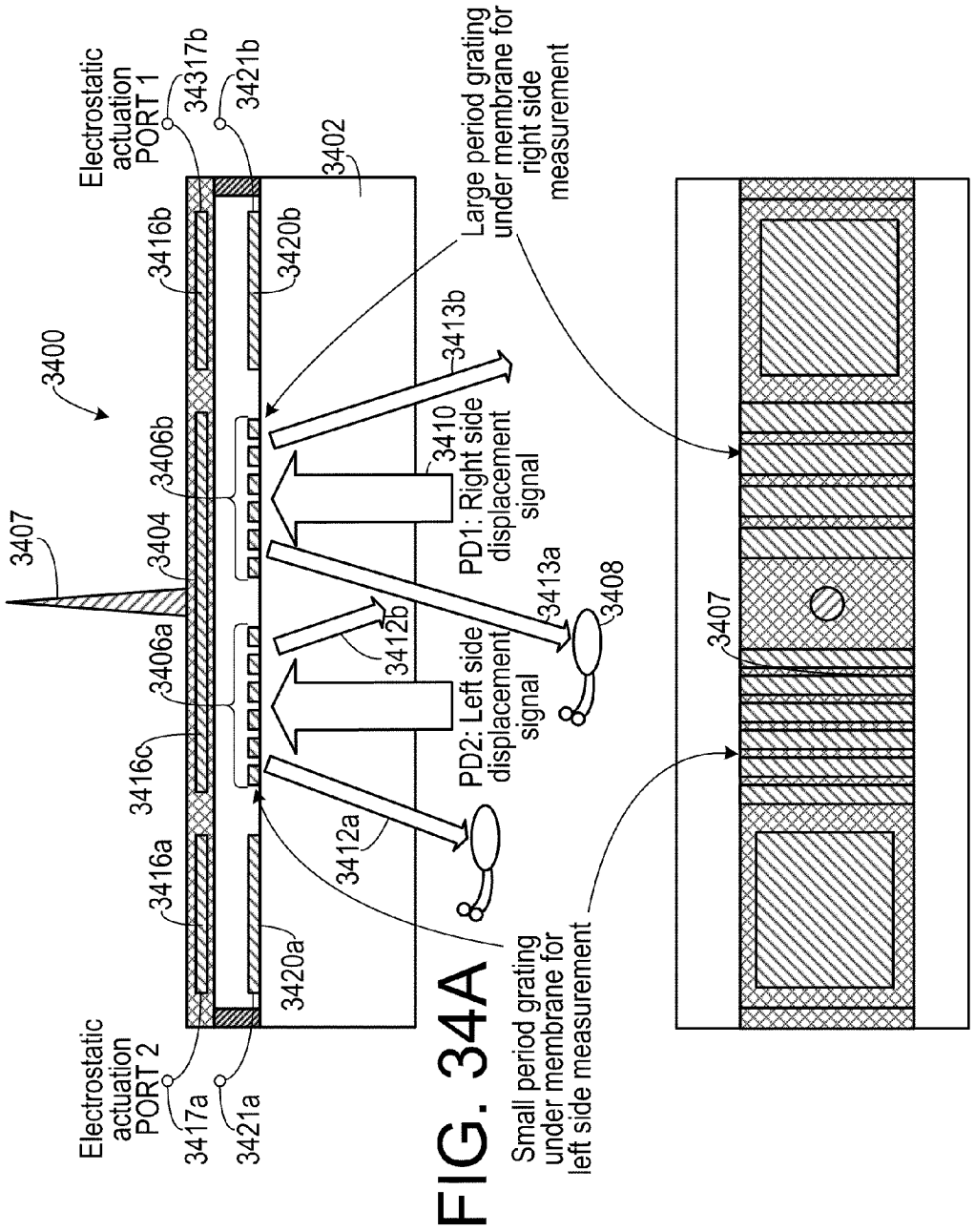

FIG. 34A

FIG. 34B

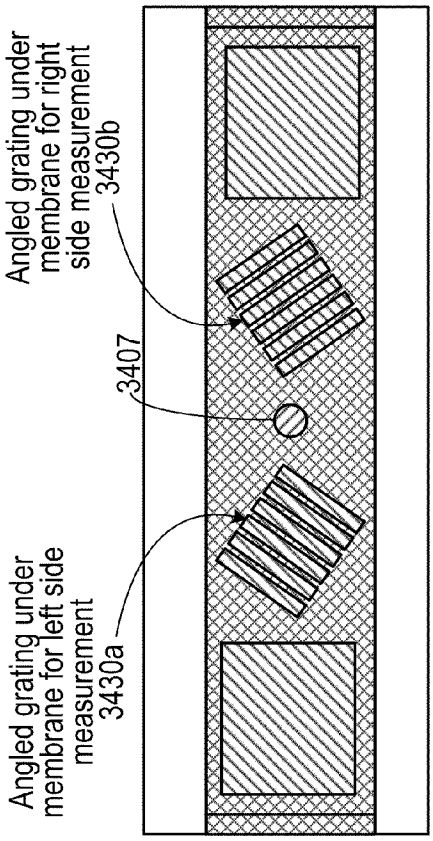

FIG. 34C

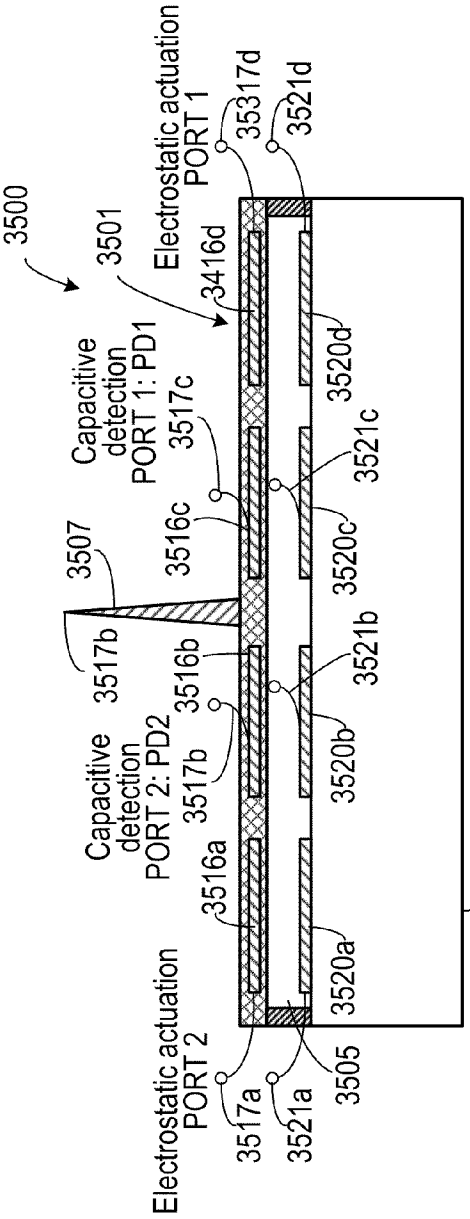

FIG. 35

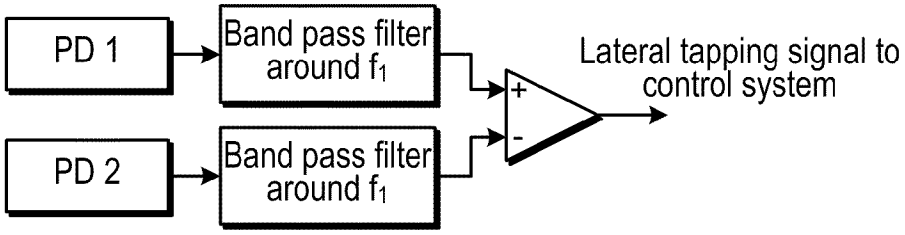

FIG. 36A

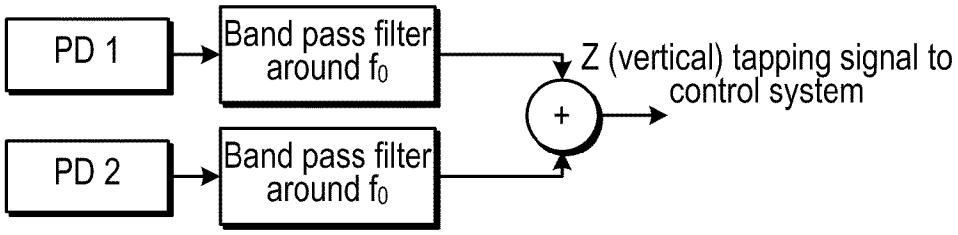

FIG. 36B

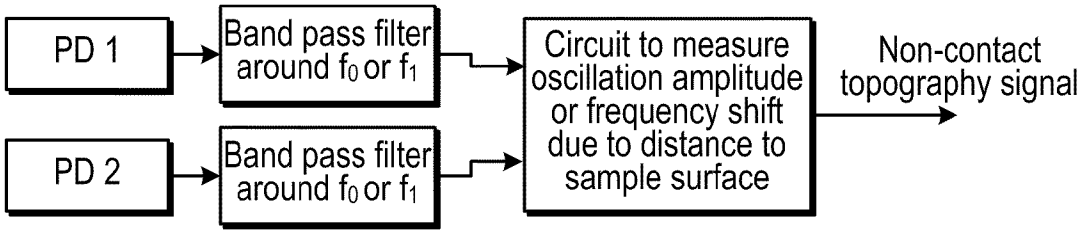

FIG. 37

THREE-DIMENSIONAL NANOSCALE METROLOGY USING FIRAT PROBE

CROSS-REFERENCE TO RELATED APPLICATION(S)

This application claims the benefit of U.S. Provisional Patent Application Ser. No. 60/730,217, filed Oct. 25, 2005, the entirety of which is hereby incorporated herein by reference.

This application is divisional of, and claims the benefit of U.S. patent application Ser. No. 12/136,399, filed Jun. 10, 2008, which is a continuation of, and claims the benefit of, U.S. patent application Ser. No. 11/552,274, filed Oct. 24, 2006, which issued as U.S. Pat. No. 7,395,698 on Jul. 8, 2008, the entirety of each of which is hereby incorporated herein by reference.

BACKGROUND OF THE INVENTION

1. Field of the Invention

The subject matter of this application relates to probe microscopy. More particularly, the subject matter of this application relates to methods and devices for probe and force microscopes with sensors having improved sensitivity.

2. Description of the Prior Art

Conventional atomic force microscope (AFM) and its variations have been used to probe a wide range of physical and biological processes, including mechanical properties of single molecules, electric and magnetic fields of single atoms and electrons. Moreover, cantilever based structures inspired by the AFM have been a significant driver for nanotechnology resulting in chemical sensor arrays, various forms of lithography tools with high resolution, and terabit level data storage systems. Despite the current rate of success, the AFM needs to be improved in terms of speed, sensitivity, and an ability to generate quantitative data on the chemical and mechanical properties of the sample. For example, when measuring molecular dynamics at room temperature, the molecular forces need to be measured in a time scale that is less than the time of the thermal fluctuations to break the bonds. This requires a high speed system with sub-nanoNewton and sub-nanometer sensitivity.

Current cantilever-based structures for AFM probes and their respective actuation methodologies lack speed and sensitivity and have hindered progress in the aforementioned areas. Imaging systems based on small cantilevers have been developed to increase the speed of AFMs, but this approach has not yet found wide use due to demanding constraints on optical detection and bulky actuators. Several methods have been developed for quantitative elasticity measurements, but the trade-off between force resolution, measurement speed, and cantilever stiffness has been problematic especially for samples with high compliance and high adhesion. Cantilever deflection signals measured during tapping mode imaging have been inverted to obtain elasticity information with smaller impact forces, but complicated dynamic response of the cantilever increases the noise level and prevents calculation of the interaction forces. Arrays of AFM cantilevers with integrated piezoelectric actuators have been developed for parallel lithography, but complex fabrication methods have limited their use.

Most of the scanning probe microscopy techniques, including tapping mode imaging and force spectroscopy, rely on measurement of the deflection of a microcantilever with a sharp tip. Therefore, the resulting force data depend on the dynamic properties of the cantilever, which shapes the frequency response. This can be quite limiting, as mechanical structures like cantilevers are resonant vibrating structures and they provide information mostly only around these resonances. For example, in tapping mode imaging it is nearly impossible to recover all the information about the tip-sample interaction force, since the transient force applied at each tap cannot be observed as a clean time signal.

Moreover, conventional methods of imaging with scanning probes can be time consuming while others are often destructive because they require static tip-sample contact. Dynamic operation of AFM, such as the tapping-mode, greatly reduces shear forces during the scan. However, the only free variable in this mode, the phase, is related to the energy dissipation and it is difficult to interpret. Further, the inverse problem of gathering the time-domain interaction forces from the tapping signal is not easily solvable due to complex dynamics of the AFM cantilever. Harmonic imaging is useful to analyze the sample elastic properties, but this method recovers only a small part of the tip-sample interaction force frequency spectrum.

Thus, there is a need to overcome these and other problems of the prior art associated with probe microscopy.

SUMMARY OF THE INVENTION

In accordance with an embodiment of the invention, there is a force sensor for a probe based instrument. The force sensor can comprise a detection surface and a flexible mechanical structure disposed a first distance above the detection surface so as to form a gap between the flexible mechanical structure and the detection surface, wherein the flexible mechanical structure is configured to deflect upon exposure to an external force, thereby changing the first distance.

According to another embodiment of the invention, there is a force sensor structure. The force sensor structure can comprise a cantilever and a force sensor positioned on a free end of the cantilever. The force sensor can comprise a gap formed by a detection surface at the free end of the cantilever and at least one sidewall for positioning a flexible mechanical structure a first distance from the detection surface.

According to another embodiment of the invention, there is a force sensor unit. The force sensor unit can comprise a force sensor and a detector. The force sensor can comprise a detection surface and a flexible mechanical structure positioned a distance above the detection surface to form a gap, the flexible mechanical structure configured to deflect upon exposure to an external stimuli. The detector can be configured to detect deflection of the flexible mechanical structure.

According to another embodiment of the invention, there is another force sensor. The force sensor can comprise a substrate comprising an optical port having an optical axis, a reflective diffraction grating positioned along the optical axis and positioned a distance from the optical port, and a cantilever positioned a distance from the substrate. The cantilever can comprise a fixed end in contact with the substrate, a free end positioned a distance from the diffraction grating, wherein a portion of the free end is positioned along the optical axis, and a probe tip in contact with the free end of the cantilever.

It can be understood that both the foregoing general description and the following detailed description are exemplary and explanatory only and are not restrictive of the invention, as claimed.

The accompanying drawings, which are incorporated in and constitute a part of this specification, illustrate several

embodiments of the invention and together with the description, serve to explain the principles of the invention.

BRIEF DESCRIPTION OF THE FIGURES OF THE DRAWINGS

FIG. **1**A shows a cross-sectional schematic diagram of an exemplary force sensor in accordance with the present teachings.

FIG. **1**B shows a scanning electron microscope (SEM) picture of an exemplary force sensor in accordance with the present teachings.

FIG. **1**C shows a photograph of a top down view of a force sensor in accordance with the present teachings.

FIG. **1**D shows a photograph of a bottom up view of a force sensor in accordance with the present teachings.

FIG. **1**E shows a cross-sectional schematic diagram of another exemplary force sensor in accordance with the present teachings.

FIG. **2**A shows a cross-sectional schematic diagram of another exemplary force sensor in accordance with the present teachings.

FIG. **2**B shows a scanning ion beam image of another exemplary force sensor in accordance with the present teachings.

FIG. **2**C shows photograph of a bottom up view of a force sensor in accordance with the present teachings.

FIG. **2**D shows a scanning electron microscope (SEM) picture of a force sensor tip in accordance with the present teachings.

FIG. **3**A shows a cross-sectional schematic diagram of another exemplary force sensor in accordance with the present teachings.

FIG. **3**B shows a cross-sectional schematic diagram of another exemplary force sensor in accordance with the present teachings.

FIG. **4**A shows a cross-sectional schematic diagram of another exemplary force sensor in accordance with the present teachings.

FIG. **4**B shows a bottom up view perspective of another exemplary force sensor in accordance with the present teachings.

FIG. **4**C shows a cross-sectional schematic diagram of an exemplary force sensor in accordance with the present teachings.

FIG. **5**A shows a cross-sectional schematic diagram of another exemplary force sensor in accordance with the present teachings.

FIG. **5**B is a graph plotting cantilever motion versus time for an exemplary force sensor in accordance with the present teachings.

FIG. **5**C is a graph plotting flexible mechanical structure grating-distance versus time for an exemplary force sensor in accordance with the present teachings.

FIG. **6** shows a partial cross-sectional schematic diagram of another exemplary force sensor in accordance with the present teachings.

FIG. **7** shows a partial cross-sectional schematic diagram of another exemplary force sensor in accordance with the present teachings.

FIG. **8**A shows a cross-sectional schematic diagram of an arrangement used to monitor sensitivity of an exemplary force sensor in accordance with the present teachings.

FIG. **8**B shows a graph plotting voltage output versus time for a tapping cantilever for a force sensor in accordance with the present teachings.

FIG. **8**C shows a close up of a portion of the graph shown in FIG. **8**B.

FIG. **9**A shows a schematic diagram of another exemplary force sensor in accordance with the present teachings.

FIG. **9**B shows a graph of interaction force versus time for an exemplary force sensor in accordance with the present teachings.

FIGS. **9**C-**9**F show graphs of a flexible mechanical structure displacement versus time for an exemplary force sensor in accordance with the present teachings.

FIGS. **9**G-**9**H show graphs of photo-detector output versus time for an exemplary force sensor in accordance with the present teachings.

FIG. **10**A shows a cross-sectional schematic diagram of another exemplary force sensor in accordance with the present teachings.

FIG. **10**B shows a cross-sectional schematic diagram of another exemplary force sensor in accordance with the present teachings.

FIG. **10**C shows a cross-sectional schematic diagram of another exemplary force sensor in accordance with the present teachings.

FIG. **10**D shows a cross-sectional schematic diagram of another exemplary force sensor in accordance with the present teachings.

FIG. **11**A shows a schematic diagram of another exemplary force sensor in accordance with the present teachings.

FIG. **11**B shows a schematic diagram of another exemplary force sensor in accordance with the present teachings.

FIG. **11**C shows a schematic diagram of another exemplary force sensor in accordance with the present teachings.

FIG. **12** shows a schematic diagram of another exemplary force sensor in accordance with the present teachings.

FIG. **13**A shows a schematic diagram of another exemplary force sensor in accordance with the present teachings.

FIG. **13**B shows a cross-sectional schematic diagram of another exemplary force sensor in accordance with the present teachings.

FIG. **14** shows a schematic diagram of an exemplary AFM system in accordance with the present teachings.

FIGS. **15**A-**15**C show graphs of interaction force versus time for an exemplary force sensor in accordance with the present teachings.

FIG. **16**A shows a graph of interaction force versus time for an exemplary force sensor in accordance with the present teachings.

FIG. **16**B shows a PAF image and a topography image of a sample using an exemplary force sensor in accordance with the present teachings.

FIG. **16**C shows a PRF image and a topography image of a sample using an exemplary force sensor in accordance with the present teachings.

FIG. **17**A shows a topographical image of a sample using an exemplary force sensor in accordance with the present teachings.

FIG. **17**B shows line scans of the sample shown in FIG. **17**A measured at different speeds.

FIG. **17**C shows a topographical image of sample in FIG. **17**A made using a conventional AFM system.

FIG. **17**D shows line scans of the sample shown in FIG. **17**C measured at different speeds using a conventional AFM system.

FIG. **18** shows a cross-sectional schematic diagram of another exemplary force sensor in accordance with the present teachings.

FIG. **19** shows a graph plotting normalized intensity versus gap thickness using a force sensor in accordance with the present teachings.

FIG. **20**A shows a graph plotting photo-detector output versus bias voltage for a force sensor in accordance with the present teachings.

FIG. **20**B shows a graph plotting photo-detector output versus time for a force sensor in accordance with the present teachings.

FIG. **21** shows a cross-sectional schematic diagram of another exemplary force sensor in accordance with the present teachings.

FIG. **22** shows a cross-sectional schematic diagram of another exemplary force sensor in accordance with the present teachings.

FIG. **23**A shows a graph plotting normalized intensity versus gap thickness using a force sensor in accordance with the present teachings.

FIG. **23**B shows a graph plotting sensitivity versus metal thickness using a force sensor in accordance with the present teachings.

FIG. **24**A shows a graph plotting detector output versus bias voltage using a force sensor in accordance with the present teachings.

FIG. **24**B shows a graph plotting detector output versus bias voltage using a force sensor in accordance with the present teachings.

FIG. **24**C shows a graph plotting photo-detector output versus time using a force sensor in accordance with the present teachings.

FIG. **25** shows a graph plotting normalized intensity versus gap thickness using a force sensor in accordance with the present teachings.

FIG. **26** shows a cross-sectional schematic diagram of another exemplary force sensor in accordance with the present teachings.

FIG. **27** shows a cross-sectional schematic diagram of another exemplary force sensor in accordance with the present teachings.

FIG. **28**A shows a cross-sectional schematic diagram of another exemplary force sensor in accordance with the present teachings.

FIG. **28**B shows a cross-sectional schematic diagram of a portion of the force sensor shown in FIG. **28**A in accordance with the present teachings.

FIG. **29**A shows a top schematic diagram of an exemplary force sensor structure with multiple integrated actuators accordance with the present teachings.

FIG. **29**B shows a cross-sectional schematic diagram of a portion of the force sensor structure shown in FIG. **29**A in accordance with the present teachings.

FIG. **30** shows a cross-sectional schematic diagram of an oscillation of the force sensor in accordance with the present teachings.

FIG. **31**A shows a side schematic diagram of a force sensor oscillation in accordance with the present teachings.

FIG. **31**B shows a side schematic diagram of a further force sensor oscillation in accordance with the present teachings.

FIG. **32** shows a side schematic diagram of a linear oscillation of the force sensor in accordance with the present teachings.

FIG. **33** shows a side schematic diagram of a lateral oscillation of the force sensor in accordance with the present teachings.

FIG. **34**A shows a side schematic diagram of a force sensor having multiple optical detection ports in accordance with the present teachings.

FIG. **34**B shows a top schematic diagram of the force sensor shown in FIG. **34**A showing the location of gratings with different periods in accordance with the present teachings.

FIG. **34**C shows a top schematic diagram of the force sensor shown in FIG. **34**A showing the location of gratings with different orientations in accordance with the present teachings.

FIG. **35** shows a side schematic diagram of a force sensor having a three-dimensional force measurement capability in accordance with the present teachings.

FIG. **36**A shows a signal process for obtaining lateral tapping signals with the force sensor in accordance with the present teachings.

FIG. **36**B shows a signal process for obtaining vertical tapping signals with the force sensor in accordance with the present teachings.

FIG. **37** shows a signal processing for non-contact three-dimensional imaging with the exemplary force sensor in accordance with the present teachings.

DETAILED DESCRIPTION OF THE INVENTION

In the following description, reference is made to the accompanying drawings that form a part thereof, and in which is shown by way of illustration specific exemplary embodiments in which the invention may be practiced. These embodiments are described in sufficient detail to enable those skilled in the art to practice the invention and it is to be understood that other embodiments may be utilized and that changes may be made without departing from the scope of the invention. The following description is, therefore, not to be taken in a limited sense.

Notwithstanding that the numerical ranges and parameters setting forth the broad scope of the invention are approximations, the numerical values set forth in the specific examples are reported as precisely as possible. Any numerical value, however, inherently contains certain errors necessarily resulting from the standard deviation found in their respective testing measurements. Moreover, all ranges disclosed herein are to be understood to encompass any and all sub-ranges subsumed therein. For example, a range of "less than 10" can include any and all sub-ranges between (and including) the minimum value of zero and the maximum value of 10, that is, any and all sub-ranges having a minimum value of equal to or greater than zero and a maximum value of equal to or less than 10, e.g., 1 to 5.

According to various embodiments there is a force sensor for use in, for example, probe based instruments, such as probe microscopy and structure manipulation. The force sensor can comprise a detection surface, a flexible mechanical structure, and a gap between the detection surface and the flexible mechanical structure. The force sensors can also comprise a tip in contact with the flexible mechanical structure.

Force sensors described herein can eliminate the corruption of utility, such as measurement information, that can arise from a cantilever. These force sensors can also be used as actuators to apply known forces, providing clean and valuable elasticity information data on surfaces, biomolecules, and other materials. Moreover, these force sensors can be integrated on cantilevers and can be compatible with existing AFM systems while providing accurate tip displacement and also act as "active tips".

According to various embodiments, a displacement measurement can be made using a flexible mechanical structure, such as a membrane, a diaphragm, a cantilever, a clamped-

clamped beam, a flexible structure comprising multiple flexible elements partially or totally fixed at one end on a substantially rigid surface and connected at a point so as to form a symmetry axis. These flexible mechanical structures can be micro-machined. These flexible mechanical structures can have uniform or non-uniform cross sections to achieve desired static and dynamic deflection characteristics. For example, the vibration modes that are symmetric and anti-symmetric with respect to the symmetry axis can be used to detect forces in different directions. These flexible mechanical structures can be made of metals such as gold, aluminum, or a semiconductor such as single crystal silicon or polycrystalline silicon, or dielectric materials such as silicon nitride, silicon oxide, or a polymer such as SU-8, or they can be a composite structure of metallic, semiconducting, polymer, or dielectric materials. While not intending to be so limited, measurements can be made to detect, for example: localized forces, such as, a force experienced by a tip contacting the flexible mechanical structure; surface topography using for example, a flexible mechanical structure with an integrated tip contacting a surface; a flexible mechanical structure with an integrated tip in close proximity of a surface or substance; and forces between a reactive substance, such as a molecule, bound to the flexible mechanical structure and another reactive substance, such as a molecule, bound on a close by structure such as a tip.

According to various embodiments, the detection surface can be a surface of a rigid substrate, or a part of a rigid substrate, with an optically reflective diffraction grating, a part of a rigid substrate with a reflective and/or electrically conductive diffraction grating for optical interferometric detection and electrostatic actuation, a part of a rigid substrate with electrically conductive members for electrostatic actuation and capacitive detection, a surface of a rigid substrate with a semi-transparent layer for optical interferometry. In some cases the detection surface can be a surface of a deformable mechanical structure such as a membrane, clamped-clamped beam or a cantilever. The rigidity of the mechanical structure with the detection surface can be substantially higher than the flexible mechanical structure of the force sensor. The detection surface can contain conductive and dielectric portions to have electrical isolation between actuation and detection electrodes. In some cases, the deformable detection surface can be actuated and therefore it can contain a separate electrode or piezoelectric film for actuation purposes. Still further, in some cases the detection surface can form a substrate.

According to various embodiments, displacement can be measured using interferometric techniques or capacitive techniques. For example, a grating, such as that used in a diffraction based optical interferometric method or any other optical interferometric method such as, for example, Fabry-Perot structures, an example of which is described in U.S. patent application Ser. No. 10/704,932, filed Nov. 10, 2003, which is incorporated herein by reference in its entirety, can be used. Capacitive measurements can use techniques used to monitor capacitance, such as that used in capacitive microphones.

The flexible mechanical structure dimensions and materials can be adjusted to have desired compliance and measurement capabilities to make static and dynamic measurements with sufficient bandwidth. The overall shape of the flexible mechanical structure can be circular, square, or any other suitable shape. Typical lateral dimensions can be from 1 μm to 2 mm, flexible mechanical structure thickness can be from 10 nm to 3 μm, and the gap can be from 1 nm to 10 μm. In some embodiments the gap can be as large as 1 mm. The flexible mechanical structure material can comprise, for example, aluminum, gold, silicon nitride, silicon, silicon oxide, or polysilicon or can be a composite structure of metallic, semiconducting, and dielectric materials. The gap can be sealed or partially sealed for applications in liquids, or it can be open for vacuum and atmospheric measurements.

For some force measurements, a soft cantilever may not be required. Using the output from the force sensors in a feedback loop, one can use an external actuator to individually adjust the tip-flexible mechanical structure, tip-sample distances. According to various embodiments, the flexible mechanical structure can be electrostatically actuated to apply desired forces. According to various embodiments, force sensors described herein can be attached to a cantilever to form a force sensor structure. Further, the force sensor structure can be combined with a detector to form a force sensor unit that can be used in a probe based instrument.

FIG. **1**A shows a cross-sectional schematic diagram of an exemplary force sensor **100** in accordance with the present teachings. The force sensor **100** comprises a detection surface **102** and a flexible mechanical structure **104**. The flexible mechanical structure **104** can be disposed distance (D) above the detection surface so as to form a gap **105** between the flexible mechanical structure **104** and the detection surface **102**. The flexible mechanical structure can be configured to move to a new position **104'** upon exposure to external stimuli **114**, such as a force. Moreover, the force sensor **100** can include elements configured to detect changes in the distance (D). Still further, the force sensor **100** can be actuated to affect the distance (D) using, for example, bottom electrode **106**, such as a grating, and a top electrode **116**, both of which are described in more detail below.

The detection surface **102** can be made of a material transparent to predetermined wavelengths of light. For example, the detection surface can be made from silicon oxide, such as quartz. The overall shape of the flexible mechanical structure **104** can be circular, square, or any other suitable shape. Typical diameters of flexible mechanical structure **104** can range from about 5 μm to about 2 mm and the thickness of flexible mechanical structure **104** can be from about 10 nm to about 10 μm. The flexible mechanical structure can be a micro-machined material that can comprise, for example, aluminum, gold, silicon nitride, silicon oxide, or polysilicon.

According to various embodiments, the distance (D) of gap **105** can be from about 50 nm to about 50 μm. Moreover, the gap **105** can be sealed for applications in liquids, or it can be open for vacuum and atmospheric measurements. In some embodiments, the gap can be formed by the flexible mechanical structure and can be supported over the detection surface by at least one sidewall. Movement of the flexible mechanical structure, or displacement measurements, can be made, for example using a grating as described below, which uses a diffraction based optical interferometric method or any other optical interferometric method or a capacitive method, such as in that used in capacitive microphones, can be used for detection. According to various embodiments, grating periods of the grating **106** can range from about 0.5 m to about 20 m. The incident light can be from the UV (with wavelengths starting at about 0.2 m) to IR (with wavelengths starting at about 1.5 m).

FIGS. **1**B-**1**D show various perspective views of exemplary force sensors. For example, FIG. **1**B shows a view using a scanning electron microscope (SEM) of the sensor **100**. FIG. **1**C is a top down photographic view of the force sensor **100** and shows flexible mechanical structure **104**. FIG. **1**D is a photographic view of the force sensor **100** as seen by pass-

ing light through the transparent detection surface **102** and shows grating **106** positioned under the flexible mechanical structure **104**.

According to various embodiments, the force sensor **100** can also include a grating **106**, as shown in FIG. **1**E. In FIG. **1**E, a beam of light **110** can be directed through the detection surface **102** to impinge on the flexible mechanical structure **104** and the grating **106**. According to various embodiments, the beam of light **110** can be directed at the detection surface **102** at an angle, such as, in the range of, for example ±10° away from normal to the detection surface **102**. A portion of the flexible mechanical structure **104** can be reflective such that light **110** can be reflected from the flexible mechanical structure **104** and another portion can be reflected by the grating **106**. As a result, different diffraction orders with different intensity levels can be generated as the light passes through the grating **106** depending on the gap thickness.

For example, FIG. **1**E shows first diffraction order light **112** reflected from the grating **106** and the flexible mechanical structure **104**. The diffracted light **112** can be detected by a detector **108**. It is to be understood that alternatively, the detectors can be used to detect changes in capacitence due to changes in the gap **105**.

As shown in FIG. **1**E, a stimuli **114**, such as a force, can be applied to the flexible mechanical structure **104**. The stimuli **114** causes the flexible mechanical structure **104** to bend, or flex, shown as **104'**. According to various embodiments, the flexible mechanical structure **104** can bend in various directions, such as toward the detection surface **102** or away from the detection surface **102**. Bending the flexible mechanical structure **104** causes the thickness (D) of the gap **105** shown in FIG. **1**A to change.

When using a beam of light, the light **110** is reflected in a different direction when the flexible mechanical structure is in the bent position **104'** than when the flexible mechanical structure is in the rest position **104**. Further, light **110** reflected from the bent flexible mechanical structure **104'** interacts differently with the grating **106** to produce changes in the intensity of different diffraction orders, shown in FIG. **1**E as **112***a*-**112***c*. The detectors **108** can then detect the intensity of the diffracted light output from the grating **106**. This provides a robust, micro-scale interferometer structure. Generally, information obtained from the detectors **108** can be used to determine the stimuli **114**, such as the amount of force, applied to the flexible mechanical structure **104**. This determination can be done using a computer processor (not shown) or other various techniques as will be known to one of ordinary skill in the art. Also shown in FIG. **1**E is a top electrode **116** that can cooperate with, for example grating **106**, to serve as an actuator, as will be described in detail below.

According to various embodiments the detector **108** can be a photo-detector, such as a silicon photodiode operated in photovoltaic or reverse biased mode or another type of photo-detector sensitive in the wavelength range of the light source. Moreover, the light **110** can be a coherent light source such as a laser. Exemplary light sources can include, but are not limited to, helium neon type gas lasers, semiconductor laser diodes, vertical cavity surface emitting lasers, light emitting diodes.

FIG. **2**A shows a cross-sectional schematic diagram of another exemplary force sensor **200** in accordance with the present teachings. The force sensor **200** comprises a detection surface **202**, a flexible mechanical structure **204**, a grating **206**, and a tip **207**. In some embodiments, the force sensor **200** can also include a top electrode **216**. Moreover, the grating **206** can be covered with a dielectric layer to prevent electrical shorting in case of flexible mechanical structure collapse.

Generally, the force sensor **200** can be used to manipulate structures, such as atoms, molecules, or micro-electromechanical systems (MEMS) or to characterize various material properties of a sample **218**. For example, the topography of the sample **218** can be determined by moving the sample **218** in a lateral direction across the tip **207**. It is also contemplated that the sample **218** can remain stationary and the tip **207** can be moved relative to the sample **218**. Changes in height of the sample **218** are detected and cause the tip **207** to move accordingly. The force on the tip **207** caused by, for example the tip motion, can cause the flexible mechanical structure **204** to bend, or flex as shown by **204'**. Light **210** can also be directed through detection surface **202** to impinge on the flexible mechanical structure **204**. The light **210** is reflected from the flexible mechanical structure and diffracted by the grating **206**. As the tip **207** applies force to the flexible mechanical structure, the thickness of the gap **205** changes. This can cause the reflected light to diffract differently than if the flexible mechanical structure were in its un-bent position. Thus, different diffraction orders of intensity can change depending on the gap thickness.

After passing through the grating **206** the diffracted light **212***a-c* can be detected by the detectors **208**. The output from the detectors **208** can be used in a feedback loop to direct an external actuator (not shown) to adjust the tip-flexible mechanical structure position (i.e., the gap height), and thus the tip-sample distance (d). The flexible mechanical structure **204** can be electrostatically actuated to apply desired forces or to adjust the flexible mechanical structure position (i.e., the gap height), and thus the tip-sample distance (d) by biasing electrodes **220***a* and **220***b* attached to the grating **206** and the top electrode **216**, respectively. Although two detectors are shown in FIG. **2**A, one of ordinary skill in the art understands that one or more detectors can be used.

According to various embodiments, the force sensor **200** can form an integrated phase-sensitive diffraction grating structure that can measure the flexible mechanical structure **204** and/or tip **207** displacement with the sensitivity of a Michelson interferometer. The displacement of the tip **207** due to stimuli acting on it can be monitored by illuminating the diffraction grating **206** through the transparent detection surface **202** with a coherent light source **210** and the intensity of the reflected diffraction orders **212***a-c* can be recorded by the detectors **208** at fixed locations. The resulting interference curve is typically periodic with $\lambda/2$, where λ is the optical wavelength in air. According to an exemplary embodiment, the displacement detection can be within the range of about $\lambda/4$ (167.5 nm for λ=670 nm) in the case of a fixed grating **206**. However, the detection surface **202** and the grating **206** can be moved by suitable actuators to extend this imaging range. Furthermore, the grating **206** can be located not at the center but closer to the clamped edges of the flexible mechanical structure to increase the equivalent detectable tip motion range. In the case of a microscope, the "active" tip can be moved by electrostatic forces applied to the flexible mechanical structure **204** using the diffraction grating **206** as an integrated rigid actuator electrode. In some applications, this actuator can be used to adjust the tip **207** position for optimal displacement sensitivity to provide a force feedback signal to an external actuator moving the transparent detection surface **202**.

In some embodiments, such as applications requiring high speeds, this integrated actuator can be used as the only actuator in the feedback loop to move the tip **207** with a speed

determined by the flexible mechanical structure **204** dynamics in liquids, air, and vacuum.

FIG. **2**B shows a focused ion beam (FIB) micrograph of a force sensor **250** according to an exemplary embodiment. In the embodiment shown in FIG. **2**B, the flexible mechanical structure **254** is 0.9 μm thick and is made from aluminum. Moreover, the flexible mechanical structure **254** is 150 μm in diameter and it can be formed by sputter deposition on a 0.5 mm thick quartz substrate over a 1.4 μm thick photoresist sacrificial layer. FIG. **2**C shows the optical micrograph of the flexible mechanical structure **254** from the backside as seen through the substrate **252**. The grating **256** and the electrical connections **270** can be seen as well as the darker spot at the position of the tip **257** at the middle of the flexible mechanical structure **254**. In FIG. **2**C, the 90 nm thick aluminum grating **256** can be formed by evaporation over a 30 nm thick titanium or titanium nitride adhesion layer and then patterned to have a 4 μm grating period with 50% fill factor. A 220 nm thick oxide layer can be deposited over the grating **256** using plasma enhanced chemical vapor deposition. In this case, the subsequent flexible mechanical structure stiffness was measured to be approximately 133 N/m using a calibrated AFM cantilever and the electrostatic actuation range was approximately 470 nm before collapse. The tip **257** was fabricated out of platinum using an FIB. The process involved ion beam assisted chemical vapor deposition of platinum using methyl platinum gas where molecules adsorb on the surface but only decompose where the ion beam interacts. The tip **257**, with a radius of curvatures down to 50 nm on the aluminum flexible mechanical structures **254**, was fabricated with this method. An SEM micrograph of a typical tip with 70 nm radius of curvature is shown in FIG. **2**D.

According to various embodiments, the force sensor **200** can have a compact integrated electrostatic actuator, where the electric field between the grating electrode **206** and the top electrode **216** is contained within the gap **205**. This structure can be replicated to form planar arrays of sensors, as described in more detail below, with good electrical and mechanical isolation. With a suitable set of flexible mechanical structure and electrode materials, the device can be operated in a dielectric or conductive fluid. According to various embodiments, the electrostatic forces may act only on the probe flexible mechanical structure **204**. As such, the actuation speed can be quite fast. Therefore, combined with array operations, the force sensor can be used in probe applications that call for high speeds.

FIG. **3**A depicts a schematic diagram of another exemplary force sensor **300** and FIG. **3**B depicts a schematic diagram of multiple force sensors **300** working in concert in accordance with the present teachings. The embodiments shown in FIGS. **3**A and **3**B can be used as force sensors for parallel force measurements, such as in the case of biomolecular mechanics. The force sensors **300** shown in FIGS. **3**A and **3**B can comprise a detection surface **302** and a flexible mechanical structure **304**. The force sensor **300** can also comprise a grating **306** and a tip **307** positioned above the flexible mechanical structure **304**. According to various embodiments, reactive substances, such as molecules, including biomolecules, labeled **318***a* and **318***b* in FIGS. **3**A and **3**B can be attached to flexible mechanical structure **304** and tip **307**, respectively. In some embodiments, the force sensors **300** can also include a top electrode **316**. FIG. **3**B shows the force sensors **300** in contact with a single detection surface **302**. However, in some cases more than one force sensor **300** can contact a separate detection surface so as to be controlled separately.

The force sensors **300** can be used to characterize various material properties of the reactive substance. For example, biomolecular bonding can be determined by moving the tip **307** contacted by a reactive substance, including, for example, inorganic molecules and/or organic molecules, such as biomolecules, over the force sensors **300**. It is also contemplated that the tip **307** can remain stationary and the force sensors **300** can be moved relative to the tip **307**. The reactive substance on the flexible mechanical structure **304** can be attracted to the reactive substance on the tip **307**. A stimuli **319**, such as a force, light, or temperature, on, for example, the force sensor **300** or the tip **307** caused by, for example the molecular attraction, a light source, or a temperature source, can cause the flexible mechanical structure **304** to bend, or flex as shown by **304'**. Light **310** can also be directed through detection surface **302** to impinge on the flexible mechanical structure. The light **310** is reflected from the flexible mechanical structure and then diffracted by the grating **306**. As the stimuli displaces the flexible mechanical structure, the thickness of the gap **305** changes. This can cause the reflected light to diffract differently than if the flexible mechanical structure were in its un-bent position. Thus, different diffraction order intensities can be generated as the light passes through the grating **306** depending on the gap thickness. After passing through the grating **306** the diffracted light **312***a-c* can be detected by the detectors **308**. The output from the detectors **308** can be used in a feedback loop to direct an external actuator (not shown) to adjust the flexible mechanical structure position (i.e., the gap height), and thus the tip-sample distance (d). According to various embodiments, the flexible mechanical structure **304** can be electrostatically actuated to apply desired forces by biasing electrodes **320***a* and **320***b* attached to the grating **306** and the top electrode **316**, respectively.

By using a variety of techniques disclosed herein, displacements from 1 mm down to 1×10^{-6} Å/√Hz or lower can be measured. As such, forces from 1N down to 1 pN can be detected with 10 kHz bandwidth with an effective spring constant of the sensor flexible mechanical structure from about 0.001N/m to about 1000N/m at its softest point. These mechanical parameters can be achieved by micro-machined flexible mechanical structures, such as MEMs microphone flexible mechanical structures. Therefore, using flexible mechanical structure surfaces and tips functionalized by interacting reactive substances, as shown in FIGS. **3**A and **3**B, force spectroscopy measurements can be performed in parallel using optical or electrostatic readout.

For example, in the case of rupture force measurements, the reactive substance, such as a molecule, is pulled and if the bond is intact, the flexible mechanical structure is also pulled out while the displacement, i.e., applied force, is measured. With the bond rupture, the flexible mechanical structure comes back to rest position. The force sensor flexible mechanical structures can be individually actuated to apply pulling forces to individual molecules and measuring their extensions allowing for array operation.

FIGS. **4**A-**4**C depict perspective views of exemplary embodiments in accordance with the present teachings. FIG. **4**A depicts a cross-sectional schematic diagram and FIG. **4**B depicts a view of the top of a force sensor structure **400**. The force sensor structure **400** can include a cantilever **422**, such as that used in AFM, and a force sensor **401** positioned on the free end of the cantilever **422**. The force sensor **401** can comprise a detection surface **402**, a flexible mechanical structure **404**, a gap **405**, grating **406**, a tip **407**, and a top electrode **416**. Further, the cantilever **422** can be transparent to allow for optical readout of the deflection of the flexible mechanical

structure, which has an integrated tip for imaging. The cantilever **422** can be made of materials similar to those of the detection surface material, described above. Indeed, in some embodiments, the cantilever **422** alone can comprise the detection surface **402**. Alternatively, the detection surface can be a substrate formed on the cantilever. In some embodiments the cantilever **422** can also include a reflector **424**.

The cantilever **422** can be used to provide periodic tapping impact force for tapping mode imaging to apply controlled forces for contact mode or molecular pulling experiments. Because the flexible mechanical structure **404** can be stiffer than the cantilever **422** and can be damped by immersion in a liquid, the measurement bandwidth can be much larger than the cantilever **422**. Furthermore, optical readout of the diffraction orders can directly provide tip displacement because the diffraction orders can be generated by the grating **406** under the flexible mechanical structure **404**.

According to various embodiments, the reflector **424** can be used to beam bounce to find cantilever deflection for feedback, if needed. In some cases, the tip-force sensor output can provide the real force feedback signal. The cantilever **422** and the flexible mechanical structure **404** dimensions can be adjusted for the measurement speed and force requirements.

FIG. **4**C depicts a cross-sectional schematic diagram of another exemplary force sensor **401***a* in accordance with the present teachings. The force sensor **401***a* is similar to the force sensor **401** but includes a thicker base region **403** of the detection surface **402**. Also shown in FIG. **4**C are electrical connections **420***a* and **420***b* that contact the grating **406** and the top electrode **416**, respectively. The electrical connections can be used to provide electrostatic actuation or capacitive detection.

FIG. **5**A shows an embodiment of a force sensor structure **500** according to the present teaching for tapping mode imaging. In addition to topography, tapping mode can also provide material property imaging and measurement if the tip-sample interaction forces can be accurately measured. The disclosed force sensor structure solves a significant problem for this mode of operation. For example, when the cantilever is vibrated using a sinusoidal drive signal, shown in FIG. **5**B, and it is brought to a certain distance to the surface, the tip starts to contact the surface during a short period of each cycle, as shown in FIG. **5**C. While the oscillation amplitude is kept constant for topography information, the contact force i.e., the tip-sample interaction force and duration can be related to the material properties of the sample and adhesion forces. With a regular cantilever, the deflection signal can be dominated by the vibration modes of the cantilever, which can significantly attenuate the information in the harmonics. According to various embodiments, the transient force that the tip **507** or the sample **518** experiences at each tap can be measured. Because the force sensors disclosed herein can directly measure the flexible mechanical structure/tip displacement directly using optical interferometry or capacitive measurement, this transient force signal can be obtained. By designing the flexible mechanical structure stiffness, broadband response is possible and short transient force signals can be measured. This situation can be valid in both air and liquids, as the information is independent of the cantilever vibration spectrum.

Using electrically isolated electrodes, the flexible mechanical structure can be actuated so as to have an "active tip". Further the actuated flexible mechanical structure can optimize the optical detection or capacitive detection sensitivity in air or in liquid environments. FIG. **6** shows an application of a force sensor structure **600** comprising a sensor **601** on a cantilever **622** where the tip **607** is active, as shown by arrow **623**. In FIG. **6**, the active tip **607** can be used to apply known forces to the surface of sample **618** using electrostatic actuation and optical interferometric displacement detection or capacitive displacement detection can be achieved. The tip **607** can be activated, for example, by applying a bias between the grating **606** and the top electrode **616**. Further, a DC force, shown by arrow **626**, can be used to keep the tip **607** in constant contact with the sample.

Light **610** can be directed to the flexible mechanical structure **604** and the orders **612***a-c* of light diffracted by the grating **606** can be detected by the detector **608**. Similar to the force sensor **401***a* shown in FIG. **4**C, designing the dimensions of the flexible mechanical structure base **603**, or choosing the operation frequency at an anti-resonance of the cantilever, the flexible mechanical structure **604** can be moved, and hence the tip **607** can be pushed into the sample **618** by known electrostatic forces. Accordingly, displacements of the flexible mechanical structure **604** can be measured optically or capacitively. Furthermore, in some embodiments there is no need for an active tip on the force sensor. Moreover for optical measurements, the gap between the flexible mechanical structure and the grating can be optimized during fabrication of the force sensor. Thus, there is no need to actively adjust that gap during tapping mode operation as shown in FIG. **6**. Similarly for capacitive detection, an electrical connection for detection of capacitance changes can be provided. In that case, the force sensor **601** can be connected to a detection circuit such as used in a capacitive microphone for measuring the force on the tip **607**.

The thickness of the base **603** (or the substrate) supporting the flexible mechanical structure **604** can be adjusted to control the operation frequency to insure that the motion of the flexible mechanical structure **604** produces an indentation in the sample surface. This measurement, therefore, directly provides surface elasticity information. According to various embodiments, the frequency of electrostatic actuation can be in the ultrasonic range. Alternatively, a wideband impulse force can be applied and resulting displacements can be detected in the bandwidth of the flexible mechanical structure displacement force sensor. For these applications, it may be desirable to move the higher cantilever vibration mode frequencies away from the first resonance. This can be achieved, for example, by increasing the mass close to the tip of the cantilever, such as by adjusting the thickness, or mass of the base **603**. With added mass, the cantilever acts more like a single mode mass spring system and can generate tapping signals without spurious vibrations and can also be effective at a broad range of frequencies.

In general, for tapping mode AFM and UAFM applications a broadband, stiff tip displacement measurement sensor/structure can be integrated into compliant structures, such as regular AFM cantilevers. Although flexible mechanical structures are primarily described here, according to another embodiment, the tip displacement measurement structure can be a stiff beam structure with the same cross-section of the flexible mechanical structure or another stiff cantilever, as shown, for example, in FIG. **7**. In FIG. **7**, there is a force sensor structure **700**, comprising a force sensor **701**, a compliant structure **722**, a tip **707**, and a flexible mechanical structure **728** such as a stiff broadband structure. In this case, the stiff broadband structure **728** can be small cantilever mounted to an end of the compliant structure **722**, also a cantilever. The small cantilever **728** can be spaced a distance (d) from the compliant structure **722**. The compliant structure **722** can be used to control the impact and/or contact force of the tip **707** mounted to a side of the stiff broadband structure **728**. Further, the stiff broadband structure **728** can be used to

measure tip displacements. Displacement of the tip **707** can be measured, for example, optically, electrostatically, capacitively, piezoelectrically or piezoresistively.

According to various embodiments, for fast imaging and tapping mode applications, the cantilever can be eliminated. In this case, a fast x-y scan of a sample or the integrated tip can be used with the described sensor/actuator for tapping and detecting forces. The large, fast z-axis motion can be generated, for example, by a piezoelectric actuator that moves the base of the force sensor, which can be a thick, rigid substrate.

The sensitivity of a force sensor in accordance with the present teachings can be described by the following exemplary embodiment, depicted in FIG. **8**A. In FIG. **8**A, a rectangular silicon AFM cantilever **822** with a tip **807** is vibrated at 57 kHz above a 150 μm diameter, ~1 μm thick aluminum flexible mechanical structure **804** with an integrated diffraction grating **806**. The force sensor **800** flexible mechanical structure **804** is built on a quartz detection surface or substrate **802**. A DC bias of 37V is applied to move the flexible mechanical structure **804** to a position of optimal detection sensitivity and the vibrating tip **807** is brought close enough to have tapping mode-like operation with intermittent contact. Diffraction order **812** can be detected by detector **808** when a beam **810** is diffracted by grating **806** upon exiting force sensor **800**.

The single shot signals collected at this position are shown at the top two rows (Row **1** and Row **2**) of the four rows of the graph in FIG. **8**B. The bottom graph, in FIG. **8**C, shows a zoomed in version of Row **2** of individual taps, where the transient displacement of the flexible mechanical structure due to impact of the tip is clearly seen. If the flexible mechanical structure material were softer or there were a compliant coating on the flexible mechanical structure **804**, the measured tap signals would be longer in duration and smaller in amplitude because the tip **807** would spend more time indenting the softer surface while transmitting less force to the flexible mechanical structure **804**. Therefore, the tapping force measurement provides elasticity information and this embodiment can be used as a material property sensor for a thin film coating on the flexible mechanical structure.

In addition, when the tip **807** leaves contact, the flexible mechanical structure **804** is pulled away due to adhesion or capillary forces, permitting force spectroscopy measurement methods. When the tip **807** is moved progressively closer, it is in contact with the flexible mechanical structure **804** for a longer duration of each cycle and finally it pushes the flexible mechanical structure **804** down during the whole cycle. Thus, the simple force sensing structures disclosed herein provide information not available by conventional AFM methods and result in more effective tools for force spectroscopy applications.

The sensitivity of another force sensor in accordance with the present teaching can be described by the following exemplary embodiment, depicted in FIGS. **9**A-**9**H. As shown in FIG. **9**A, a quartz substrate **902** with a sensor flexible mechanical structure **904** is placed on a piezoelectric stack transducer **927**, which can be used to approach to the tip **907** and obtain force distance curves. The flexible mechanical structure **904** is aluminum and can be 150 μm in diameter, 1 μm thick, and located over a 2 μm gap **905** above the rigid diffraction grating electrode **906**. In this case, the grating period is 4 μm. The gap **905** is open to air through several sacrificial layer etch holes (not shown). The grating **906** can be illuminated at **910** through the quartz substrate **902** using, for example, a HeNe laser (λ=632 nm) at a 5° angle away from normal to the substrate. The output optical signal can be obtained by recording the intensity of the 1st diffraction order beam **912***b*.

For measuring the AFM dynamic tip-sample interaction forces, the cantilever **922** can be glued on a piezoelectric AC drive transducer **926** that can drive the cantilever **922** at its resonant frequency. The flexible mechanical structure **904**, with a stiffness of approximately 76N/m as measured at the center using a calibrated AFM cantilever **922**, can be used. The DC bias on the flexible mechanical structure **904** is adjusted to 27V to optimize the optical detection, and the sensitivity is calibrated as 16 mV/nm by contacting the flexible mechanical structure **904** with a calibrated AFM cantilever **922** and a calibrated piezo driver. In this case, the broadband RMS noise level of the system was about 3 mV (0.18 nm) without much effort to reduce mechanical, laser, or electrical noise.

A force curve can be produced by moving the piezoelectric stack **927** supporting the substrate **902** with a 20 Hz, 850 nm triangular signal and making sure that there is tip-flexible mechanical structure contact during a portion of the signal period. The cantilever **922** can be, for example, a FESP from Veeco Metrology, Santa Barbara, Calif., with k=2.8N/m.

FIG. **9**B shows a force curve **950** where the inset drawings (i)-(v) indicate the shape of the cantilever **922** and flexible mechanical structure **904**, and the hollow arrow indicates the direction of motion of the piezo stack **927** and the quartz substrate **902**. Moreover, the insert drawings (i)-(v) correspond to sections (a)-(e), respectively, of the curve **950**. Before measurement, the flexible mechanical structure **904** is at rest, as seen in insert (i) and section (a). Tip-flexible mechanical structure contact happens starting in section (b) at around 3 ms and the tip bends the flexible mechanical structure **904** downwards, as shown in insert drawings (ii) and (iii). Tip-flexible mechanical structure contact continues through section (c) until about 26 ms, which is in section (d). The piezoelectric motion is reversed starting at section (c). Section (d) shows that attractive forces due to adhesion pulls the flexible mechanical structure **904** up, as seen in insert (iv), for 2 ms and then the flexible mechanical structure **904** moves back to its rest position, as seen in insert (v) after a 180 nN jump at the end of the retract section. Curve **950** in section (e) shows the rest position.

For direct observation of time resolved dynamic interaction forces along the force curve, a similar experiment can be performed while the cantilever **922** is driven into oscillation by applying a sinusoidal signal to the AC drive piezo **926** at 67.3 kHz. The single shot, transient flexible mechanical structure displacement signal **960** obtained during a cycle of the 20 Hz drive signal is shown in FIG. **9**C. Dynamic interaction force measurements provide various types of information, as indicated by the various interaction regimes (A)-(C) during the measurement. The data of FIG. **9**C is shown expanded in FIGS. **9**D-F in the initial tapping region (A), intermittent to continuous contact region (B), and continuous to intermittent contact transition region (C), respectively.

Starting from the left, the cantilever tip **907** is first out of contact with the flexible mechanical structure **904**. At around 1 ms it starts intermittent contact (tapping) with the flexible mechanical structure **904** as individual taps are detected, as shown in FIG. **9**D. As the cantilever **922** gets closer to the flexible mechanical structure **904**, the pulses become unipolar and the distortion is more severe as there are double peaked tap signals when the cantilever **922** gets into contact due to non-linear interaction forces, as shown FIG. **9**E. When the tip **907** is in continuous contact, which happens around 4.2 ms, the displacement signal has the periodicity of the drive

signal in addition to distortion that can be caused by contact non-linearities and higher order vibration modes of the cantilever **922** with its tip **907** hinged on the flexible mechanical structure **904**. Similarly, around 15 ms, the cantilever **922** starts breaking off the flexible mechanical structure surface and tapping resumes, as shown in FIG. **9**F. Between 7 ms and 12 ms the curve is not linear.

Individual tapping signals can be filtered by the dynamic response of the flexible mechanical structure **904**. In this example, the force sensor was not optimized and the flexible mechanical structure **904** acted as a lightly damped resonator with a resonant frequency at 620 kHz rather than having broadband frequency response that is ideal for fast interaction force measurements. Nevertheless, the transfer function of the flexible mechanical structure **904** can be obtained using, for example, integrated electrostatic actuators, as described herein.

Still further, FIG. **9**G shows the measured temporal response of the flexible mechanical structure **904** when a 2V square pulse 100 ns in length is applied in addition to the 27V DC bias at the actuator terminals. Comparing the trace waveform in FIG. **9**G with averaged data from individual tap signals shown in FIG. **9**H, it can be seen that the stiff cantilever tap is nearly an impulsive force, which can be recovered by inverse filtering.

Thus, according to various embodiments, minimum displacement detection levels down to 10^{-4} Å/√Hz can be measured and mechanical structures with spring constants in the 0.001 to 10N/m range can be built that can monitor force levels in the pico-Newton range. These sensitivity levels can make it useful for a wide range of probe microscopy applications including quantitative interaction force measurements, fast imaging in liquids and in air, and probe arrays for imaging, lithography, and single molecule force spectroscopy.

While FIGS. **8**A-**9**H are examples of sensitivity testing made by applying a force from a tip to the force sensor, similar sensitivities can be achieved when a tip is mounted to the force sensor and the force sensor is used to characterize a sample.

FIG. **10**A depicts a cross-sectional schematic diagram of another exemplary force sensor **1000** in accordance with the present teachings. The sensor **1000** can comprise a substrate **1002**, a flexible mechanical structure **1004**, a gap **1005**, a tip **1007**, a plurality of separate top electrodes, such as electrodes **1016***a-c*, and a bottom electrode **1030**. The force sensor **1000** substrate **1002** can be positioned at an end of a cantilever **1022**. According to various embodiments, the flexible mechanical structure **1004** can be fully clamped around its circumference as described above and shown in FIG. **10**A. Alternatively, the flexible mechanical structure **1004** can be a clamped-clamped beam with a rectangular or H-shape, as shown in FIGS. **10**B and **10**C, respectively, where the short edges **1040** at the ends are clamped. Still further, the flexible mechanical structure **1004** can be a cantilever structure or a similar structure that changes shape in a predictable manner in response to a force applied to the tip **1007**, as shown in FIG. **10**D.

Each of the plurality of separate top electrodes **1016***a-c* can be electrically isolated and formed in the flexible mechanical structure **1004**. Moreover, the bottom electrode **1030** can spaced apart from the separate top electrodes **1016***a-c* by the gap **1005**. Further, the bottom electrode can be positioned in the substrate **1002** and can be contacted by electrode terminals **1020***d*. Similarly, each of the separate top electrodes **1016***a-c* can be contacted by electrode terminals **1020***a-c*. In some cases, the electrode terminals **1020***a-c* and **1020***d* can be capacitive sensing terminals that can detect a capacitance change formed between the separate top electrodes **1016***a-c* and the bottom electrode **1030**.

In FIG. **10**A, a voltage can be applied between the electrode terminals **1020***a-c* and **1020***d*. The voltage can be used to independently control and move any of the separate top electrodes **1016***a-c*, so that they can serve as actuators. Further, the separate top electrodes **1016***a-c* can also perform sensing, similar to that of a dual electrode capacitive micromachined ultrasonic transducer where the vibrations of the sensor flexible mechanical structure are converted to electrical current signals through change in capacitance.

For example, the force sensor **1000** can be used for fast imaging where bias voltages are applied between the electrode terminals **1020***a*, **1020***c* and the bottom electrode terminal **1020***d* and alternating voltages of the same or reverse phase are applied to the electrode terminals **1020***a* and **1020***c* to vibrate the tip **1007** vertically or laterally to have intermittent contact with a sample surface. In some cases, the forces between the tip **1007** and a close by surface can be sensed without contact for non-contact imaging. The bias voltages applied to the electrode terminals **1020***a*, **1020***c* also control the position of the tip **1007** in response to changes in capacitance detected between the electrode terminals **1020***b* and the bottom electrode terminal **1020***d*. An external controller (not shown) can read the detected capacitance change and generate the control signals (bias voltages) applied to the electrode terminals **1020***a*, **1020***c* and the bottom electrode terminal **1020***d*.

FIG. **11**A depicts a cross-sectional schematic diagram of another exemplary force sensor unit **1100** in accordance with the present teachings. The force sensor unit **1100** can comprise a force sensor **1101**, a detection surface **1102**, a flexible mechanical structure **1104**, a gap **1105**, a tip **1107**, a plurality of separate top electrodes, such as electrodes **1116***a-c*, a plurality of gratings, such as first grating **1106***a* and second grating **1106***b*, at least one detector **1108**, and a cantilever **1122**. The first grating **1106***a* can have a different grating spacing than the grating spacing of **1106***b*. Furthermore, the first grating **1106***a* can have a different orientation as compared to the grating **1106***b*. It is to be understood that other force sensor embodiments described herein can also comprise multiple gratings.

The detection surface **1102** can be positioned at a free end of the cantilever **1122**. Moreover, the flexible mechanical structure **1104** can be fully clamped around its circumference, it can be a clamped-clamped beam with a rectangular or H shape where the short edges at the ends are clamped, or it can be a cantilever structure or a similar structure that changes shape in a predictable manner in response to a force applied to the tip **1107**.

The force sensor **1101** shown in FIG. **11**A can be used for lateral force or friction measurements. For example, force sensor **1101** can be used to sense torsion created on the flexible mechanical structure, shown as **1104'**. Separate top electrodes **1116***a-c* can be positioned on the flexible mechanical structure **1104** to excite the torsional motion or resonances. Similarly, the flexible mechanical structure **1104** can be bent asymmetrically, shown as **1104'**, due to torsion created by the tip **1107** or due to out of phase actuation from the first grating **1106***a*, the second grating **1106***b*, and the top electrodes **1116***a-c* acting as electrostatic actuators. In particular, a voltage can be applied to the electrical contacts **1120***a* and **1120***b* that contact the first grating **1106***a* and the top electrode **1116***a*, respectively. The same voltage can be applied to the electrical contacts **1120***c* and **1120***d* that contact the top electrode **1116***c* and the second grating **1106***b*, respectively. Applying this same voltage can cause the flex-

ible mechanical structure **1104** to bend up and down. In contrast, similarly applying a differential voltage can cause torsion of the flexible mechanical structure **1104**.

A light beam **1110** can be directed through the detection surface **1102** to impinge on the flexible mechanical structure **1104**. The beam **1110** reflects off of the flexible mechanical structure **1104**, a portion of which can be reflective, and is diffracted differently by the first grating **1106***a* and the second grating **1106***b*. As shown in FIG. **11**A, the first grating **1106***a* can generate a first set of diffraction orders **1112***a-d* and the second grating **1106***b* can generate a second set of diffraction orders **1113***a-d*. The detectors **1108** can detect the different diffraction orders. The detector outputs can be added to obtain up and down bending displacement detection. Similarly, the outputs can be subtracted to obtain torsional motion and force detection. This information can be obtained when the spring constant for the second bending mode (torsion around the mid axis) of the flexible mechanical structure **1104**, clamped-clamped beam or a cantilever is known. Thus, in addition to acting as actuators, the first grating **1106***a* and second grating **1106***b* can be used to optically or capacitively decouple the bending motion from the torsional motion. As such, the sensed outputs of these detectors yield both bending and torsional motion information. One can also use separate beams **1110** to illuminate the plurality of gratings.

FIG. **11**B depicts a cross-sectional schematic diagram of another exemplary force sensor unit **1150** in accordance with the present teachings. The force sensor unit **1150** can comprise a force sensor **1151**, a first detection surface **1152** such as a substrate, a flexible mechanical structure **1154**, a gap **1155**, a tip **1157**, a top electrode **1166**, a grating **1156**, grating flexible mechanical structure actuation inputs **1170***a* and **1170***b*, and tip flexible mechanical structure actuation inputs **1172***a* and **1172***b*. The force sensor **1151** can be affixed to a free end of a cantilever (not shown). The grating flexible mechanical structure actuation input **1170***a* can contact a transparent conductor **1173**, such as indium tin oxide, formed on the first detection surface **1152**. According to various embodiments, the flexible mechanical structure **1154** can be separated from the grating by a distance (d). Moreover, the flexible mechanical structure **1154** can comprise the top electrode **1166** and the grating **1156** can be spaced away from the first detection surface **1152**.

The force sensor **1151** shown in FIG. **11**B can extend the tip actuation range without degradation in optical displacement measurement sensitivity. For example, the tip **1157** can be positioned at a relatively large distance away from the grating **1156**. In this manner, the tip **1157** can be moved large distances without shorting or damaging the sensor **1150**. Moreover, the grating **1156** can be actuated to keep the detection sensitivity at an optimal level. For example, the grating can be actuated a distance of $\lambda/4$, where λ is the wavelength of light **1161**, to provide proper sensitivity.

The tip **1157** and flexible mechanical structure **1154** can be spaced away from the grating in various ways. For example, rigid supports **1179** can be formed on the first detection surface **1152** to support the flexible mechanical structure **1154**. In this manner, the flexible mechanical structure **1154** is separated from the grating **1156** at a predetermined distance. A second detection surface **1184** can be separated from the first detection surface **1152** by a gap so as to provide a predetermined separation distance. The grating **1156** can be formed on the second detection surface **1184**.

Operation of the sensor **1150** is similar to that described above. For example, light **1161** is directed through the first detection surface **1152**, which can be transparent. The light **1161** passes through the transparent conductor **1173** and through the grating **1156** and impinges the flexible mechanical structure **1154**. The light is reflected from the flexible mechanical structure **1154** and is diffracted by grating **1156** before being detected by detectors **1158**.

FIG. **11**C depicts a cross-sectional schematic diagram of another exemplary force sensor **1190** in accordance with the present teachings. The force sensor **1190** can comprise a detection surface **1192**, a piezoelectric actuator **1193** comprising a thin piezoelectric film **1193***a* disposed between a pair of electrodes **1193***b* and **1193***c*, a flexible mechanical structure **1194**, a gap **1195**, a tip **1197**, and a grating **1196**. The force sensor **1190** can be combined with at least one detector and a cantilever to form a force sensor unit.

According to various embodiments, the thin piezoelectric film can comprise a piezoelectric material such as, for example, ZnO or AlN. The piezoelectric film can be deposited and patterned on the flexible mechanical structure **1194** along with the tip **1197**. The piezoelectric actuator **1193** can form, for example, a bimorph structure that can be bent and vibrated by applying DC and AC signals through the electrodes **1193***b* and **1193***c*. According to various embodiments, the grating **1196** can be placed off-center so as to provide a large range of tip motion that can be detected without losing sensitivity.

FIG. **12** depicts a cross-sectional schematic diagram of an array **1200** of force sensors **1201***a-c* in accordance with the present teachings. The array **1200** can comprise multiple force sensors, such as force sensors **1201***a-c*, formed on a detection surface **1202**. Each of the force sensors **1201***a-c* can comprise a flexible mechanical structure **1204**, a gap **1205**, a tip **1207**, an electrode, such as electrodes **1216***a-c*, and a grating **1206**. According to various embodiments, the array **1200** of force sensors can be used for imaging and sensing at the same time so as to enable simultaneous sensing of a physical, chemical, or biological activity and imaging of the sample **1218** surface. The force sensors **1201***a-c* can be combined with at least one detector **1208** and a cantilever (not shown) to form a force sensor unit. Some of the force sensors **1201***a-c* can be modified to include, for example, electrodes, sensitive films, or optical waveguides, while the others can be used for regular probe microscopy imaging of topography. Thus, each force sensor can perform the same or different function.

For example, force sensor **1201***a* can be used to measure and image the elasticity or adhesion of the surface of sample **1218**. Further, the grating **1206** can be used with electrode **1216***a* to provide actuation of the flexible mechanical structure **1204** by applying a voltage between contacts **1220***a* and **1220***b*, respectively. The elasticity information can be measured by applying known dynamic and quasi-static forces to the surface with the tip **1207** using an external actuator or by applying voltage to the terminals **1220***a* and **1220***b*. At the same time, the diffraction order intensities can be monitored by the optical detectors **1208** or a capacitance change can be detected by electrical means to determine the resulting tip displacement. Viscoelasticity or adhesion can be calculated using computer models well known by those who are skilled in the art of probe microscopy.

Force sensor **1201***b* can be used to measure and image the topography of the surface of sample **1218** similarly as described herein using beam **1210** to generate diffraction orders **1212***a-c* that can be detected by detectors **1208**. In the case of force sensor **1201***b*, the grating **1206** can be used with electrode **1216***b* to provide actuation of the flexible mechanical structure **1204** by applying a voltage between contacts **1220***c* and **1220***d*, respectively.

Still further, the force sensor **1201***c* can be used to measure and image the surface potential of sample **1218**. In the case of

force sensor **1201***c*, the grating **1206** can be used with electrode **1216***c* to provide actuation of the flexible mechanical structure **1204** by applying a voltage between contacts **1220***e* and **1220***f*, respectively. Moreover, the sample **1218** can be biased with respect to the tip **1207** of the force sensor **1201***c* using the electrical terminal **1220***g* to assist in surface potential measurements. The tip **1207** on the force sensor **1216***c* can have a separate electrical terminal **1220***h* which is electrically isolated from the other electrodes **1220***f* and **1220***e* and placed in the dielectric sensor flexible mechanical structure **1204**. The surface potential can then be measured using an electric potential measurement device connected between terminals **1220***g* and **1220***h*. Furthermore, an external source (not shown) can be connected to terminals **1220***g* and **1220***h* and the current flow in that electrical circuit can be measured to locally determine the flow of ions or electrons available from the sample **1218** or in a solution that the force sensor **1216***c* is immersed.

As described previously, the force sensors **1216***a* and **1216***b* can be used to obtain surface topography and elasticity information. This information can be used by an external controller to adjust the position of the tips **1207** of individual force sensors to optimize the measurements. As such, the array **1200** can be used to measure elasticity, electrochemical potential, optical reflectivity, and fluorescence while also imaging the surface.

FIGS. **13**A and **13**B depict top-down and cross-sectional schematic diagrams of an exemplary force sensor **1300** in accordance with the present teachings. In FIGS. **13**A and **13**B, the force sensor **1300** can comprise a detection surface **1302**, a grating **1306**, a tip **1307**, an electrostatic cantilever actuator flexible mechanical structure **1317**, and a cantilever **1322**. As shown in FIG. **13**B, the force sensor **1300** can also include an optical port that can be created, for example, by etching a hole **1332** through the detection surface **1302**. According to various embodiments, the grating **1306** can be a diffraction grating comprising a plurality of conductive fingers that can be deformable and that can be electrostatically actuated independently of the cantilever **1322** in order to control the relative gap **1305** distance (d) between the grating **1306** and the reflecting cantilever **1322**. Further, the cantilever **1322** can have its own electrostatic actuation mechanism **1317**. With the cantilever **1322** having its own electrostatic actuation mechanism **1317**, displacement measurements can be optimized on each cantilever **1322** of an array of independent force sensor structures. With this capability, the initial positions from topography, misalignment with the imaged sample, and/or process non-uniformities can be measured and corrected.

In operation, as shown, for example, in FIG. **13**B, a light **1310** can be directed at the cantilever **1322** through the hole **1332**. The light **1310** is reflected from the cantilever and then diffracted by the grating **1306**. Various diffraction orders **1312***a-c* can be detected by detectors **1308**.

FIG. **14** shows a force sensor structure **1400** used in an AFM system **1401** according to various embodiments. The AFM system **1401** can comprise a force sensor **1403**, a detector **1408**, such as a photodiode, a light source **1411**, such as a laser diode, and a computer **1430** comprising a first processor **1440** to generate a control loop for imaging material properties and a second processor **1450** to generate a control loop for fast tapping mode imaging. The second processor **1450** can further control an integrated electrostatic actuator, as described herein.

As shown in FIG. **14**, the force sensor **1403** can be fabricated, for example, on a detection surface **1402** and placed on a holder **1428**, which can be attached to an external piezoelectric actuator (piezo tube) **1427**. The intensity of, for example, the $+1^{st}$ diffraction order of light diffracted by a grating **1406** in the force sensor **1403** is detected by the detector **1408** as the tip **1407** displacement signal. For example, with a 4 μm grating period and a 670 nm laser wavelength, the $+1^{st}$ diffraction order is reflected at a 9.6° angle from the grating normal. Tilting the detection surface **1402** by 6.2° with respect to the incident beam **1410** provides a total of 22° angular deflection. According to various embodiments with the force sensor **1403**, significantly all of the light **1410** can be reflected from the grating **1406** and the flexible mechanical structure **1404**, eliminating optical interference problems due to reflections from the sample **1418**. This can provide a clean background for tip displacement measurements.

The performance of the AFM **1401** having a force sensor, such as those described herein, can be characterized using an integrated electrostatic actuator. For example, an optical interference curve with a DC bias range of 24-36 V was traced and the bias was adjusted for optimum sensitivity point at 30 V. The displacement sensitivity at this bias level was 204 mV/nm. The RMS noise measured in the full DC-800 kHz bandwidth of the photodetector **1408** was 18 mV RMS. This value, confirmed by spectrum analyzer measurements, corresponds to 1×10^{-3} Å/√Hz minimum detectable displacement noise with 1/f corner frequency of 100 Hz. Using the laser power available from the 0^{th} and -1^{st} orders and differential detection, this value can be lowered well below 5×10^{-4} Å/√Hz without increasing the laser power or using etalon detection. The dynamic response of a typical flexible mechanical structure was also measured using electrostatic actuation, indicating a resonance frequency of 720 kHz with a quality factor of 4.1, suitable for fast tapping mode imaging.

Two controller schemes interfaced with the AFM system **1401** can be used. The first scheme is used with the first processor **1440** comprising a controller **1443** and an RMS detector **1445** for material property measurement and imaging using transient interaction force signals. The Z-input of the piezo tube **1427** is driven to generate a 2 kHz 120 nm peak sinusoidal signal while the controller **1443** keeps constant the RMS value of the photo-detector signal generated by the force sensor **1403** when it taps on the sample **1418**. The 2 kHz signal frequency is chosen as a compromise between the ability to generate adequate vertical (Z direction) displacement of the piezo tube and the frequency response of the internal RMS detector **1445** for a typical force sensor structure **1401**. The second controller scheme is used with the second processor **1450** for fast tapping mode imaging. In this case, the Z-input of the piezo tube is disabled and the integrated electrostatic actuator is used to generate a 10 nm peak-to-peak free air tapping signal in the 500-700 kHz range as well as the signals to control the force sensor **1403** tip **1407** position keeping the RMS value of the tip vibration at the desired set point.

FIGS. **15**A-**15**C show the results of a force sensor described herein used in a dynamic mode in an AFM system, such as that shown in FIG. **14**. The results shown in FIGS. **15**A-**15**C provide information about the transient interaction forces with a resolution that exceeds conventional systems. In this example, the detection surface, such as a substrate, can be oscillated, and can be driven by a suitable actuator. Both the attractive and repulsive regions of the force curve are traced as the tip **1407** contacts the sample **1418** during some phases (I-V) of each cycle. The inserts (i)-(v) in FIG. **15**A show the shape of the flexible mechanical structure **1404** during different phases of a cycle while the substrate is oscillated at 2 kHz by the Z-piezo. FIG. **15**A also shows the measured detector

output signal during each phase corresponding to each cycle. The detector **1408** output is proportional to the force acting on the tip **1407**.

In this particular case, during phase I, the tip **1407** is away from the sample **1418** surface where it experiences long range attractive forces. When brought close to the surface, the tip **1407** jumps to contact (0.2 nm change in tip position, phase II) and remains in contact for about 14% of the cycle. In the middle of the period, the repulsive force applied to the sample **1418** reaches to a peak value of 163 nN (1.22 nm tip displacement, phase III). When the tip **1407** is withdrawn, the tip **1407** experiences capillary forces of 133 nN (phase IV) before breaking off from the liquid film on the sample **1418** surface (phase V). As shown in FIG. **15**B, the controller **1443** of FIG. **14** can be used to stabilize the signal with a constant RMS, so that the output signal of the force sensor shows individual and repeatable taps on the sample **1418**. The signals shown are averaged 100 times on a digitizing oscilloscope, and the noise level is less than 1 nN with 800 kHz measurement bandwidth.

An application of this mode of operation is the measurement of local viscoelastic properties. For example, in FIG. **15**C individual tap signals obtained on (100) silicon (E=117 GPa) and photoresist (PR, Shipley 1813) (E=4 GPa) samples using a sensor with having a tip 50 nm radius of curvature were compared. The maximum repulsive force is significantly larger for the silicon sample even though the tip-sample contact time is less than that of photoresist (PR) indicating that the silicon is stiffer than PR. Consequently, the positive slope of the time signal during the initial contact to silicon sample is significantly larger than it is when in contact with the PR sample. The silicon sample also shows higher capillary hysteresis. Both of these results are consistent with existing models and data. Moreover, the tip **1407** can encounter different long range van der Waals or electrostatic forces on these two samples. Since this information is obtained with nanometer scale lateral resolution and applying nanoNewton level forces, this mode of operation can be referred to as "nano-characterizer" mode of operation.

The results shown in FIGS. **15**A-**15**C demonstrate a unique feature of the force sensors described herein for dynamic force measurements. In particular, the output signal is generated only when there is an interaction force on the tip. With broad bandwidth and high sensitivity, the force sensors enable direct measurement of transient interaction forces during each individual tap with high resolution and without background signal. This provides information on properties of the sample such as adhesion, capillary forces, as well as viscoelasticity.

The force sensor can be used to image various material properties by recording at each pixel the salient features of the tap signal. For example, the AFM system **1401** shown in FIG. **14** can be used to monitor transient interaction forces. The first controller **1440** of system **1401** can be used to maintain a constant RMS value of the output signal while scanning the tapping tip **1407**. FIG. **16**A shows the transient tap signals on the PR and silicon regions of a sample having 360 nm thick, 2 μm wide PR strips with 4 μm periodicity patterned on silicon surface. Significant differences exist between the tap signals in terms of both the attractive and repulsive forces acting on the tip **1407**. For example, the silicon surface exhibits a much larger adhesion force when compared to the PR surface. Because the first controller **1440** attempts to maintain a constant RMS value over the sample, it forces the tip **1407** to indent more into the PR region. As such, the tip **1407** experiences a larger repulsive force. The shape of the individual tap signals in the attractive region has a strong dependence on the environment.

To form an image in which sample adhesion dominates the contrast mechanism, a peak detector circuit can be used to record the peak attractive force (PAF) as the pixel value, such as points A_{si}, A_{PR} in FIG. **16**A. Simultaneously, the sample topography can be recorded using a fixed RMS value set point. FIG. **16**B shows the resulting adhesion (PAF) and topography images, **1661** and **1662**, respectively, of the sample. In the topography image **1662**, the stripes **1664** correspond to the 360 nm high PR pattern (Shipley **1805**) and stripes **1665** correspond to the silicon surface. In the PAF image **1661**, the silicon surface appears brighter than PR due to higher adhesion forces. By recording the peak repulsive force (PRF) as the pixel value, images where sample viscoelasticity dominates the contrast, such as at points R_{si}, R_{PR} in FIG. **16**A, can be obtained.

Simultaneously recorded PRF and topography images of the same sample region are shown in FIG. **16**C at **1671** and **1672**, respectively. The PRF image **1671** shows a reversed contrast when compared to the PAF image, while the topography image is repeatable. The PR strips **1674** appear brighter in the PRF image as indicated by the individual tap signals shown in FIG. **16**A. Also, many more contamination particles are adhered to the silicon **1675** surface as compared to the PR strips **1674**, and these particles are seen with high contrast. This is consistent with higher adhesion measured on the silicon in the PAF image **1661**.

Although a simple controller based on the RMS value set point is described in this embodiment, it is contemplated that different control schemes, such as those sampling individual tap signals at desired time instants and using those values in the control loop can also be used. For example, if the peak value of the repulsive force is kept constant as the control variable, images where the contact-to-peak force time determines the contrast—a direct measure of sample stiffness can be obtained. Several existing models can then be used to convert these images to quantitative material properties. Similarly, by detecting the attractive force peaks before and after the contact one can obtain quantitative information on the hysteresis of the adhesion forces.

FIGS. **17**A and **17**B show the results of fast tapping mode imaging of sample topography with a single sensor probe using the setup shown in FIG. **14**. In this mode, the Z-input of the piezo tube **1427** is disconnected and used only for x-y scan. The integrated electrostatic actuator is used for both oscillating the tip **1407** at 600 kHz and controlling the flexible mechanical structure **1404** bias level in order to keep the oscillation amplitude constant as the tapping mode images are formed.

A standard calibration grating with 20 nm high, 1 μm wide, sharp steps with 2 μm periodicity was used as the fast imaging sample (NGR-22010 from Veeco Metrology). FIG. **17**A shows the images of a 4 μm×250 nm area (512×16 pixels) of the grating with line scan rates of 1 Hz, 5 Hz, 20 Hz, and 60 Hz. FIG. **17**B shows the cross sectional profiles of individual scan lines for each image. The AFM system **1401** had an x-y scan capability that can go up to 60 Hz.

For comparison, FIGS. **17**C and **17**D, show the tapping mode images and line scans using a conventional AFM system on the same sample used in the example of FIGS. **17**A and **17**B. The commercial AFM system used a tapping mode cantilever. The cantilever was made of silicon and had a 300 kHz resonance frequency (TESP-A from Veeco Metrology). In this case, the tapping piezo on the cantilever holder was used as the actuator.

As can be seen in the figures, AFM systems described herein are able to resolve the grating with at least a 20 Hz line scan rate and in some cases a 60 Hz line scan rate. In contrast,

conventional AFM systems are not able to follow the sharp steps starting at 5 Hz, and fail to produce a viable image after 20 Hz line scan rate. The imaging bandwidth of the AFM system **1401** described herein was about 6 kHz. However, controlling the dynamics of the air flow in and out of etch holes on two sides of the flexible mechanical structure, such as those shown at **280** in FIG. **2**C. With a sealed cavity, the imaging bandwidth of various force sensors described herein can be increased to more than 60 kHz. Moreover, since the force sensor unit is a well damped system even in air, methods other than RMS detection can be used to implement faster controllers.

FIG. **18** depicts a cross-sectional schematic diagram of another exemplary force sensor unit **1800** in accordance with the present teachings. FIG. **18** shows a light source **1811** and a photodiode **1808** on the surface of an opaque, rigid, detection surface **1802**. The detection surface **1802** can be a printed circuit board, a silicon wafer, or any other solid material. Furthermore, the light source **1811** and photodiode **1808** can be constructed or sourced externally and attached to the detection surface or fabricated directly into the material using integrated circuit or micromachining fabrication techniques.

The light source **1811** can be an optical fiber or the end of a microfabricated waveguide with an appropriate reflector to direct the light to the desired location in the force sensor unit **1800**, such as a diffraction grating **1806**. The optical diffraction grating structure **1806** exists above the light source **1811**, and is characterized by alternating regions of reflective and transparent passages. A gap **1805** defining a cavity is formed between the grating **1806** and the detection surface and can be sealed at some desired pressure (including low pressures) with any gas or gas mixture, or can be open to ambient. Further, a flexible mechanical structure **1804** (also called a reflective surface or reflective diaphragm) exists above the diffraction grating **1806** that reflects light back towards the detection surface **1802**. The diffraction grating **1806** and the reflective surface **1804** together form a phase sensitive diffraction grating.

When illuminated with the light source **1811** as shown, diffracted light reflects back towards the detection surface **1802** in the form of diffracted orders **1812***a* and **1812***b* with intensity depending on the relative position between the reflective surface **1804** and the diffraction grating **1806**, or the gap **1805** thickness. The diffracted orders **1812***a* and **1812***b* emerge on both the right and left side and are traditionally numbered as shown in FIG. **18**. For the phase sensitive diffraction grating with 50% fill factor, i.e. reflective and transparent passages with the same width, only the zero order and all odd orders emerge. The intensity of any one or any subset of these orders can be measured with photo-diodes **1808** to obtain information about the relative distance between the diffraction grating **1806** and the reflective surface **1804**. The angles of the orders are determined by the diffraction grating period, Λ_g, and the wavelength of the incident light, λ. For example, in the far field the angle of the order n, θ_n, will be given by the relation [1]:

$$\sin(\theta_n) = n\frac{\lambda}{\Lambda_g}. \quad [1]$$

In order to illustrate how the intensity of the reflected orders depends on the gap thickness, the normalized intensity of the zero and first orders are plotted versus the gap in FIG. **19** assuming normal incidence. The remaining odd orders (i.e. 3^{th}, 5^{th}, etc.) are in phase with the 1^{st} but have decreasing peak intensities. This behavior can be obtained when the light source **1811** remains coherent over the distance between the reflector and the diffraction grating **1806**.

Furthermore, the diffracted orders can be steered to desired locations using structures such as Fresnel lenses. For this purpose, the gratings **1806** can be curved or each grating finger can be divided into sections of sub-wavelength sized gratings.

Also using wavelength division multiplexing, light with different wavelengths can be combined and used to illuminate a multiplicity of force sensors with different grating periods. The reflected diffraction orders from different force sensors can either be converted to electrical signals by separate photodetectors, or the reflected light at different wavelengths can be combined in an optical waveguide or optical fiber to minimize the number of optical connections to a processor that subsequently decodes the information carried at different wavelengths. Therefore, a multiplicity of force sensors can be interrogated using a single physical link or a reduced number of physical links to a processing system.

According to various embodiments, such as chemical and biological sensors, the reflective surface **1804** can be made of single material or a multi layered material that changes its optical properties, such as reflectivity, in response to a chemical or biological agent. Similarly, the reflective surface **1804** can be a micromachined cantilever or a bridge structure made of single or layered material that deforms due to thermal, chemical, magnetic, or other physical stimulus. For example, an infrared (IR) sensor can be constructed by having a bimorph structure including an IR absorbing outer layer and a reflective layer facing the light source **1811**. In other embodiments, such as a microphone or a pressure sensor, the reflector **1804** can be in the shape of a diaphragm.

In many applications, moving or controlling the position of the reflective surface **1804** may be desired for self-calibration, sensitivity optimization, and signal modulation purposes. For example, if the reflective surface **1804** is a diaphragm or flexible mechanical structure, as in the case of a microphone or a capacitive micromachined transducer, vibrating the diaphragm to produce sound in a surrounding fluid may be desired for transmission and self-calibration. Also, while measuring the displacement of the diaphragm, controlling the nominal gap **1805** height to a position that will result in maximum possible sensitivity for the measurement may be desired. These positions correspond to points of maximum slope on the curves in FIG. **19**, where it can be seen graphically that a change in gap thickness results in a maximum change in intensity of the diffracted order. These examples can use an added actuation function that can be accomplished with electrostatic actuation. In one exemplary embodiment, the entire diaphragm structure **1804** or just a certain region thereof can be made electrically conductive. This can be accomplished by using a non-conductive material for the reflective surface **1804** such as a stretched polymer flexible mechanical structure, polysilicon, silicon-nitride, or silicon-carbide, and then making the material conductive in the desired regions either through doping or by depositing and patterning a conductive material such as aluminum, silver, or any metal or doping the flexible mechanical structure **1804**, such as when the flexible mechanical structure comprises polysilicon.

In another exemplary embodiment, the entire diffraction grating **1806** or a portion of the grating **1806** can be made conductive. The flexible mechanical structure **1804** and diffraction grating **1806** can together form a capacitor which can hold charge under an applied voltage. The strength of the attraction pressure generated by the charges can be adjusted

by controlling the voltage, and precise control of the flexible mechanical structure **1804** position is possible.

FIGS. **20**A and **20**B demonstrate this function. First, increasing voltage levels were applied to pull the flexible mechanical structure **1804** towards the detection surface **1802**, which resulted in decreasing gap **1805** height (i.e. a movement from right to left on the curve in FIG. **19**). The change in light intensity of the first diffracted order that resulted was measured with a photodiode and plotted at the top. To illustrate why controlling the flexible mechanical structure position may be important, a displacement measurement of the flexible mechanical structure **1804** was made at different gap **1805** heights as follows. At different applied voltages, sound was used to vibrate the flexible mechanical structure **1804** with constant displacement amplitude and the resulting change in light intensity of the first diffracted order was again measured with a photodetector. As shown in the bottom of FIG. **20**A, voltage levels that move the gap height to a point corresponding to a steep slope of the optical curve are desirable as they produce larger measurement signals for the same measured input. Although sound pressure was used to displace the flexible mechanical structure **1804**, the device can be tailored to measure any physical occurrence, such as a change in temperature or the exposure to a certain chemical, or an applied force so long as the flexible mechanical structure **1804** was designed to displace as a result of the occurrence.

This displacement measuring scheme has the sensitivity of a Michelson interferometer, which can be used to measure displacements down to 1.4×10^{-5} Å for 1 Hz bandwidth for 1 mW laser power. Various embodiments disclosed herein can provide this interferometric sensitivity in a very small volume and can enable integration of light source, reference mirrors and detectors in a mechanically stable monolithic or hybrid package. This compact implementation further reduces the mechanical noise in the system and also enables easy fabrication of arrays. The high sensitivity and low noise achieved by the various embodiments far exceed the performance of other microphones or pressure sensors based on capacitive detection.

FIG. **21** depicts a cross-sectional schematic diagram of another exemplary force sensor **2100** in accordance with the present teachings. FIG. **21** shows a force sensor comprising a detection surface **2102**, which allows the light source **2111** to be placed at a location behind the substrate **2102**. The detection surface **2102** also allows the reflected diffracted orders **2112** to pass through, and the light intensity of any of these orders can measured at a location behind the substrate **2102**. The force sensor **2100** can also comprise a flexible mechanical structure **2104**, such as a diaphragm, and a diffraction grating **2106** that can be made moveable so that its position may be controlled via electrostatic actuation, with a region of the substrate serving as a bottom electrode **2116**. Changing the flexible mechanical structure—grating gap thickness can be used to optimize the displacement sensitivity of the flexible mechanical structure, as discussed above with reference to FIG. **18**.

Several material choices exist for the detection surface **2102** that is transparent at the wavelength of the incident light. These include quartz, sapphire, and many different types of glass, and it can be silicon for light in the certain region of the IR spectrum. Furthermore, several manufactures sell these materials as standard 100 mm diameter, 500 μm thick wafers, which make them suitable for all micro-fabrication processes including lithographic patterning. As in the force sensor **1800**, several different material types may be used for the flexible mechanical structure **2104**, and the cavity between the platform and diaphragm may be evacuated or filled with any type of gas mixture.

The diffraction grating **2106** may be made of any reflective material, as long as the dimensions are chosen to produce a compliant structure that may be moved electrostatically. As explained for force sensor **1800**, electrostatic actuation requires a top and bottom electrode. According to various embodiments, the diffraction gating **2106** can serve as the top electrode and the bottom electrode **2116** can be formed on the substrate **2102**. Furthermore, the distance between these electrodes can be small (order of a micrometer) to be able to perform the actuation with reasonable voltage levels (<100V). For example, for force sensor **2100** this means regions of both the diffraction grating **2106** and the detection surface **2102** can be made electrically conductive. If a metal or any other opaque material is chosen to form the bottom electrode **2116** on the detection surface **2102**, the electrode region should exist in a region that will not interfere with the propagation of light towards the diffraction grating **2106** and the flexible mechanical structure **2104**. Alternatively, a material that is both optically transparent and electrically conductive, such as indium-tin oxide, may be used to form the bottom electrode **2116** on the platform. Force sensor **2100** enables one to use the advantages of electrostatic actuation while having a large degree of freedom in designing the flexible mechanical structure **2104** in terms of geometry and materials.

FIG. **22** depicts a cross-sectional schematic diagram of another exemplary force sensor in accordance with the present teachings. FIG. **22** shows the implementation of a resonant-cavity-enhanced (Fabry-Perot cavity) optical force sensor **2200** that can be used to improve displacement sensitivity, which may be defined as the intensity variation of the diffracted beam per unit flexible mechanical structure displacement (i.e., the change of the cavity gap) due to the external excitation. The force sensor **2200** can comprise a detection surface **2202**, two parallel mirror layers, such as a bottom mirror **2203** and a top mirror **2204**, and a grating **2206**. According to various embodiments, the bottom mirror **2203** can be formed on the detection surface **2202** and can include the grating **2206**. Further, the top mirror **2204** can also serve as a diaphragm or flexible mechanical structure.

The bottom mirror **2203** and the top mirror **2204** can be separated by the grating-embedded gap or cavity **2205**, as illustrated in FIG. **22**. As mentioned, the flexible mechanical structure **2204** can have a high reflectance and can act as the top mirror, and the bottom mirror **2203** can be placed beneath the diffraction grating **2206**. The mirror layers can be built, for example, using a thin metal film, a dielectric stack of alternating quarter-wave ($\lambda/4$) thick media, or combination of these two materials.

FIG. **23**A shows the calculated intensity of the first order versus the gap **2205** for the case of a metal mirror made of silver, but any other metal with a high reflectivity and low loss at the desired wavelength can be used. It can be noticed that the change in the diffracted order intensity with cavity gap **2205** in the resonant-cavity-enhanced optical force sensor **2200** departs from that shown in FIG. **19**, depending on optical properties of the mirror layers, such as reflectance. As seen in FIG. **23**A, the slope of the intensity curve increases with increasing metal layer thickness, hence the mirror reflectivity. The sensitivity in the unit of photocurrent per flexible mechanical structure displacement (A/m) is also evaluated when the intensity of the first-order, diffracted from an incident light of 1 mW optical power, is detected by a detector, such as a photo-diode with 0.4 A/W responsivity. The calcu-

lation result for various metals is presented in FIG. **23**B. For example, the displacement sensitivity can be improved by 15 dB using a 20 nm thick silver layer for the mirror. For different metals with higher optical loss, the improvement may be less or the sensitivity may decrease as in the case of aluminum.

FIG. **24**A shows the experimental data obtained by two structures with and without an approximately 15 nm thick silver mirror layer with an aluminum diaphragm. FIG. **24**A shows data for an embodiment without a mirror. Similar to FIG. **20**A, increasing the DC bias voltage helps one to trace the intensity curve in FIG. **24**A from right to left. Because there is no Fabry-Perot cavity formed in this embodiment, the intensity curve is smooth.

FIG. **24**B shows the same curve for the Fabry-Perot cavity with a silver mirror. In this embodiment, the intensity curve has sharper features and large slopes around 16-18V DC bias. This is similar to the change predicted in FIG. **23**A. The sensitivity dependence is also verified by subjecting the diaphragm to an external sound source at 20 kHz and recording the first order intensity at different DC bias levels. FIG. **24**C shows the result of such an experiment and verifies that the optical detection signal is much larger for the 16V DC bias as compared to 40V, where the average intensity is the same. For a regular microphone without the Fabry-Perot cavity structure, one would expect to obtain larger signal levels with 40V DC bias.

FIG. **25** shows the calculated intensity of the first order versus the gap **2205** for the case of the dielectric mirrors. In this embodiment the dielectric mirrors are made of silver and SiO_2/Si_3N_4 pairs but any other dielectric material combination resulting in a high reflectivity and low loss at the desired wavelength can be used. The reflectance of the mirror can be controlled by the change in the thickness of the metal film and the number of alternating dielectric pairs for a given choice of mirror materials. In FIG. **25**, the number of pairs is increased from 2 to 8 and which in turn increases the slope of the intensity curve resulting in a higher sensitivity.

In contrast to the dielectric mirror case, peak intensity amplitude of the first order decreases with the metal mirror reflectance due to the optical loss in the metal film (FIG. **23**A), and thus metals of low absorption loss provide good results for the metal-mirror applications. In addition, the optimal bias position moves toward to a multiple of $\lambda/2$ with the reflectance of the metal mirror. However, the optimal bias position can be easily achieved through electrostatic actuation of the flexible mechanical structure **2204**.

The scheme of the resonant-cavity-enhanced optical force sensor can be also applied to the other microstructures described herein with a simple modification of fabrication process.

FIG. **26** depicts a cross-sectional schematic diagram of another exemplary force sensor in accordance with the present teachings. FIG. **26** shows a force sensor **2600** comprising a detection surface **2602**, a flexible mechanical structure **2604** (also called a diaphragm), a gap **2605** (also called a cavity), and a grating **2606**. The grating **2606** can be reflective and can be formed on the flexible mechanical structure **2604**, which can be transparent. Further, the grating can comprise reflective diffraction fingers. According to various embodiments, the detection surface **2602** can be reflective. The force sensor **2600** can form a phase-sensitive diffraction grating when illuminated from the topside of the flexible mechanical structure **2604** as shown in FIG. **26**. Similar to the embodiment shown in FIG. **18**, the zero and all odd orders of light are reflected back and have intensities that depend on the gap **2605** between the diffraction grating **2606** and the detection surface **2602**. The thickness of the gap **2605** can also include the thickness of the flexible mechanical structure **2604**, which may be made of any transparent material. Examples of transparent materials include silicon dioxide, silicon nitride, quartz, sapphire, or a stretched polymer membrane such as parylene. Because the detection surface **2602** is reflective, any material, including semiconductor substrates or plastics, can suffice given that they are coated with a reflective layer, such as metal. To add electrostatic actuation, as described herein, a region of both the detection surface **2602** and the flexible mechanical structure **2604** can be made electrically conductive. For the flexible mechanical structure **2604**, this can be accomplished by using a material that is both reflective and electrically conductive for the diffraction grating **2606**. For example, any reflective metal would be suitable. In various embodiments, because the light source **2611** and detectors (not shown) exist on the top side of the flexible mechanical structure **2604**, this particular embodiment offers remote sensing capabilities. For example, if measuring the displacement of the flexible mechanical structure **2604** due to a change in pressure is desired (as would be the case for a pressure sensor or a microphone), the detection surface **2602** can be attached to a surface and the light source **2611** and detectors can be stationed in a remote location, not necessarily close to the diaphragm.

In addition to remote measurements, the force sensor **2600** can be remotely actuated to modulate the output signal. For example, an acoustic signal at a desired frequency can be directed to the flexible mechanical structure **2604** with the grating **2606** and the output signal can be measured at the same frequency using a method such as a lock-in amplifier. The magnitude and phase of the output signal can give information on the location of the flexible mechanical structure **2604** on the optical intensity curve in shown in FIG. **19**, which in turn may depend on static pressure, and other parameters such as temperature, etc. Similar modulation techniques can be implemented using electromagnetic radiation, where an electrostatically biased flexible mechanical structure with fixed charges on it can be moved by applying electromagnetic forces. In this case, the flexible mechanical structure can be made of some dielectric material with low charge leakage.

FIG. **27** depicts a cross-sectional schematic diagram of another exemplary force sensor in accordance with the present teachings. FIG. **27** shows a force sensor **2700** comprising a detection surface **2702**, a transparent support comprising electrodes **2703**, a flexible mechanical structure **2704** (also called a diaphragm), a gap **2705** (also called a cavity), a grating **2706**, and a detector **2708**. The detection surface **2702** in force sensor **2700** can be transparent so that the light source **2711** and detectors **2708** can be placed at a location behind the detection surface. However, placing the light source and detectors **2708** on the surface of the detection surface is equally viable and allows the usage of substrates such as silicon wafers or printed circuit boards. According to various embodiments, the grating **2706** can be moveable. As discussed herein, controlling the gap **2705** between the grating **2706** and the reflective flexible mechanical structure **2704** can be used to optimize detection sensitivity.

Various methods can be used to control the thickness of the gap **2705**, such as, for example, controlling the flexible mechanical structure **2704** position, the grating **2706** position, or both. Furthermore, the force sensor **2700** allows placement of the grating **2706** anywhere in the cavity **2705** between the light source **2711** and the flexible mechanical structure **2704**.

According to various embodiments, the use of highly reflective semi-transparent layers to enhance displacement sensitivity using Fabry-Perot cavity, as described by, for

example the embodiment shown in FIG. **22**. For example, a Fabry-Perot cavity can be implemented with any of the other embodiments mentioned so far, when the semitransparent layer is placed in close proximity to the diffraction grating.

For example, the sensors shown in FIGS. **18** and **21** can place a semi-transparent layer on the top or bottom surface of the grating. Further, the force sensor shown in FIG. **26** can place a semi-transparent layer on either the top or backside of the flexible mechanical structure, which is where the diffraction grating is located in this case.

FIG. **28**A depicts a cross-sectional schematic diagram of another exemplary force sensor in accordance with the present teachings. FIG. **28**A shows a force sensor **2800** comprising a detection surface **2802**, a flexible mechanical structure **2804** (also called a diaphragm), a first gap **2805**A (also called a first cavity), a second gap **2805**B (also called a second cavity), a first grating **2806**A (also called a reference grating), a second grating **2806**B (also called a sensing grating), a detector **2808**, and a light source **2811**. The second grating **2806**B can be formed on the flexible mechanical structure **2804**, which can be transparent. Moreover, the flexible mechanical structure **2804** can be formed over the first grating **2806**A.

In this embodiment, the flexible mechanical structure **2804** is or has a reflective diffraction grating, second grating **2806**B, rather than a mirror-like uniform reflector surface described above. Moreover, the second grating **2806**B on the flexible mechanical structure **2804** reflector can have the same periodicity as the first grating **2806**B, but can be offset and can have diffraction fingers whose widths are smaller than the gap between the first grating **2806**A. This offset allows some of the incident light to pass through. This structure, as shown in FIG. **28**A, allows some of the incident light from light source **2811** to transmit through the whole force sensor **2800** and also introduces new diffraction orders in the reflected field. As such, this provides a different kind of phase grating than those described above.

FIG. **28**B is provided to assist in understanding the operation of a sensor having two gratings. For example, one can consider the phase of the light reflected from the first grating **2806**A (also called the reference grating) (ϕ_1) and the second grating **2806**B on the flexible mechanical structure **2804** (ϕ_2). When the difference between ϕ_1 and ϕ_2 is $2k\pi$, k=0, 2, 4, . . . , the apparent period of the grating is Λ_g (apparent reflectivity of 1, 0, 1, 0 regions assuming perfect transmission through the transparent diaphragm **2804**) and the even diffraction orders are reflected with angles

$$\sin(\theta_n) = n\frac{\lambda}{\Lambda_g},\ n = 0, \pm 2, \pm 4 \ldots \quad [2]$$

In contrast, when the difference between ϕ_1 and ϕ_2 is $m\pi$, m=1, 3, 5, . . . , the apparent period of the grating is $2\Lambda_g$ (apparent reflectivity of 1, 0, −1, 0, 1 regions assuming perfect transmission through the flexible mechanical structure **2804**) and the odd diffraction orders are reflected with angles

$$\sin(\theta_n) = n\frac{\lambda}{2\Lambda_g},\ n = 1, \pm 3, \pm 5 \ldots \quad [3]$$

Here it is assumed that the width of the reflective fingers on the reference grating **2806**A and the second grating **2806**B on the flexible mechanical structure **2804** are the same. This does not have to be the case if the interfering beams go through different paths and experience losses due to reflection at various interfaces and also incidence angle variations. The diffraction grating geometry can then be adjusted to equalize the reflected order intensities for optimized interference.

In this double grating structure, shown, for example in FIG. **28**A, the intensity of the odd and even numbered orders change to 180° out of phase with each other when the gap **2805**B between the reference grating **2805**A and sensing grating **2806**B changes. The even numbered diffraction orders are in phase with the zero order reflection considered in the previous embodiments.

One advantage of having other off-axis even diffraction orders in phase with the specular reflection is that it enables one to easily use differential techniques. This is achieved by taking the difference of the outputs of two detectors positioned to detect odd and even orders, respectively. Hence the common part of the laser intensity noise which is common on both orders can be eliminated.

The sensors described herein can be used with various AFM systems and methods to measure, for example, the attractive and repulsive forces experienced by the tip to provide information on various surface forces and sample properties. Moreover, the force sensors described herein can be used with several AFM methods, including nanoindentation, force modulation, ultrasonic AFM, pulsed force mode, and dynamic force spectroscopy that have been developed to characterize the viscoelastic properties of the material under investigation.

Thus, a force sensor for probe microscope for imaging is provided that can offer the unique capability for measuring interaction forces at high speeds with high resolution. In addition to optical interferometer, various integrated readout techniques including capacitive, piezoelectric or piezoresistive can be used. Similarly, the actuators described herein can be a thin film piezoelectric, a magnetic, or a thermal actuator. Further, force sensors with multiple tips, where several sensing and actuation functions are implemented in the same device are also envisioned. Still further, electrical measurements, chemical measurements, information storage and nanoscale manipulations can be performed all while simultaneously obtaining topography images of the sample in gas or liquid media. As such, the sensors and the methods of imaging described herein open a new area in the field of probe microscopy. This new device can enable high speed imaging and provide images of elastic properties and surface conditions of the sample under investigation.

Force sensors of the type described above in connection with the several exemplary embodiments are particularly suitable for probe microscope designs and imaging methods. In the following exemplary embodiments, multi-directional manipulation of the described force sensors will be explained for measurement of structures having three-dimensional topography. Movement of the force sensors is described with minimal contact and with non-contact. In particular, the force sensors described can be manipulated to measure the topography of microscale and nanoscale three dimensional structures with nanometer and sub-nanometer resolution.

The above described exemplary force sensors suitable for the multi-directional manipulation can be characterized as force sensing integrated readout and active tip (FIRAT) type. Upon manipulating one or more FIRAT probes in three-dimensional space with respect to an object or surface, topography of the surface or object can be obtained. Even further, imaging can occur within a topographical trench or other

recessed configuration without using an external scanner and controller loop to scan the sample or the substrate of the FIRAT probe.

Currently, an atomic force microscope (AFM) is used as a calibration tool for imaging critical dimensions in microelectronics due to its capability of examining three dimensional structures. These three dimensional structures typically include those having sidewalls from 10 nm to 5 μm in height. However, when measuring the sidewall structure in deep trenches, AFM cantilevers need to be tilted to have the tip interact with the sidewall being measured. This can be inconvenient and can prohibit imaging of both the top to bottom and sidewall profiles with acceptable throughput.

Accordingly, the exemplary embodiments that follow describe the maneuvering of the force sensor structure and more particularly the probe tip of the force sensor structure, in different directions to provide multiple degrees of freedom for tip motion and orientation.

Referring to FIGS. **29**A and **29**B, there is shown a top schematic and side sectional schematic views of a force sensor structure **2900** in which electrostatic actuation is employed to enable three dimensional imaging in accordance with the present teachings.

In the exemplary embodiment, the force sensor structure **2900** can comprise a support surface such as a substrate **2902**, a flexible mechanical structure **2904**, a gap **2905**, plural top electrodes such as electrodes **2916***a-b*, plural bottom electrodes such as electrodes **2920***a-b*, and a tip **2907**. In some embodiments, the force sensor **2900** can also include a grating (not shown). According to various embodiments, the flexible mechanical structure **2904** can be fully clamped around its circumference. Alternatively, the flexible mechanical structure **2904** can be a clamped-clamped beam with a rectangular or H-shape, where the short edges at the ends are clamped. Still further, the flexible mechanical structure **2904** can be a cantilever structure or a similar structure that changes shape in a predictable manner in response to a force applied to the tip **2907**. These types of structures are described above in connection with FIGS. **10**B through **10**D and are applicable to the various exemplary embodiments herein.

The tip **2907** of the force sensor structure **2900** can be made from a variety of materials that enable a high aspect ratio for the tip. The high aspect ratio will ensure that deep trenches or holes of a dimensional structure can be probed. For example, the tip **2907** of the sensor structure can be made from any of single crystal silicon, silicon nitride, tungsten, platinum, or other nanostructures such as carbon-based or ZnO nanotubes. The tip **2907** can be fabricated as an integral part of the flexible mechanical structure **2904** or can be attached to the mechanical structure **2904** using different techniques such as adhesives, focused ion beam deposition, or welding by help of focused ion beam deposition.

Each of the plurality of separate top electrodes **2916***a-b* can be electrically isolated and formed in the flexible mechanical structure **2904**. Moreover, the bottom electrodes **2920***a-b* can be spaced apart from the separate top electrodes **2916***a-b* by the gap **2905**. In some cases, where the flexible mechanical structure **2904** is electrically conductive, separate bottom electrodes **2920***a-b* may be required. Further, the bottom electrodes can be positioned in the substrate **2902** and can be contacted by electrode terminals **2921***a-b*, respectively. Similarly, each of the separate top electrodes **2916***a-b* can be contacted by electrode terminals **2917***a-b*, respectively. In some cases, the electrode terminals **2921***a-b* and **2917***a-b* can be capacitive sensing terminals that can detect a capacitance change formed between the separate top electrodes **2916***a-b* and the bottom electrodes **2920***a-b*.

In FIGS. **29**A and **29**B, a voltage can be applied between the electrode terminals **2917***a* and **2921***a* as well as between electrode terminals **2917***b* and **2921***b*. The electrode terminals therefore integrate the various electrodes and the voltage can be used to selectively control and move any of the separate top electrodes **2916***a-b*, so that they can serve as actuators. Further, the separate top electrodes **2916***a-b* or separate bottom electrodes **2920***a-b* can also perform sensing, similar to that of a dual electrode capacitive micromachined ultrasonic transducer where the vibrations of the sensor flexible mechanical structure are converted to electrical current signals through change in capacitance.

Selected ones of the electrode terminals **2917***a-b* and **2921***a-b* are operable as actuators to manipulate the flexible mechanical structure **2904**, and thereby direct the tip **2907** of the force sensor **2900**. Actuation of the actuatable electrode terminals is by known controllers which apply different DC bias or AC voltages of different amplitude, frequency and phase. Typically, for a clamped-clamped beam structure, at least two of the electrostatic actuator electrodes, such as electrostatic actuators **2917***a-b*, can be selectively actuated. In the case of a four sided beam structure, four selectively actuated independent actuators can be utilized as will be further described. This multiple electrode configuration, in addition to application of DC bias or AC voltages of different amplitude, frequency and phase enables actuation of the fundamental and higher order symmetrical and anti-symmetrical modes of the flexible mechanical structure **2904**. These different modes can be useful for imaging the topography of three-dimensional structures. Furthermore, they can be useful to apply forces in three-dimensions to sample surfaces and measure their reaction. Particular applications can include measurement of friction forces, local piezoelectric and magnetic forces.

The force sensor **2900** can be used as described above in connection with FIG. **10**A for fast imaging where bias voltages are applied between the electrode terminals **2917***a*, **2917***b* and the bottom electrode terminals **2920***a-b* and alternating voltages of the same or reverse phase are applied to the electrode terminals **2917***a* and **2917***b* to vibrate the tip **2907** vertically or laterally to have intermittent contact with a sample surface. In some cases, the forces between the tip **2907** and a close by surface can be sensed without contact for non-contact imaging. The bias voltages applied to the electrode terminals **2917***a*, **2917***b* also control the position of the tip **2907** in response to changes in capacitance detected between the electrode terminals **2917***a-b* and the bottom electrode terminals **2921***a-b*. An external controller (not shown) can read the detected capacitance change and generate the control signals (bias voltages) applied to the electrode terminals **2917***a-b* and the bottom electrode terminals **2921***a-b*.

In the exemplary embodiment, the clamped-clamped beam structure is used to move the tip in vertical and one of the lateral directions by applying different DC bias or AC voltages of different amplitude, frequency and phase using the two electrostatic actuator electrodes. Likewise, the structure can be extended in the other lateral direction by having a four-sided beam structure with four independent actuators. The tip **2907** of the probe can be made from a variety of materials such as silicon, silicon nitride, tungsten, platinum or other nanostructures such as carbon-based or ZnO nanotubes. The important aspect of the tip structure for topography measurement is that it has a high aspect ratio so that deep trenches or holes can be probed.

FIG. **30** shows a cross-sectional schematic diagram of generating an oscillation of the flexible mechanical structure **3004**, and thereby the force sensor tip **3007** in vertical and

lateral orientations. The probe tip **3007** can be vibrated in a vertical planar motion with respect to the substrate **3002** by exciting the first symmetric resonance of the force sensor structure **3000**. By applying a large bias voltage to control the bias position for the control loop and adding a small sinusoidal signal at the resonant frequency f_0 to the electrostatic actuation ports **3017***a-b*, the probe **3007** can be used for fast tapping mode or non-contact mode imaging of planar, lateral structures.

In order to impart the vertical motion, the sinusoid generated by electrostatic actuation at **3017***a* is IN PHASE with the sinusoid generated by the electrostatic actuation at **3017***b*. With in-phase vibrations between the electrostatic actuators **3017***a-b*, the flexible mechanical structure **3004** is oscillated to an offset position **3004'**. The offset position of the mechanical structure at **3004'** is offset from or bowed away from its original plane which is parallel to the substrate **3002**.

In addition to the vertical and horizontal oscillation of the mechanical structure **3004** of the force sensor **3000**, the embodiments described herein enable an oscillation of the probe tip **3007** an at angle normal to a three-dimensional structure as in FIG. **31**A and in an elliptical orbit as shown in FIG. **31**B.

A typical dimensional structure **3100** can be, for example, a portion of a microelectronic device structure. The structure **3100** can include a substrate or support **3102**, and surface variations such as protrusions **3104** and **3016** generated as a result of etching, patterning and the like during fabrication of a circuit or semiconductor device, for example. The surface structures **3104** and **3106** can include trenches or holes **3108** between adjacent surface structures as defined by sidewalls **3110** of the surface topography. In particular, the sidewalls **3110** can be patterned to include undercut portions **3112** as shown.

As shown in FIG. **31**A, oscillating the probe tip **3107** in a desired motion pattern at an angle normal to a surface structure **3106** is suitable for inspecting a sidewall **3112** thereof. In FIG. **31**B, the probe tip **3107** is moved in an elliptical orbit to simultaneously provide both lateral tapping and vertical tapping signals. Similar motion patterns can be used for non-contact operation where the frequency shifts or oscillation amplitude variations are used to control parameters. The following describes how these probe tip **3107** motion patterns can be obtained with the force sensor of FIGS. **29**A-B.

FIG. **32** is a side schematic diagram of a lateral oscillation of the force sensor in accordance with the present teachings. It will be apparent that the force sensor shown in FIG. **32** employs the force sensor elements as described in connection with FIGS. **29**A and **29**B. In order to impart motion to the probe tip **3207**, different bias signals are selectively applied to the actuation ports **3217***a* (also labeled as Port **2**) and **3217***b* (also labeled as Port **1**).

By applying the different bias signals to the actuation ports **3217***a* and **3217***b*, the portions of the flexible mechanical structure **3204** close to the fixed edges thereof can each be pulled down toward the substrate **3202** by different amounts. For example, the edge of the flexible mechanical structure **3204** closer to the actuation port **3217***b* can be pulled down toward the substrate **3202** by a greater distance than the edge adjacent the actuation port **3217***a*.

Since the electrodes **3216***a-b* are positioned close to the edges of the flexible mechanical structure **3204**, an actuation range can be the full distance of the gap **3205** between the flexible mechanical structure **3204** and the substrate **3202**. For example, with a 1-10 μm gap and a 50 μm long flexible mechanical structure **3204**, the flexible mechanical structure **3204** can be manipulated to form an angle in the range of 1.1° to 10° with respect to normal. Accordingly, with the probe tip **3207** seated on the flexible mechanical structure, **3204**, the probe tip will be directed at similar angles. This described range of angles is adequate for tapping on a sidewall **3110**. For a 5 μm high probe tip **3207**, this corresponds to a 100 nm to 800 nm lateral distance from the base to the tip of the probe **3207**. Therefore, small objects can be imaged by selectively directing the probe tip.

In order to vibrate the tip **3207** in a linear direction at one of the described angles, sinusoidal signals with proper amplitudes are added to the actuator input signal as shown in FIG. **32**. In this case a higher bias voltage is applied to the right side of the flexible mechanical structure **3204** as compared to the left side ($V_{Dc1}>V_{DC2}$). The frequency of this signal can be chosen to be the resonant frequency of the symmetric mode of the structure taking into account the effect of the bias voltage in the system dynamics. A similar result can be obtained using separate piezoelectric actuators (not shown) integrated to the flexible mechanical structure **3204**. Similar motion can be obtained by applying AC signals higher or below the resonance frequencies of the flexible mechanical structure **3204**.

Referring now to FIG. **33**, a lateral oscillation of the probe tip **3307** can also be generated according to the present teachings. As with the linear oscillation, the flexible mechanical structure **3304** is manipulated by selective electrostatic actuation at the electrostatic actuation ports **3317***a-b*. In general, the probe tip **3307** is moved laterally using the first anti-symmetric resonance of the vibration mode of the flexible mechanical structure **3304** where the probe tip **3307** is located at a nodal point of the structure. More specifically, the sinusoid at electrostatic actuation port **3317***b* (Port **2**) is excited at a first anti-symmetric resonance of the flexible mechanical structure **3304** while the sinusoid at the electrostatic actuation port **3317***a* (Port **1**) is excited to be OUT of phase with the sinusoid of Port **1**. This arrangement generates a lateral movement of the probe tip **3307** with respect to the substrate **3302**.

With the probe tip **3307** at the node of this vibration mode as shown in FIG. **33**, the resultant lateral motion can be used for tapping or non-contact mode imaging of sidewalls **3110**. In order to efficiently excite this mode, the same polarity bias (control) voltages are applied in addition to out-of-phase sinusoidal signals at the resonant frequency, f_1. Alternatively, in-phase sinusoidal signals at the resonant frequency f_1 can be applied in addition to bias (control) voltages of reversed polarity. Since the frequencies f_0 and f_1 can be designed to be far from each other and non-harmonically related, these two modes can be independently excited to achieve the tip motion depicted in FIG. **31**B. In general, the voltages that can be applied to the electrical actuation Ports **1** and **2** can be described as below.

$$V_1=V_{1bias}(t)+A\cos(2\pi f_0 t)+B\cos(2\pi f_1 t) \text{ and } V_2=V_{2bias}(t)+C\cos(2\pi f_0 t)+D\cos)2\pi f_1 t)$$

By way of further explanation, $V_{1bias}(t)$ is large for controlling and bending; $A\cos(2\pi f_0 t)$ is for symmetric mode actuation; and $B\cos(2\pi f_1 t)$ is for anti-symmetric mode actuation.

The relatively slowly varying V_{1bias} and V_{2bias} voltages control the shape of the beam, enable linearized operation of the electrostatic actuators, and are used as the actuator in the control loop. The coefficients A, B, C, D determine the orbit of the tip oscillation. It is possible to have simultaneously non-zero values for all these amplitudes to have the tip move laterally at one frequency and vertically at another. Similarly, the tip can be moved vertically using more than one symmetrical vibrational mode by applying appropriate signals. By decoding and separately detecting the motions, it is pos-

sible to run separate control loops to image lateral and vertical dimensions using model-based control and imaging software.

For fast imaging the force sensor probe tip **2907** can provide a motion range of 2-5 μm in the vertical direction and up to 0.5 μm in the X-Y directions by using the integrated actuators **2917***a-b*. This can enable movement of the probe tip **2907** by a range sufficient to image 100-200 nm high and 20 nm~100 nm wide photoresist structures and their sidewalls encountered in microelectronics processing. The resonant frequencies can be in the range of 1 kHz to 10 MHz depending on the speed, actuation range, and detection limitations. Micromachined membrane, beam and cantilever based structures have been successfully developed and used in this frequency range. The imaging described has position control accuracy on the order of 0.1 nm in three-dimensional space.

As indicated, the detection methods available by the present embodiments also include multi-directional, multi-frequency probe tip motion.

The exemplary force sensors including the tip probe **2907** enables detection of a force applied to the tip in different directions by measuring its effect on the flexible mechanical structure **2904** with multiple detectors, and processing the detector output signals in different ways. These multiple detectors can use optical, capacitive, piezoresistive or piezoelectric methods.

As an example, FIG. **34**A shows a side sectional schematic and FIGS. **34**B, and **34**C show top schematic views of a force sensor having multiple optical detection ports in accordance with the present teachings. In these figures, the force sensor unit **3400** can comprise a force sensor **3401**, a detection surface **3402**, a flexible mechanical structure **3404**, a gap **3405**, a tip **3407**, a plurality of separate top electrodes, such as electrodes **3416***a-c*, a pair of bottom electrodes, such as electrodes **3420***a* and **3420***b*, a plurality of gratings, such as first grating **3406***a* and second grating **3406***b*, and at least one detector **3408**. The first grating **3406***a* can have a different grating period than the grating period of **3406***b*. Furthermore, the first grating **3406***a* can have a different orientation as compared to the grating **3406***b*. These variations in grating structures help separate the readout beams to measure displacement of different parts of the flexible mechanical structure **3404** corresponding to different grating locations. It is to be understood that other force sensor embodiments described herein can also comprise multiple gratings and gratings fabricated at different elevations on the detection surface **3402** to increase the deflection detection range.

Each of the plurality of separate top electrodes **3416***a-c* can be electrically isolated and formed in the flexible mechanical structure **3404**. Moreover, the bottom electrodes **3420***a-b* can be spaced apart from the separate top electrodes **3416***a-c* by the gap **3405**. Further, the bottom electrodes can be positioned in the substrate **3402** and can be contacted by electrode terminals **3421***a-b*. Similarly, the separate top electrodes **3416***a* and **3416***b* can be contacted by electrode terminals **3417***a* and **3417***b*.

The detection surface **3402** can be positioned at a free end of a cantilever (not shown). Moreover, the flexible mechanical structure **3404** can be fully clamped around its circumference, it can be a clamped-clamped beam with a rectangular or H shape where the short edges at the ends are clamped, or it can be a cantilever structure or a similar structure that changes shape in a predictable manner in response to a force applied to the tip **3407**.

A light beam **3410** can be directed through the detection surface **3402** to impinge on the flexible mechanical structure **3404**. The beam **3410** reflects off of the flexible mechanical structure **3404**, a portion of which can be reflective, and is diffracted differently by the first grating **3406***a* and the second grating **3406***b*. As shown, the first grating **3406***a* can generate a first set of diffraction orders **3412***a-b* and the second grating **3406***b* can generate a second set of diffraction orders **3413***a-b*. The detectors **3408** can detect the different diffraction orders. The detector outputs can be added to obtain up and down bending displacement detection. Similarly, the outputs can be subtracted to obtain torsional motion and force detection. This information can be obtained when the spring constant for the second bending mode (torsion around the mid axis) of the flexible mechanical structure **3404**, clamped-clamped beam or a cantilever is known. Thus, in addition to acting as actuators, the first grating **3406***a* and second grating **3406***b* can be used to optically or capacitively decouple the bending motion from the torsional motion. As such, the sensed outputs of these detectors yield both bending and torsional motion information. Similarly, by having a flexible mechanical structure **3404** supported by 3 or 4 beams, the forces acting on the tip **3407** in three-dimensions can be obtained by proper processing of the output signals from multiple displacement sensors, such as the gratings **3406***a*, **3604***b*. One can also use separate beams **3410** to illuminate the plurality of gratings.

More specifically, FIG. **34**A further shows that the two gratings each have different grating periods. The first grating **3406**A is positioned placed on the left and right side of the probe tip **3407** while the second grating **3406***b* is positioned on the right side of the probe tip **3407**. When illuminated by the light beam **3410**, such as a laser beam, each of these gratings **3406***a* and **3406***b* will direct the position detection (PD) signals **3412***a-b* and **3413***a-b* each at a different angle. By placing the photo detectors at these particular locations the displacement of each side of the beam can be determined. This is made clear by the top view shown in FIG. **34**B. In a similar fashion, gratings **3430***a* with the same periodicity but different orientation from gratings **3430***b* can be used to separate the optical signals coming from each side of the probe tip **3407** as shown in FIG. **34**C. Since the gratings are not connected to an electrical source, their asymmetry does not affect the electromechanical actuation of the probe tip **3407**.

Capacitive detection can be implemented into the force sensor structure **3500** as shown in the exemplary embodiment of FIG. **35**. The force sensor structure **3500** includes two capacitive detection ports **3550***a* and **3550***b* as shown. Capacitive detection can be particularly useful when an array of probe tips (not shown) is formed on the same substrate for imaging large areas in parallel.

Similar to the force sensor structures described above, the force sensor structure unit **3500** can comprise a force sensor **3501**, a detection surface **3502**, a flexible mechanical structure **3504**, a gap **3505**, a tip **3507**, a plurality of separate top electrodes, such as electrodes **3516***a-d*, and a plurality of separate bottom electrodes, such as electrodes **3520***a-d*.

Each of the plurality of separate top electrodes **3516***a-d* can be electrically isolated and formed in the flexible mechanical structure **3504**. Moreover, the bottom electrodes **3520***a-d* can be spaced apart from the separate top electrodes **3516***a-d* by the gap **3505**. Further, the bottom electrodes can be positioned in the substrate **3502** and can be contacted by electrode terminals **3521***a-d*. Similarly, each of the separate top electrodes **3516***a-d* can be contacted by electrode terminals **3517***a-d*. In the present embodiment, the electrode terminals **3517***b-c* can be capacitive sensing terminals that can detect a capacitance change formed between the separate top electrodes **3516***b-c* and the bottom electrodes **3520***b-c*.

Similar to the embodiments described above, the force sensor structure **3500** of FIG. **35** includes the electrostatic

actuation via electrostatic actuation ports **3517***a* and **3517***d*. The electrostatic actuation imparts vertical, lateral, and multidirectional motion to the probe tip **3507** as described and the details are omitted herein for the sake of brevity.

FIG. **36**A shows a signal processing method for obtaining lateral tapping signals and FIG. **36**B shows a signal processing method for obtaining vertical tapping signals with the exemplary force sensors in accordance with the present teachings. More specifically, a simple difference taking and adding scheme is utilized to generate lateral (X or Y) and vertical (Z) tapping signals during tapping mode imaging. Since the lateral motion of the tip is driven by a signal at frequency f_1, as shown in FIG. **33**, and the two ends of the flexible mechanical structure **3304** move out-of-phase with each other, this signal can be extracted by filtering the input around f_1 and taking the difference of signals from each end. Therefore, the common mode signal indicating any motion in the vertical direction is eliminated. Similarly, the commonly known vertical (Z) tapping signal can be separated by filtering the signal around frequency f_0 and summing the outputs. By designing the flexible mechanical structure to have a large separation between f_0 and f_1, large imaging bandwidths can be achieved around these frequencies while significantly decoupling the signals. More complicated algorithms can be used to separate these signals and generate control signals to be applied to the integrated electromechanical actuators on the sensor structure as well as to the scanning stages.

FIG. **37** shows a signal processing for non-contact three-dimensional imaging with exemplary force sensors in accordance with the present teachings. For non-contact imaging, the information to run the control loop comes from the changes in the oscillation characteristic of the force sensor due to long range interaction forces between the tip and the sample surface. These changes can be detected either in the oscillation amplitude or in the resonance frequency. The shifts in these parameters can be detected by suitable circuits and can be used to run control loops in the Z and X-Y directions to form three-dimensional images. For sensitive non-contact operation, the quality factor of the oscillator should be high. This can be ensured by designing the force sensor structure to vibrate in a mode with low loss or operate the device in vacuum environment.

While the invention has been illustrated with respect to one or more implementations, alterations and/or modifications can be made to the illustrated examples without departing from the spirit and scope of the appended claims. In addition, while a particular feature of the invention may have been disclosed with respect to only one of several implementations, such feature may be combined with one or more other features of the other implementations as may be desired and advantageous for any given or particular function. Furthermore, to the extent that the terms "including", "includes", "having", "has", "with", or variants thereof are used in either the detailed description and the claims, such terms are intended to be inclusive in a manner similar to the term "comprising."

Other embodiments of the invention will be apparent to those skilled in the art from consideration of the specification and practice of the invention disclosed herein. It is intended that the specification and examples be considered as exemplary only, with a true scope and spirit of the invention being indicated by the following claims.

What is claimed is:

1. A method of causing a probe tip of a force sensor structure to move in three dimensions, comprising the steps of:

a. forming a flexible mechanical structure a first distance above a detection surface so as to form a gap between the flexible mechanical structure and the detection surface;

b. placing the probe tip on the flexible mechanical structure so as to point toward the detection surface;

c. arranging at least a pair of actuator electrodes on the flexible mechanical structure and opposed to electrodes arranged on the detection surface;

d. selectively activating at least one of the actuator electrodes thereby deflecting the flexible mechanical structure at a selected location so that the flexible mechanical structure causes the probe tip to move in more than one dimension.

2. The method according to claim **1**, wherein the multi-directional motion comprises vertically oscillating the probe tip with respect to the detection surface.

3. The method according to claim **2**, wherein vertically oscillating the probe tip comprises exciting a symmetric resonance of the flexible mechanical structure.

4. The method according to claim **1**, wherein multi-directional motion comprises laterally oscillating the probe tip with respect to the detection surface.

5. The method according to claim **4**, wherein laterally oscillating the probe tip comprises applying different bias signals to the actuator electrodes such that portions of the flexible mechanical structure are deflected by correspondingly different amounts.

6. The method according to claim **1**, wherein multi-directional motion comprises oscillating the probe tip at an angle to the normal with respect to the detection surface.

7. The method according to claim **6**, wherein oscillating the tip at an angle to the normal with respect to the support surface comprises applying different bias signals to the actuator electrodes such that portions of the flexible mechanical structure are deflected by correspondingly different amounts.

8. The method according to claim **7**, wherein an angle with respect to normal is from about 0.1° to about 10°.

9. The method according to claim **1**, wherein multi-directional motion comprises an orbital motion.

10. The method according to claim **9**, wherein orbitally oscillating the tip comprises independently exciting the actuation electrodes at non-harmonic frequencies.

11. The method according to claim **9**, wherein the orbital motion is elliptical.

12. The method according to claim **11**, wherein resonant frequencies of the flexible mechanical structure are from about 1kHz to about 10MHz.

13. The method according to claim **1**, wherein the probe tip has a vertical range of motion of from about 2 μm to about 10 μm and a lateral range of up to 1 μm.

* * * * *